Unlocking hidden phage diversity to complete the BASEL collection for systematic exploration of phage-host interactions

Dorentina Humolli[1], Enea Maffei[1,2,#], Yannik Heyer[2,#], Elia Agustoni[2,#], Damien Piel[1], Aisylu Shaidullina[1,2], Luc Willi[2], Patrick Sauer[2], Fabienne Estermann[2], Aline Cuénod[3], Dominik P. Buser[2], Adrian Egli[3,4], Sebastian Hiller[2], Matthew Dunne[5], Alexander Harms[1,2]*

[1]Institute of Food, Nutrition, and Health (IFNH), ETH Zürich, Zürich, Switzerland

[2]Biozentrum, University of Basel, Basel, Switzerland

[3]Division of Clinical Bacteriology and Mycology, University Hospital Basel, Basel, Switzerland

[4]current address: Institute for Medical Microbiology, University of Zürich, Zürich, Switzerland

[5]Micreos GmbH, Wädenswil, Switzerland

[#]These authors contributed equally.

*Correspondence should be addressed to Prof. Alexander Harms (alexander.harms@hest.ethz.ch)

Short title: New BASEL phages requiring O-antigen or inhibited by K-12 prophages

Abstract

Research on bacteriophages, the viruses infecting bacteria, has fueled the development of modern molecular biology and inspired their therapeutic application to combat bacterial multidrug resistance. However, most work has so far focused on a few model phages which impedes direct applications of these findings in clinics and suggests that a vast potential of powerful molecular biology has remained untapped. We have therefore recently composed the BASEL collection of *Escherichia coli* phages (BActeriophage SElection for your Laboratory) which made a relevant diversity of phages infecting the *E. coli* K-12 laboratory strain accessible to the community. These phages are widely used, but their assorted diversity had remained limited by the *E. coli* K-12 host. We have therefore now genetically overcome the two major limitations of *E. coli* K-12, its lack of O-antigen glycans and the presence of resident bacterial immunity. Restoring O-antigen expression resulted in the isolation of diverse additional viral groups like *Kagunavirus*, *Nonanavirus*, *Gordonclarkvirinae*, and *Gamaleyavirus*, while eliminating all known antiviral defenses of *E. coli* K-12 additionally enabled us to isolate phages of genus *Wifcevirus*. Even though some of these viral groups appear to be common in nature, no phages from any of them had previously been isolated using *E. coli* laboratory strains and they had thus remained largely understudied. Overall, 36 new phage isolates have been added to complete the BASEL collection. These phages were deeply characterized genomically and phenotypically with regard to host receptors, sensitivity to antiviral defense systems, and host range. These results highlighted dominant roles of the O-antigen barrier for viral host recognition and of restriction-modification systems in bacterial immunity. We anticipate that the completed BASEL collection will propel research on phage-host interactions and their molecular mechanisms, deepening our understanding of viral ecology and fostering innovations in biotechnology and antimicrobial therapy.

38 # Introduction

39 Bacteriophages, the viruses infecting bacteria, have attracted great interest due to their abundance
40 and diversity in all ecosystems, their key roles as inspiration for biotechnology, and their therapeutic
41 potential in the fight against resilient bacterial infections [1-4]. Most cultured phages are so-called tailed
42 phages or *Caudoviricetes* that characteristically use a tail structure at the virion to inject their genome into
43 host cells. Morphologically, tailed phages can be classified as myoviruses (contractile tail), siphoviruses
44 (long, flexible, non-contractile tail), and podoviruses (short stubby tail). Following the "phage treaty"
45 declared by Max Delbrück in 1944 [5], a few tailed phages infecting *Escherichia coli* have become key
46 model systems for studying the molecular biology of phage-host interactions [6]. We therefore know
47 comparably much about the molecular mechanisms underlying infections of *E. coli* with these seven "T
48 phages" T1 – T7 [7, 8] and a few additional ones infecting *E. coli* or other major model organisms like
49 *Bacillus subtilis*. While this work has resulted in many major breakthroughs since the "golden era" of
50 molecular biology [3, 9], the limited number and diversity of these model phages is a severe limitation for
51 systematic research that could inform the effective use of natural phage diversity for therapeutic or
52 biotechnological applications. We and others have therefore proposed broader sets of model phages
53 infecting commonly studied host organisms such as *E. coli* [10-12], *Klebsiella* [13], or *Pseudomonas*
54 *aeruginosa* and other pseudomonads [14-16]. Our previous work had presented 68 well-characterized new
55 *E. coli* phages as the BASEL (BActeriophage SElection for your Laboratory) collection which we have
56 made accessible to the academic community.

57 The value of these BASEL phages lies in their "assorted diversity", providing access to a broad
58 spectrum of biological diversity both within and between phage groups when exploring any aspect of phage-
59 host interactions [6, 10]. For example, the BASEL collection has been used to study phage host recognition
60 [17], viral dependence on host codons [18], porin functionality [19], phage replication rates [20], and
61 bacterial immunity [21-25]. A key prerequisite for broad applicability of the BASEL phages is that they
62 have deliberately been isolated using the *E. coli* K-12 laboratory strain as host, the most important model

63 organism in fundamental microbiology research [9, 26]. However, phage isolation with *E. coli* K-12 as host
64 has also conflicted with the goal of assorted phage diversity by introducing inherent biases that prevented
65 us from sampling a complete overview of *E. coli* phage diversity [10]. Firstly, the domesticated *E. coli*
66 K-12 laboratory strain has lost the O-antigen glycan chains on the lipopolysaccharide (LPS) core that form
67 a dense barrier on wild *E. coli* and shield cell surface receptors from viral recognition [27-30]. While the
68 absence of this barrier made it easier to isolate multiple phages from different viral groups, it naturally
69 excluded the isolation of phages which depend on the O-antigen as host receptor [31]. Furthermore, a
70 second level of sampling bias may have been caused by known (and possibly unknown) antiviral defenses
71 encoded by *E. coli* K-12, although we had deleted some of them already in the host strain used to isolate
72 and study the original BASEL collection [10].

73 In the current study we have addressed both limitations of our previous work by expanding the
74 BASEL collection with 36 new phages that depend on (restored) O-antigen expression and / or seem to be
75 inhibited by resident antiviral defenses in the K-12 genome. Notably, while almost none of these phages
76 belong to groups of which other representatives have previously been found to infect *E. coli* K-12, all these
77 phages do infect *E. coli* K-12 with a few easily implemented modifications and can thus be used for
78 systematic fundamental research as an expansion of the original BASEL collection. Similar to our previous
79 study, we have performed a systematic phenotypic and genomic characterization of these phages with view
80 to host receptors, bacterial immunity, and host range, and we make them accessible to the scientific
81 community. These results extend some of our previous observations and complement them with new
82 discoveries on previously understudied phage groups such as the *Gordonclarkvirinae* podoviruses that are
83 abundant in nature, highly resistant to common phage-defense systems, and have a comparably broad host
84 range. The dependence of many newly included phages on O-antigen as host receptor highlights the
85 dominant role of viral adsorption for *E. coli* phage host range and provides a valuable tool for studying
86 diverse mechanisms of glycan recognition using the well-studied model strain *E. coli* K-12. Taken together,
87 our findings provide novel insights into the ecology and evolution of bacteriophages as well as into their

88 arms race with each other and bacterial immunity. We anticipate that our work will serve as a reference
89 point for future studies in fundamental phage biology and strengthen the BASEL collection as an effective
90 and widely used tool in the scientific community.

91 Results

92 Overview: Including O-antigen-dependent phages in the BASEL collection

93 The cell surface of Gram-negative bacteria is dominated by LPS and proteins embedded in the outer
94 membrane on which additional layers of protective exopolysaccharides such as a capsule can be present
95 [32]. To recognize their host and pass through these layers, phages typically directly bind exposed glycans
96 as an initial host receptor before moving down to the cell surface [10, 31, 33, 34]. There, the virus typically
97 binds a second so-called terminal receptor which results in irreversible adsorption and DNA ejection [34].
98 The receptor-binding proteins (RBPs) that target primary and terminal receptors are typically displayed on
99 different structures with longer, lateral tail fibers or stubby tailspikes commonly targeting primary receptors
100 followed by central tail fibers or tail tip complexes binding terminal receptors [reviewed in reference 34].

101 Bacterial exopolysaccharides and the dense O-antigen layer of the LPS effectively shield the cell
102 surface from the access of tailed phages unless the phage carries enzymatic tailspikes or glycan-targeting
103 tail fibers to specifically bind them as part of primary receptor recognition [28, 29, 31, 33, 34] (Fig. 1A).
104 Consequently, the variability of the nearly 200 different types of O-antigen and other surface structures
105 greatly contribute to the observed narrow host range of most enterobacterial phages [10, 30, 35, 36].
106 However, laboratory strains of the *E. coli* K-12 lineage do not express protective exopolysaccharides such
107 as capsules and lack even the O-antigen layer due to disruption of the *wbbL* gene by a transposon [27]
108 (Fig. 1A). Phages can therefore readily access the bacterial cell surface which enabled broad sampling of
109 *E. coli* phages for the original BASEL collection [10, 28]. However, most of these phages are unable to
110 infect *E. coli* K-12 with restored O16-type O-antigen with few exceptions that likely carry RBPs targeting
111 this glycan such as *Hanrivervirus* JakobBernoulli (Bas07) or *Tequintavirus* IrisvonRoten (Bas32; Figs. 1A
112 and 1B).

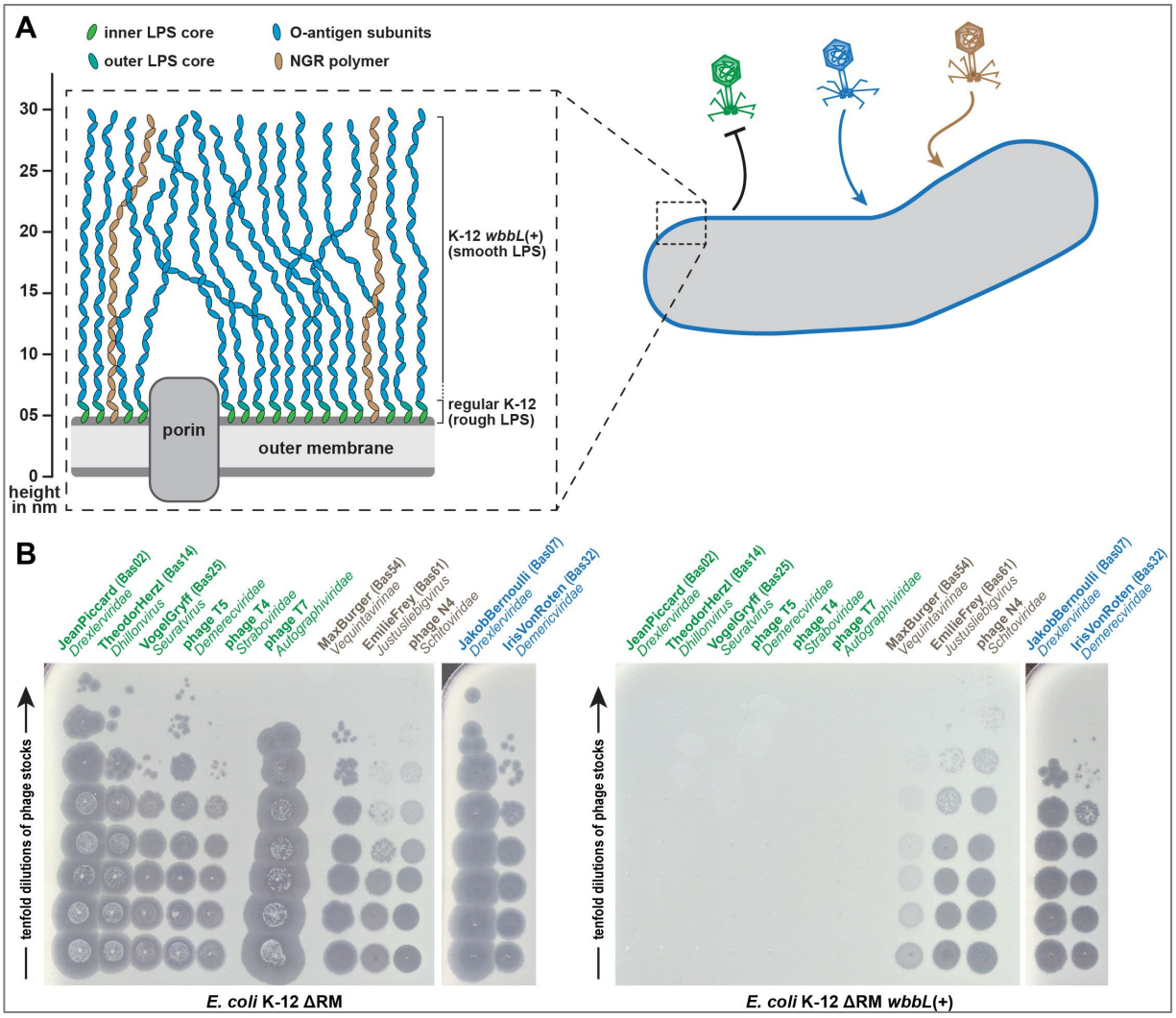

Figure 1. O-antigen glycans as barrier or host receptor for phage infections.

(A) The illustration shows cell surface glycans of *E. coli* K-12 laboratory strains including rough LPS without O-antigen and smooth LPS (with genetically restored O16-type O-antigen; see details in *Materials and Methods*). The O-antigen can be a barrier to phage infection (green), used as a host receptor (blue), or be bypassed by phages that target the NGR glycans (brown). **(B)** Serial dilutions of different phages characterized previously [10] were spotted on the *E. coli* K-12 ΔRM strain without (left) or with (right) genetically restored O-antigen expression to illustrate the three different modes of interaction with these surface glycans (same color code as in (A)).

In addition, some phages like N4 or the *Vequintavirinae* can bypass the O-antigen layer by targeting the "N4 glycan receptor" (NGR), a recently described glycan that is broadly conserved among enterobacteria [10, 17] (Figs. 1A and 1B). The shielding of surface receptors by the O-antigen layer seems to be primarily due to its density because it is not more than 30nm deep while the tail fibers of model phages T4 (ca. 145nm [37]), T5 (80nm [38]), or T7 (30nm [39]) could otherwise easily reach through it to the cell

surface. However, these phages are completely blocked by restored O16-type O-antigen expression [10].

While the absence of an O-antigen barrier in the K-12 strain used for sampling the BASEL phages made it much easier to isolate many diverse phages, it also meant that phages which depend on this glycan for host recognition could not be sampled. Using different sewage samples, we had previously shown that these are quantitatively rare though they would of course be qualitatively interesting to expand the assorted diversity of the BASEL collection [10]. We have thus now systematically isolated and characterized diverse phages that infect *E. coli* K-12 with O16-type O-antigen but not the isogenic strain without it (Figs. 2A/B). Fortuitously, we observed that phages requiring O16-type O-antigen as host receptor are much more common in environmental samples than in sewage (Table S1). Most but not all of these viruses belonged to phage groups that had already been known for their dependence on surface glycans including O-antigen such as podoviruses of *Gamaleyavirus* genus or siphoviruses of the *Kagunavirus* genus [33] (see Fig. 2B).

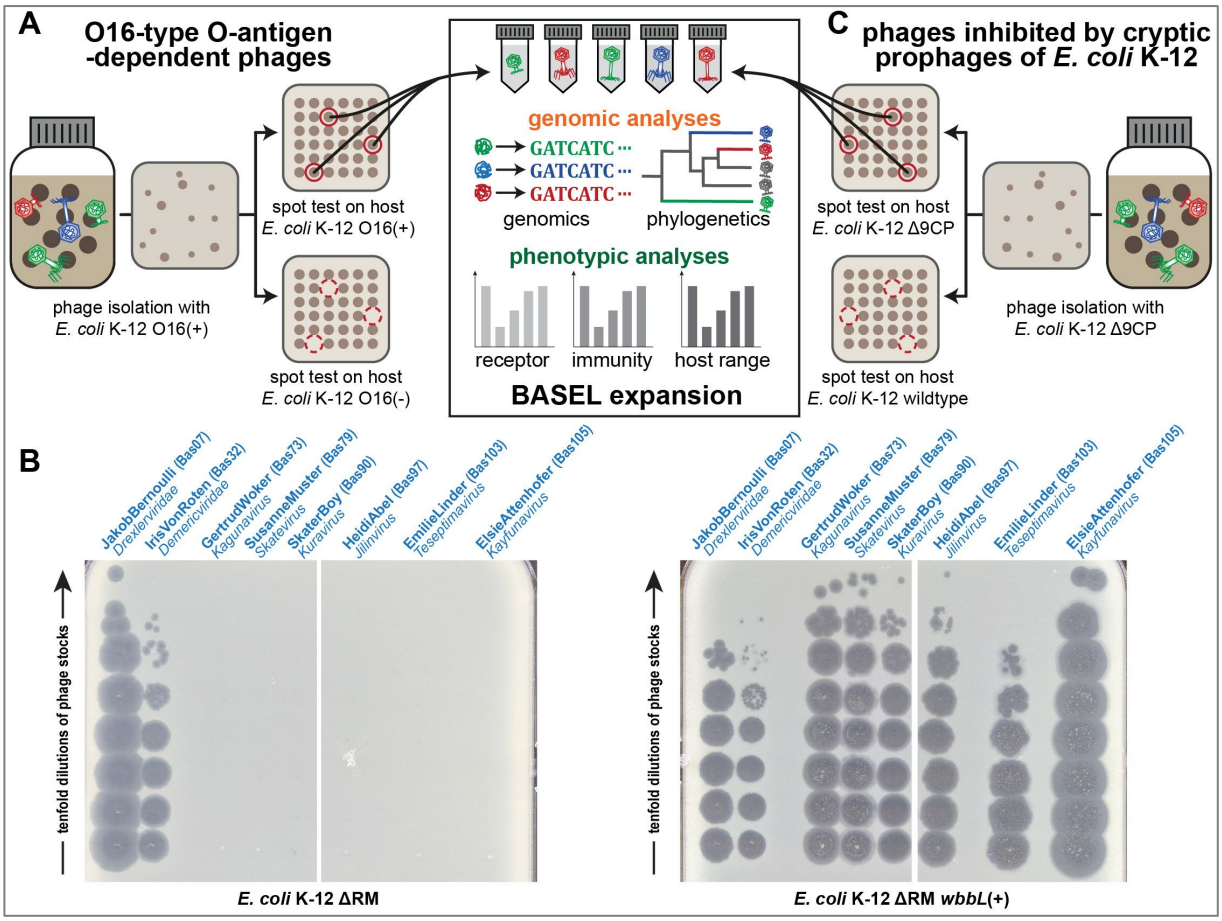

Figure 2. Expanding the BASEL collection with phages dependent on O-antigen or inhibited by K-12 cryptic prophages.

(A) Phages dependent on O16-type O-antigen were isolated and characterized as shown in the illustration (analogous to our previous work [10]). **(B)** O-antigen dependence of diverse newly isolated phages characterized in this work compared to JakobBernoulli and IrisVonRoten from our previous study that can infect *E. coli* K-12 without (left) and with (right) O-antigen [10]. **(C)** Phages inhibited by the cryptic prophages in the K-12 genome were isolated analogously to those dependent on O-antigen (see (A)) with help of the *E. coli* K-12 Δ9CP strain (details outlined in *Materials and Methods*).

129 ## Overview: Including phages inhibited by resident immunity of *E. coli* K-12

130 Bacteriophages encounter multiple layers of antiviral defenses outside and inside their host cells
131 that must be overcome for successful viral replication [40]. Some of these defenses prevent phage
132 adsorption or DNA ejection while others directly attack the invading virus such as restriction-modification
133 (RM) systems which cleave foreign DNA based on self / non-self recognition through certain DNA
134 modifications. Beyond direct attack, a deeper layer of defense systems protect the bacterial population
135 through abortive infection, i.e., the altruistic suicide of infected cells prior to successful phage replication
136 [41]. Recent work on anti-phage defense systems has vastly expanded our knowledge about their abundance
137 and diversity through the discovery of many new systems that target various aspects of phage biology and
138 are countered by phages in diverse ways [40-44].

139 The phages of the original BASEL collection had been sampled with a derivative of the commonly
140 used *E. coli* K-12 MG1655 laboratory strain in which we had knocked out all known RM systems, i.e., the
141 EcoKI type I RM system and three type IV restriction systems [10]. This enabled broad sampling of *E. coli*
142 phages including several taxonomic groups of phages that displayed considerable sensitivity to EcoKI and
143 would otherwise have been excluded [10]. However, the literature and commonly used prediction tools
144 such as DefenseFinder and PADLOC indicate that *E. coli* K-12 encodes several additional *bona fide* defense
145 systems that might limit the range of phages accessible with this genomic background [45, 46] (see details
146 at *Bacterial strains* in *Materials and Methods)*. We had not considered this to be a widely relevant factor
147 when composing the original BASEL collection because phage defenses beyond RM systems were thought
148 to be rather specific. However, our own results showing broad antiviral defense by the Fun/Z system and
149 the work of others, e.g., on the Zorya system revealed that this is not necessarily the case [10, 24].

150 Notably, all these *bona fide* defense systems are encoded on the cryptic prophages of *E. coli* K-12
151 that are genomic islands descended from once active prophages, i.e., the facultatively host-integrated form
152 of so-called temperate phages [45, 46]. This is in line with the common observation that anti-phage defenses
153 are frequently encoded on mobile elements and genomic islands [47, 48]. To overcome possible sampling
154 biases caused by these *bona fide* phage-defense systems (and possibly others that are yet unknown), we
155 thus performed phage isolation experiments with a variant of *E. coli* K-12 in which a previous study had
156 removed all cryptic prophages, *E. coli* K-12 BW25113 Δ9CP (both with and without restored O-antigen)
157 [49] (Fig. 2C). In these experiments we indeed obtained additional phages from groups of the original
158 BASEL collection or those recently isolated with restored O-antigen expression as well as another genus
159 that could never be isolated using *E.-coli* K-12 with cryptic prophages as host (*Wifcevirus* myoviruses).

160 ## Composition of the BASEL expansion

161 The original BASEL phage collection had been composed of 68 new handpicked phage isolates
162 that we characterized alongside a panel of ten well-studied model phages such as the classic T-phages [10].
163 These phages represent many major groups of *E. coli* phages which have been previously described in
164 phage isolation studies with *E. coli* K-12 [50, 51]. The (mostly genus-level) groups comprising these phages
165 showed characteristic and specific patterns of features regarding receptor usage, host range / recognition,
166 and sensitivity or resistance to bacterial immunity in our data and those from other studies [10, 20-25].
167 These observations make it possible to learn about the properties of newly isolated phages merely from
168 their genome sequences or taxonomic position, e.g., to inform a targeted selection or engineering of
169 effective phages for individual cases of phage therapy [52-54].

170 However, a close look at published work describing phages isolated with *E. coli* hosts beyond the
171 K-12 laboratory strain reveals important gaps in the assorted diversity of the original BASEL collection.
172 These include, e.g., several groups of podoviruses such as the *Gordonclarkvirinae* with characteristic
173 prolate virions [55], diverse small siphoviruses such as the genus *Kagunavirus*, and a few myoviruses such
174 as the genus *Wifcevirus* [35, 56, 57]. Using *E. coli* K-12 with restored O-antigen expression and / or without

175 cryptic prophages we have now isolated and characterized more than a hundred new phages that are unable

176 to grow on the regular *E. coli* K-12 host used for the original BASEL collection.

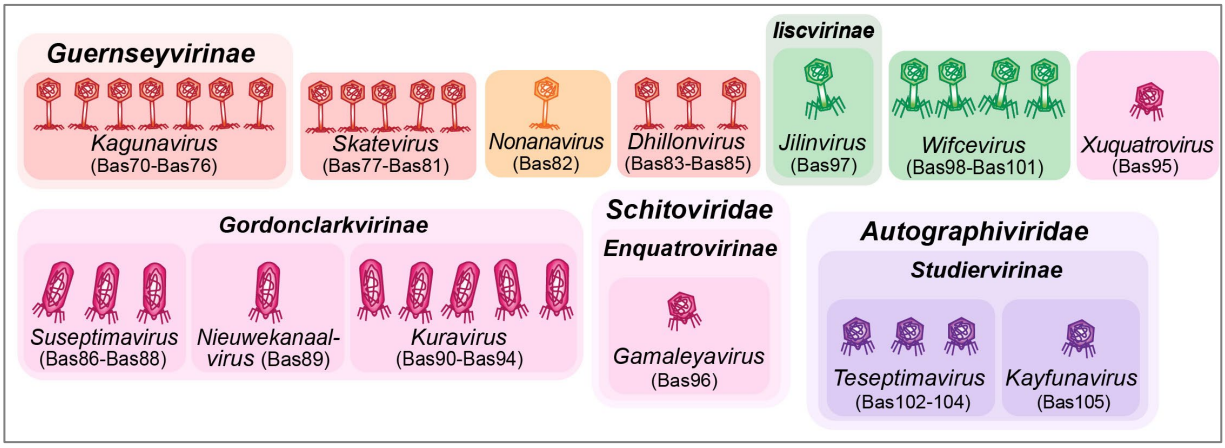

Figure 3. Overview of new phages included in the BASEL collection.
The illustration shows new phage isolates included in the BASEL collection with their Bas## identifiers. Isolates are sorted by morphotype and their current ICTV classification [58]. The color code distinguishes phages based on morphotype and genome size. For siphoviruses, small phages (ca. 30-50 kb) are shown in red and medium-sized phages (ca. 50-100 kb) are shown in orange. Small myoviruses (ca. 30-100 kb) are shown in green. For podoviruses, small phages (ca. 30-50 kb) are shown in violet and medium-sized phages (ca. 50-100kb) are shown in pink.

177 These new isolates cover all major groups of phages (and some rarely isolated ones) that have been

178 reported to infect *E. coli*, and we selected 36 isolates for an expansion of the BASEL collection based on

179 their genomic and phenotypic diversity (Fig. 3 and Table S2). We systematically characterized these phages

180 analogous to the phages in our previous study (Figs. 4A-D) and used several original BASEL phages that

181 could overcome the O16 O-antigen barrier as controls for the phenotypic experiments. For these, no relevant

182 differences to their phenotypes in the original paper were observed when the host strain expresses O16 O-

183 antigen (Fig. S1B). These results suggest that the O-antigen barrier and other defenses are largely

184 orthogonal and that our results from this study are comparable to the original publication on the BASEL

185 collection.

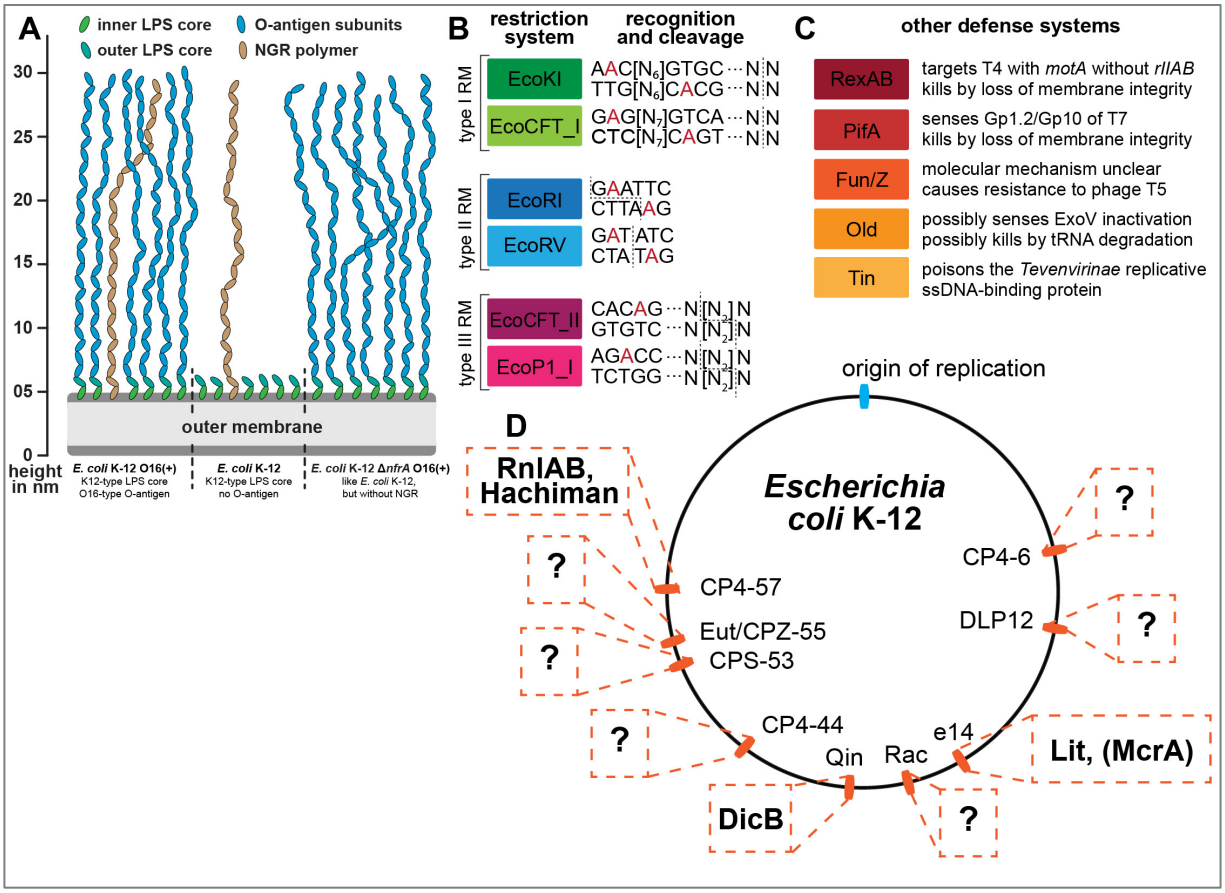

Figure 4. Overview of *E. coli* surface glycan variants and the immunity systems used in this study. (A) Surface glycans of different *E. coli* K-12 variants are shown schematically (compare Fig. 1A and see further details in *Materials and Methods*). None of the newly isolated phages in this work showed any dependence on the NGR glycan (see Fig. S1A) which has thus been omitted from the other illustrations. **(B, C)** Restriction-modification (B) and other defense systems (C) used to characterize phage isolates are summarized schematically (same as used in our previous work [10]) **(D)** The genome of *E. coli* K-12 contains nine cryptic prophages that encode all remaining antiviral defense systems predicted by DefenseFinder or PADLOC after deletion of all restriction systems in our previous work (including McrA; see details on these defense systems in *Materials and Methods* under *Bacterial strains*) [10, 45, 46]. Due to the known accumulation of antiviral defenses in prophages [47, 48], it seems likely that also many of the possibly still unknown defense systems of *E. coli* K-12 would be encoded in these loci (indicated by question marks). The *E. coli* K-12 Δ9CP variant of Wang et al. [49] which we use in the current study has been cured of all nine cryptic prophages.

Properties of siphoviral genus *Kagunavirus*

Small siphoviruses like the *Drexlerviridae* family (relatives of phage T1) or genus *Dhillonvirus* are frequently isolated using *E. coli* as host and typically have genomes of 40-50kb size. The diverse representatives of these groups in the original BASEL collection mostly showed considerable sensitivity to RM systems and – as expected from previous work – targeted different porins as terminal host receptor [10,

191 59, 60]. Only one of these phages, JakobBernoulli (Bas07), is able to infect *E. coli* K-12 with restored O-
192 antigen expression, suggesting that its lateral tail fibers can target O16-type O-glycans [10] (see also Fig.
193 S1B and below). Our targeted search for phages that depend on O16-type O-antigen resulted in the isolation
194 of various small siphoviruses of genus *Kagunavirus* within the subfamily of *Guernseyvirinae* (Fig. 5A-D).
195 These phages have small genomes of ca. 41-44kb which makes them attractive models for synthetic biology
196 applications, e.g., in case of phage CM001 [61]. While all our isolates fully depend on restored O-antigen
197 expression, only some of them (Bas70-73) infect a regular *E. coli* K-12 host while others (Bas74-76) could
198 only be isolated using a K-12 host devoid of cryptic prophages (Fig. 5D). Phenotypically, both groups of
199 *Kagunavirus* isolates behave very similarly and display the high sensitivity to RM systems and a variable
200 sensitivity to the Old anti-phage defense system that is typical for small siphoviruses [10] (Fig. 5D). The
201 dependence on glycans as host receptor seems to be a general property of *Guernseyvirinae* phages
202 including, e.g., the prototypic *Kagunavirus* K1G targeting the K1 capsule of *E. coli* [15] or the *Jerseyvirus*
203 SETP3 and several relatives targeting O-antigen of *Salmonella enterica* [62].

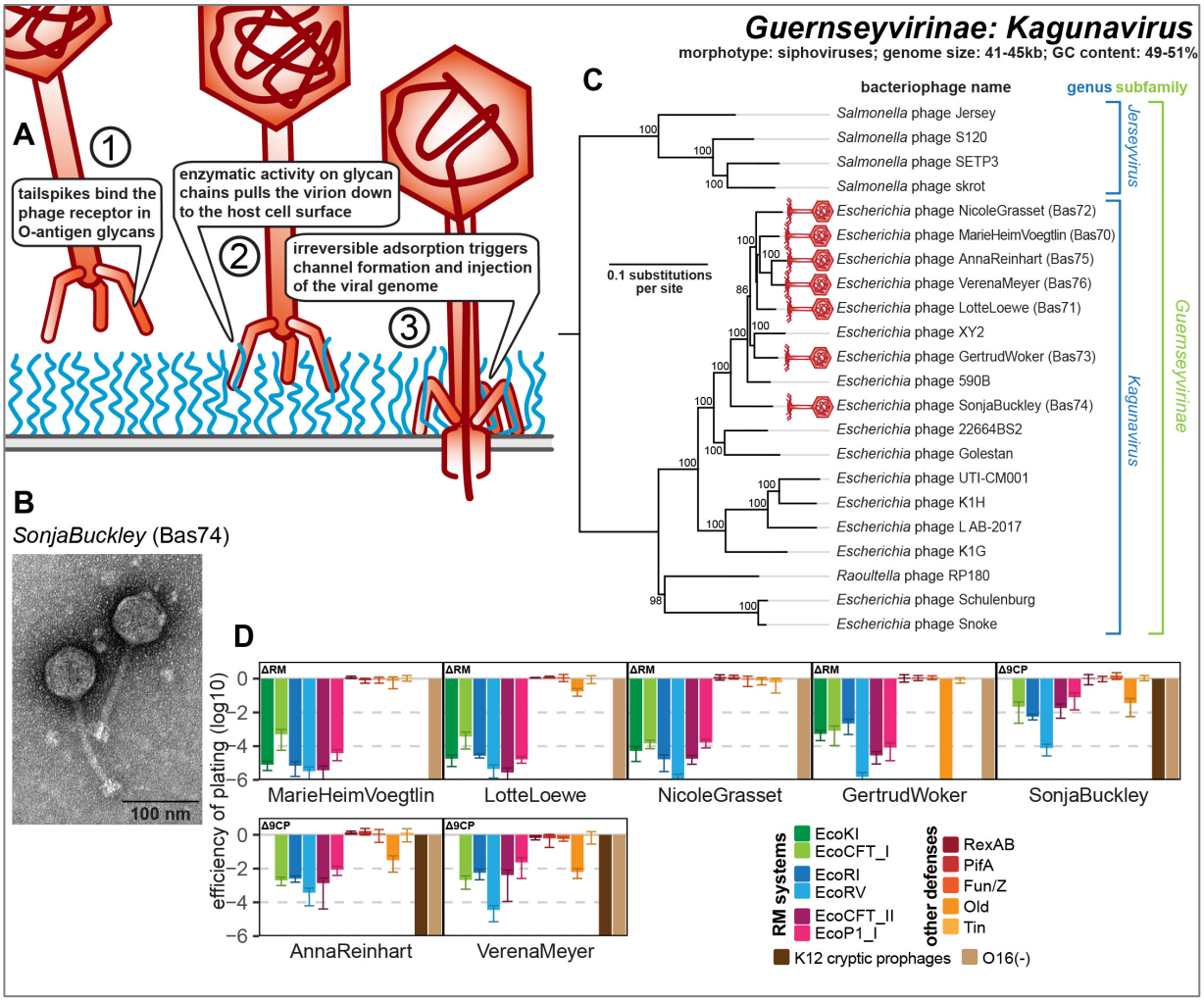

Figure 5. Overview of *Guernseyvirinae* genus *Kagunavirus* phages.

(A) Schematic illustration of host recognition by *Kagunavirus* phages (O-antigen chains in blue). In analogy to other small siphoviruses like lambda or T5, we anticipate that these phages also use a phage-derived conduit for DNA injection across the outer membrane after the tail fibers recognizing the terminal host receptor have bent off [63, 64]. **(B)** Representative TEM micrograph of phage SonjaBuckley (Bas74). **(C)** Maximum-Likelihood phylogeny of *Kagunavirus* phages and relatives based on a curated whole-genome alignment with bootstrap support of branches shown if > 70/100. Newly isolated phages of the BASEL collection are highlighted by red phage icons. The phylogeny was rooted between the genera *Kagunavirus* and *Jerseyvirus*. **(D)** The results of quantitative phenotyping experiments with *Kagunavirus* phages regarding sensitivity to altered surface glycans and bacterial immunity systems are presented as efficiency of plating (EOP). Small notes of "ΔRM" or "Δ9CP" indicate on which host strain the respective phage has been characterized (see *Materials and Methods*). Data points and error bars represent average and standard deviation of at least three independent experiments. Raw data and calculations are available in S1 Data.

Properties of other O16-dependent small siphoviruses and *Dhillonvirus*

Besides phages of the genus *Kagunavirus*, we also obtained different other small siphoviruses that depend on restored O16-type O-antigen to infect *E. coli* K-12 and new isolates of the *Dhillonvirus* genus

207 (Fig. 6A-G). Some of the new O16-dependent isolates belong to a cluster of siphoviruses formed primarily
208 by the genus *Skatevirus* (Bas77-81, Fig. 6D). These viruses have genomes of 46-48kb which is well within
209 the typical range for small siphoviruses. Additionally, we present phage KarinMuster (Bas82), belonging
210 to the rarely reported *Nonanavirus* genus comprising relatives of the more commonly known *Salmonella*
211 phage 9NA (Fig. 6E) [65]. The genome of this phage is ca. 58.5kb and thus around 10kb larger than that of
212 the other small siphoviruses presented here, reminiscent of the *Queuovirinae* characterized in our previous
213 work [10]. This latter group encodes a 7-deazaguanosine modification pathway in their additional genome
214 content which provides considerable resistance to RM systems [10, 66]. However, there is no recognizable
215 additional locus in KarinMuster and its relatives that could encode such supplemental biological functions
216 [65], though their distant relationship to other known phages and limited knowledge about their biology
217 make it difficult to draw conclusions about this. Very similar to small siphoviruses characterized previously
218 and the *Kagunavirus* phages shown above, all these phages are markedly sensitive to RM systems and to
219 the Old defense system which in the latter case results in quantifiable decrease of plaque counts only for
220 some phages (Fig. 6G). The additional genome size of KarinMuster therefore does not seem to make this
221 phage more robust than other small siphoviruses when facing bacterial immunity.

222 Finally, the phage isolation using a host without prophages identified additional members of the
223 *Dhillonvirus* genus (Bas83-85) which – unlike their relatives of the original BASEL collection (Bas14-18)
224 – fail to form plaques on regular *E. coli* K-12 (Figs. 6B and 6G). These new isolates do not cluster separately
225 within the *Dhillonvirus* genus but are rather split widely across this group, suggesting that no vertically
226 inherited feature but rather highly variable aspects of phage biology are responsible for this difference (Fig.
227 6F). Phenotypically, the three additional phages selected for this work behave mostly similar to the original
228 *Dhillonvirus* phages, e.g., by showing an only moderate sensitivity to RM systems [10] (Fig. 6G). Like the
229 other siphoviruses characterized for the foriginal BASEL collection, these *Dhillonvirus* phages display the
230 typical arrangement of two separate types of tail fibers with distinct receptor-binding proteins [10, 34] (see

231 below and Fig. S2A). Their central tail fiber has a *bona fide* target recognition module that predicted to

232 encode LptD specificity (Fig. S2B) [10].

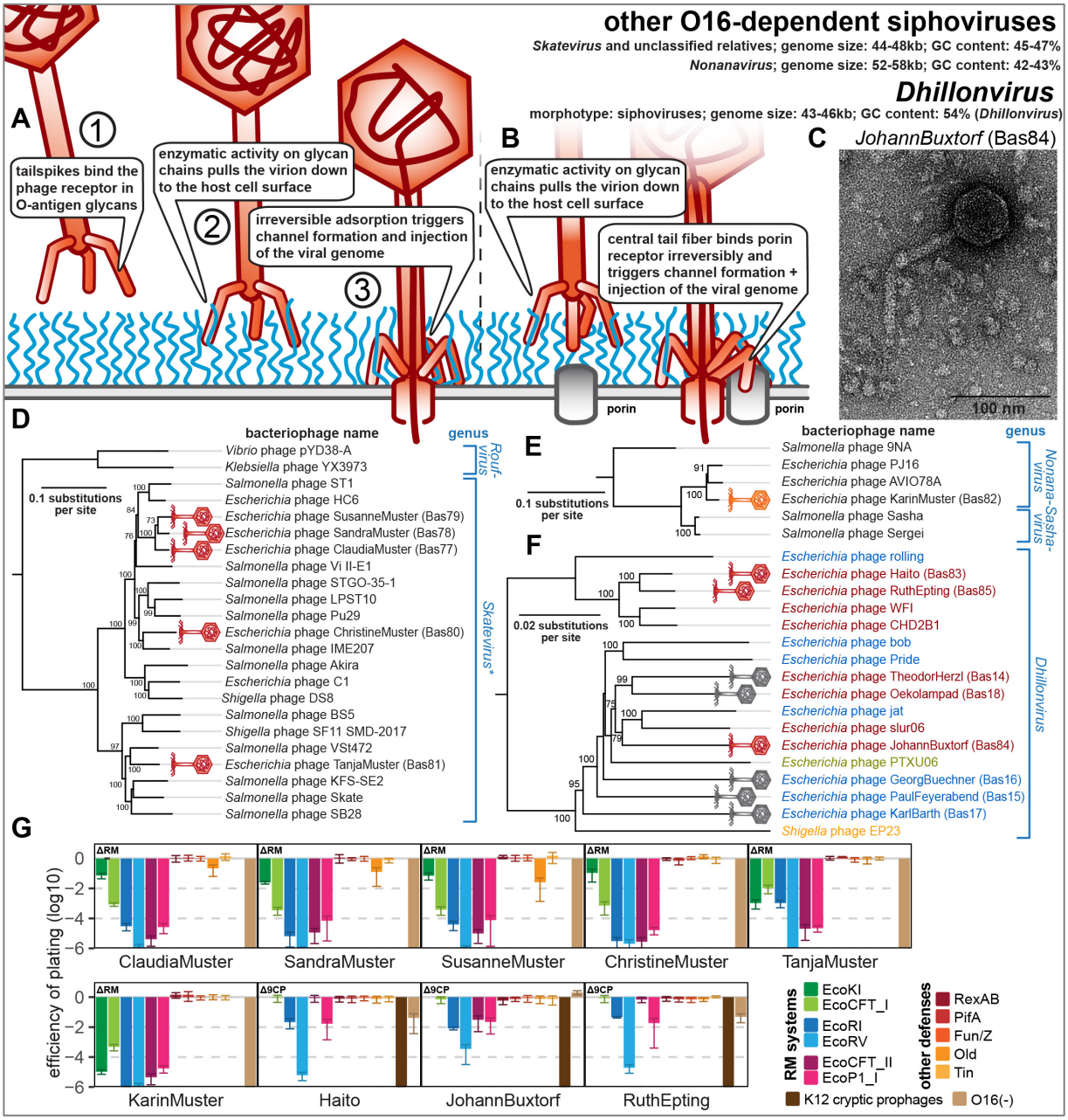

Figure 6. Overview of other O16-dependent siphoviruses of genera *Skatevirus* and *Nonanavirus* as well as new isolates of siphoviral genus *Dhillonvirus*

(A) Schematic illustration of host recognition by O16-dependent small siphoviruses as shown for *Kagunavirus* phages in Fig. 1A. **(B)** Schematic illustration of host recognition by small siphoviruses of the *Dhillonvirus* genus that use first a lateral tail fiber to overcome the O-antigen barrier before binding a porin receptor with the central tail fiber (instead of only glycan-targeting tailspikes for the LPS-dependent small siphoviruses). **(C)** Representative TEM micrograph of *Dhillonvirus* JohannBuxtorf (Bas84). **(D)** Maximum-Likelihood phylogeny of the *Skatevirus* genus and relatives based on a curated

whole-genome alignment with bootstrap support of branches shown if > 70/100. The phylogeny was rooted between genus *Roufvirus* and the others. Note that most reference phages presented here as *Skatevirus* have no formal ICTV classification while others are scattered over several seemingly paraphyletic genera, prompting us to show all phages as *Skatevirus* [58]. **(E)** Maximum-Likelihood phylogeny of the *Nonanavirus* genus and relatives based on a curated whole-genome alignment with bootstrap support of branches shown if > 70/100. The phylogeny was rooted between phage 9NA and the other relatives based on their much closer relationship. Note that *Sasha* and *Sergei* are formally classified as *Sashavirus* while 9NA and AVIO78A are classified as *Nonanavirus* [58] which – according to this phylogeny – would be paraphyletic. **(F)** Maximum-Likelihood phylogeny of the *Dhillonvirus* genus based on a curated whole-genome alignment with bootstrap support of branches shown if > 70/100. The phylogeny was rooted as previously [10] between the group of isolates including phage WFI and the others. In (D-F), newly isolated phages of the BASEL collection are highlighted by red or orange phage icons. The color code of phage names in (F) refers to porin host receptors with blue indicating FhuA, red LptD, green BtuB, and orange LamB [10] (see also Fig. S2B). **(G)** The results of quantitative phenotyping experiments with *Skatevirus*, *Nonanavirus*, and new *Dhillonvirus* isolates regarding sensitivity to altered surface glycans and bacterial immunity systems are presented as efficiency of plating (EOP). Small notes of "ΔRM" or "Δ9CP" indicate on which host strain the respective phage has been characterized (see *Materials and Methods*). Data points and error bars represent average and standard deviation of at least three independent experiments. Raw data and calculations are available in S1 Data.

233 **Properties of podoviruses of *Gordonclarkvirinae* genus *Kuravirus* and relatives**

234 Besides small siphoviruses, our phage isolation with *E. coli* K-12 expressing its O16-type
235 O-antigen resulted in multiple phages belonging to podoviruses in the *Gordonclarkvirinae* subfamily (Fig.
236 7A-D). These phages form characteristic prolate virions of the rare C3 morphology [67] (Fig. 7B) and have
237 been frequently isolated using diverse strains of *E. coli*. However, so far no representatives infecting the
238 *E. coli* K-12 or B model strains have been obtained and the molecular biology of these phages has been
239 only poorly studied. The genome sizes of this group differ widely from 67-69kb for one clade of the
240 *Kuravirus* genus (at the bottom of Fig. 7C) to 76-77kb for other *Kuravirus* phages and genera
241 *Suseptimavirus* as well as *Nieuwekanaalvirus* (see details for all in Table S2). Our phylogeny largely
242 reproduces the previously identified subgroups of *Gordonclarkvirinae* which have in the meantime been
243 recognized as different genera in the ICTV taxonomy [58, 68] (Fig. 7C). Our isolates are widely scattered
244 over the different genera of *Gordonclarkvirinae*, highlighting that no vertically inherited factor plays major
245 roles in the ability of these phages to infect our engineered *E. coli* K-12 (Fig. 7C).

246 All our isolates completely depend on the restored expression of O16-type O-antigen for infection,
247 suggesting that the O-antigen and possibly other surface glycans are the conserved host receptor of these

248 phages (Fig. 7D). This is in line with previous work reporting that spontaneous *E. coli* mutants resistant to
249 *Kuravirus* phage ES17 had always lost O-antigen expression [69]. In one of the few dedicated studies on
250 *Gordonclarkvirinae*, the Plevka group reported the virion structure of *Kuravirus* SU10 which – in the
251 absence of decades-long research available for standard model phages – was critical for the functional
252 understanding and annotation of structural genes in *Kuravirus* genomes [55]. Unlike O-antigen-dependent
253 siphoviruses (see above) and other well-studied podoviruses such as T7 [70, 71], the *Gordonclarkvirinae*
254 have two separate *bona fide* RBPs, identifiable as long tail fibers and short tail fibers, that likely recognize
255 different host receptors. These two sets of tail fibers appear to be used successively analogous to classical
256 T-even myoviruses where the long tail fibers mediate initial host recognition by targeting porins and O-
257 antigen while the short tail fibers subsequently bind conserved motifs in the LPS core as the terminal
258 receptor [10, 37, 55, 72-74]. The functionality of long and short tail fibers of T-even phages is linked in a
259 way that host recognition by long tail fibers is required for the deployment of short tail fibers and,
260 consequently, viral genome injection [10, 73, 74]. Similarly, direct observation of *Kuravirus* SU10 infection
261 using cryogenic electron tomography shows how the lateral tail fibers initially target an exposed receptor –
262 likely O-antigen glycans – before the short tail fibers target the cell surface and contribute to the formation
263 of a nozzle which extends the virion tail for genome delivery [55] (see Fig. 7A).

264 The *Gordonclarkvirinae* are remarkably resistant to RM systems despite the lack of known
265 pathways of covalent genome modification or restriction inhibitors (Fig. 7D). However, they encode a *bona*
266 *fide* dCTP deaminase and a nucleotidyltransferase with their DNA replication genes (Fig. S3), suggesting
267 that these phages might feature a covalent DNA modification – most simply deoxyuracil instead of
268 thymidine like *Bacillus* phage PBS1 – which may protect their genome from restriction [75]. Like most
269 phages with larger genomes (above ca. 60 kb) [10], the *Gordonclarkvirinae* are also sensitive to the Fun/Z
270 defense system, though a detectable decrease in the efficiency of plating was only observed for the
271 *Kuravirus* genus (Fig. 7D).

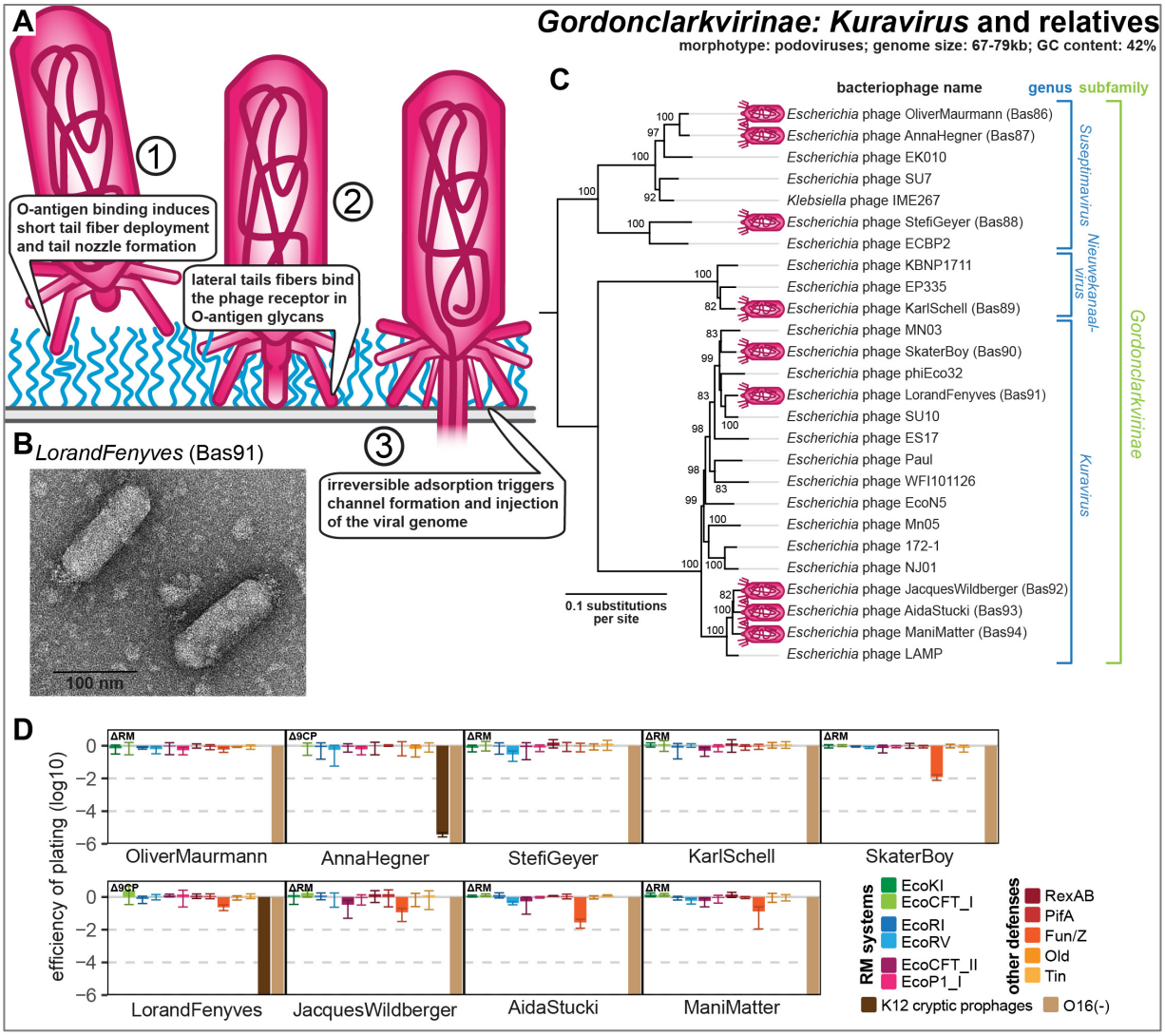

Figure 7. Overview of *Gordonclarkvirinae* phages.

(A) Schematic illustration of host recognition by *Gordonclarkvirinae* phages based on different molecular studies [55, 76]. **(B)** Representative TEM micrograph of phage LorandFenyves (Bas91). **(C)** Maximum-Likelihood phylogeny of the *Gordonclarkvirinae* subfamily based on a curated whole-genome alignment with bootstrap support of branches shown if > 70/100. Phages of the BASEL collection are highlighted by little violet phage icons. The phylogeny was rooted between the genus *Suseptimavirus* and the genera *Nieuwekanaalvirus* + *Kuravirus* based on closer relationship of the latter two. **(D)** The results of quantitative phenotyping experiments with *Gordonclarkvirinae* phages regarding sensitivity to altered surface glycans and bacterial immunity systems are presented as efficiency of plating (EOP). Small notes of "ΔRM" or "Δ9CP" indicate on which host strain the respective phage has been characterized (see *Materials and Methods*). Data points and error bars represent average and standard deviation of at least three independent experiments. Raw data and calculations are available in S1 Data.

274 ## Properties of other groups of podoviruses and myoviruses

275 ### *Xuquatrovirus* relative HelliStehle (Bas95)

276 Besides small siphoviruses and *Gordonclarkvirinae* podoviruses, all other phage groups isolated
277 for this work were individually much rarer and only one or a few isolates of each could be obtained. This
278 includes two podoviruses and one myovirus that are each the only isolates of their respective groups (Figs.
279 8A-G). One of these is a podovirus related to the *Xuquatrovirus* genus for which there are only two closely
280 related representatives, the original PTXU04 of the study by Korf et al. [56] and phage Pondi of Sidi
281 Mabrouk et al. [77] (Fig. 8D). These phages have an intermediate genome size for a podovirus of around
282 60kb which is ca. 20kb larger than *Autographiviridae* (T7 relatives; see below) but ca. 15-20kb smaller
283 than *Gordonclarkvirinae* (see above). Our new isolate HelliStehle (Bas95) is clearly related to the
284 *Xuqutatovirus* phages with a largely colinear genome of similar size (Fig. S4) but is phylogenetically
285 distinct (Fig. 8D). The biology of these phages has largely remained enigmatic besides a genomic and
286 proteomic analysis of PTXU04 when it had originally been described, which was crucial for a functional
287 annotation of at least the structural genes due to low sequence similarity to well-characterized phages [56].
288 Consequently, a recent transcriptome-wide CRISPR interference study determined the essential genes of
289 PTXU04 but could in the absence of additional phenotypic data not use this information for deeper insights
290 as has been possible, e.g., with model phages T4 and T5 [78]. Our experiments show that phage HelliStehle
291 is completely dependent on restored O-antigen expression, suggesting that it is using this glycan as an
292 essential receptor (Fig. 8G) Furthermore, this phage is very sensitive to RM systems, suggesting that –
293 unlike other larger podoviruses like N4 or *Kuravirus* – it lacks potent mechanisms to protect its genomic
294 DNA (Fig. 8G).

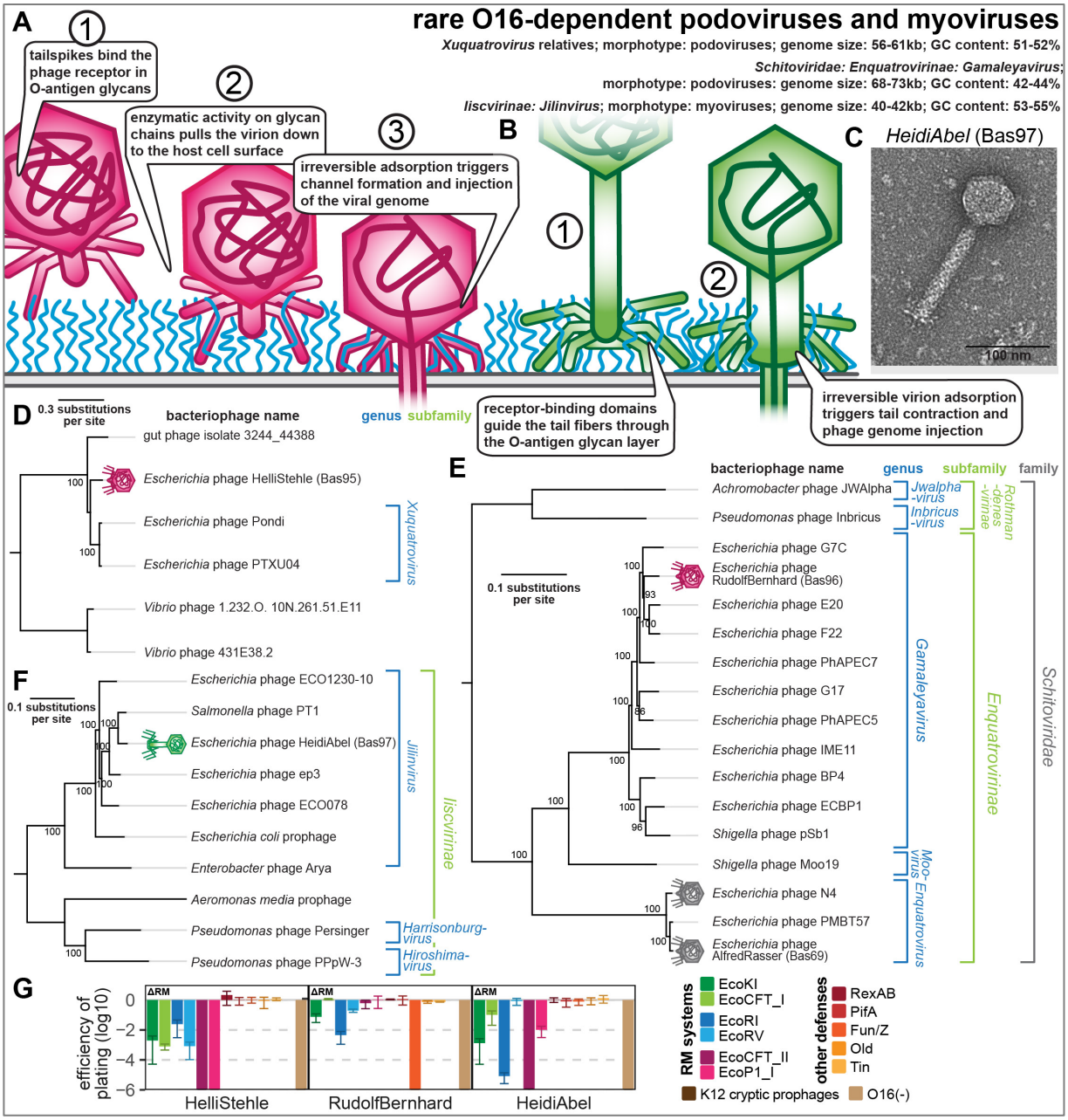

Figure 8. Overview of rare O-antigen-dependent phage groups (*Xuquatrovirus* relatives, *Gamaleyavirus*, *Jilinvirus*).

(A) Schematic illustration of host recognition by podoviruses with enzymatic tailspikes targeting O-antigen (e.g., *Gamaleyavirus*) based on previous work on phage T7 [71, 79]. **(B)** Schematic illustration of host recognition by myoviruses targeting O-antigen with a tail fiber (e.g., *Jilinvirus*). Note that *Jilinvirus* HeidiAbel encodes two sets of tail fibers (see below) whose relationship is unknown, so only a simple schematic with one set is shown. **(C)** Representative TEM micrograph of *Jilinvirus* phage HeidiAbel (Bas97). This phage forms myovirus virions with similar appearance to other Jilinvirus phages and relatives that have been studied previously [80-82]. **(D)** Maximum-Likelihood phylogeny of the genus *Xuquatrovirus* and relatives based on a curated concatenated alignment of major capsid protein, portal protein, and terminase large subunit protein sequences with bootstrap support of branches shown if > 70/100. The phylogeny was rooted between two marine *Vibrio* phages and the others based on a

large phylogenetic distance between these groups. **(E)** Maximum-Likelihood phylogeny of the *Enquatrovirinae* subfamily of *Schitoviridae* and relatives based on a curated whole-genome alignment with bootstrap support of branches shown if > 70/100. The phylogeny was rooted between subfamilies *Rothmandenesvirinae* and subfamily *Enquatrovirinae*. **(F)** Maximum-Likelihood phylogeny of the *Iiscvirinae* subfamily based on a curated whole-genome alignment with bootstrap support of branches shown if > 70/100. The phylogeny was rooted between the genus *Jilinvirus* and the other genera. The exemplary prophages of *E. coli* and *Aeromonas media* were identified in strains USECESBL382 (NCBI GenBank AATBGZ010000031) and T0.1-19 (NCBI GenBank CP038441), respectively, using PHASTEST [83]. In (D-F), phages of the BASEL collection are highlighted by pink (new) or grey (old) phage icons. **(G)** The results of quantitative phenotyping experiments with the three newly describe phage isolates regarding sensitivity to altered surface glycans and bacterial immunity systems are presented as efficiency of plating (EOP). Small notes of "ΔRM" or "Δ9CP" indicate on which host strain the respective phage has been characterized (see *Materials and Methods*). Data points and error bars represent average and standard deviation of at least three independent experiments. Raw data and calculations are available in S1 Data.

295 ***Gamaleyavirus* RudolfBernhard (Bas96)**

296 Podoviruses of the *Gamaleyavirus* genus within the *Enquatrovirinae* subfamily are close relatives
297 of the genus *Enquatrovirus* including N4 and AlfredRasser which we have characterized previously [10].
298 They typically target O-antigen glycans as essential host receptor [33, 84], and our isolate RudolfBernhard
299 (Bas96) is also completely dependent on restored O16 O-antigen expression to infect *E. coli* K-12 (Fig.
300 8G). This isolate is closely related to previously studied phage G7C (targeting O22-type O-antigen; Fig.
301 8E) but encodes different tailspikes that likely mediate O-antigen recognition (see in the dedicated section
302 below) [84]. Consequently, RudolfBernhard does not depend on the NGR glycan unlike N4 and
303 AlfredRasser which target this enigmatic polysaccharide as their essential host receptor (Figs. 8G and S1B)
304 [10, 17]. Like its relatives N4 and AlfredRasser, RudolfBernhard shows considerable resistance to RM
305 systems despite not encoding any known genome protection mechanism, but unlike those phages it does
306 have a detectable sensitivity to some systems (Fig. 8G). It is also sensitive to the Fun/Z defense system
307 which targets most phages with a genome length above ca. 60kb [10]), but the molecular basis of this
308 antiviral defense system has remained unknown.

309 ***Jilinvirus* HeidiAbel (Bas97)**

310 The genus *Jilinvirus* of the *Iiscvirinae* subfamily of myoviruses comprises only a few isolates that
311 have not been well characterized but that all infect enterobacteria (Figs. 8B and 8F). Related genera infect

312 other hosts such as pseudomonads (Fig. 8F). These phages have very small genomes for phages of the
313 myovirus morphotype (41-44 kb) and their lifestyle has remained enigmatic. On one hand, previous work
314 has never observed any temperate behavior of *Jilinvirus* phages or their relatives [80-82, 85], and also our
315 isolate HeidiAbel (Bas97) forms regular clear plaques with no signs of lysogen growth (Fig. S5A). On the
316 other hand, some *Jilinvirus* phages including HeidiAbel feature seemingly intact genes encoding an
317 integrase and a cI-like repressor – indicative of a temperate lifestyle - which are deteriorated or absent in
318 other representatives as noted previously (Fig. S5B and S5C) [82, 85]. In addition, diverse bacterial
319 genomes indeed contain *bona fide* prophages that would be classified in this viral group (see examples in
320 Fig. 8F) [81]. It thus appears that these phages may have a facultatively temperate lifestyle that is lost in
321 different representatives, possibly as an adaptation to mostly lytic growth. We therefore also interpret
322 HeidiAbel as a virulent phage, though it would be interesting to see future work exploring if or when the
323 phage makes use of its seemingly intact lysogeny control module. Notably, there also appear to be temperate
324 members of the well-studied *Autographiviridae* family of virulent podoviruses which may even be their
325 ancestral state [86], suggesting that such a transition between temperate and virulent lifestyles would not
326 be unprecedented.

327 Our data show that HeidiAbel is very sensitive to RM systems except EcoRV for which its genome
328 does not contain a recognition site (Fig. 8G and Table S2). This property is shared with all temperate phages
329 that we have tested in our previous work, but it is also very common among virulent phages with small
330 genomes that encode no dedicated protection mechanisms (see, e.g., the small siphoviruses presented in
331 this study or our previous work [10]). The infectivity of HeidiAbel depends totally on the presence of
332 restored O16-type O-antigen on *E. coli* K-12, suggesting that the viral tail fibers target this glycan as
333 essential host receptor (Fig. 8G)

334 Properties of myoviruses in genus *Wifcevirus*

335 Phages of the genus *Wifcevirus* within *Caudoviricetes* have been described comparably rarely with
336 currently less than 20 sequenced isolates in NCBI GenBank that all infect *Escherichia coli* or *Shigella* (Fig.

337 9A-E). They have genomes of ca. 66-70kb and were described as a genus when two new isolates, WFC and
338 WFH, had been linked to several phages that had been sequenced earlier [56]. Interestingly, distant relatives
339 of these phages in the *Pbunavirus* genus are among the *P. aeruginosa* phages most used for personalized
340 therapy [87, 88]. Based on clear homology, the cryogenic electron microscopy structure of virions of a
341 *Pbunavirus* has greatly helped us to annotate the structural genes of *Wifcevirus* phages [89]. No *Wifcevirus*
342 infecting *E. coli* laboratory models K-12 or B has ever been reported, limiting our knowledge about the
343 biology of these phages and their interaction with the host. However, one previous study on two *Wifcevirus*
344 isolates reported remarkably fast replication with only 3-5 minutes between adsorption and release of
345 progeny [90]. This is much faster than even mutants of phage T7 – another phage considered to be fast –
346 that had been evolved for rapid replication but did not get faster than seven minutes in comparable assays
347 [91]. This property of *Wifcevirus* phages could be of great interest for biotechnology or clinical applications,
348 but the underlying molecular mechanisms have not been explored.

349 Our four isolates (Bas98-101) belong to both major subgroups of *Wifcevirus* phages (Fig. 9B) and
350 all depend totally on restored O16-type O-antigen as host receptor (Fig. 9E), suggesting that their tail fibers
351 target this glycan as host receptor (see also the dedicated section below). This is reminiscent of their
352 *Pbunavirus* relatives which are known to target the LPS of *P. aeruginosa* as host receptor [89, 92, 93]. All
353 of our isolates could only be obtained using *E. coli* K-12 without cryptic prophages as host and their plaque
354 formation is severely impaired in their presence (Fig. 9D), though a quantitative reduction of plaque counts
355 was only observed for *VerenaGrendelmeier* (Bas101; Fig. 9E). All isolates are not sensitive to any tested
356 bacterial defense system including RM systems despite the lack of any known genome protection
357 mechanism (Fig. 9E). One notable exception is the EcoP1_I type III RM system to which they are very
358 sensitive even though they have similar numbers of recognition sites for this system as for the EcoCFT_II
359 machinery to which they are highly resistant (Fig. 9E and Table S2).

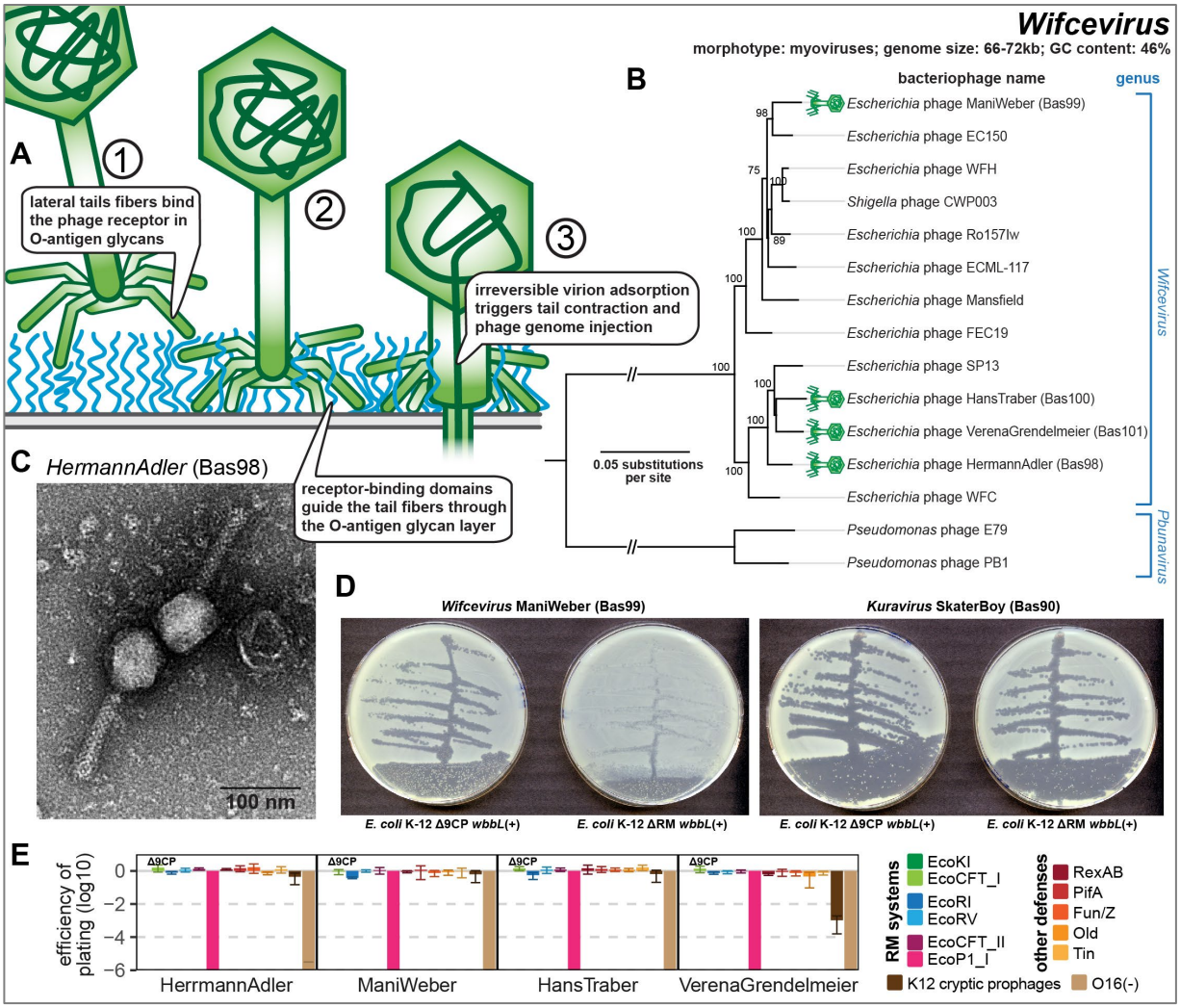

Figure 9. Overview of *Wifcevirus* phages.

(A) Schematic illustration of host recognition by *Wifcevirus* myoviruses targeting host O-antigen (blue) using tail fibers. Note that these phages carry two sets of tail fibers (see below) whose relationship is unclear, so only a simple schematic with one set is shown. **(B)** Maximum-Likelihood phylogeny of the *Wifcevirus* genus and relatives based on a curated whole-genome alignment with bootstrap support of branches shown if > 70/100. The phylogeny was midpoint-rooted between the distantly related *Wifcevirus* and *Pbunavirus* genera. Phages of the BASEL collection are highlighted by little green phage icons. **(C)** Representative TEM micrograph of phage HermannAdler (Bas98) with a virion morphology very similar to other representatives that have been visualized previously [56]. **(D)** *Wifcevirus* isolate ManiWeber (Bas99) was streaked for single plaques on *E. coli* K-12 strains with and without cryptic prophages. *Kuravirus* SkaterBoy (Bas90; see Fig. 7) is shown as a control without sensitivity to the presence of cryptic prophages. **(E)** The results of quantitative phenotyping experiments with *Wifcevirus* phages regarding sensitivity to altered surface glycans and bacterial immunity systems are presented as efficiency of plating (EOP). Small notes of "ΔRM" or "Δ9CP" indicate on which host strain the respective phage has been characterized (see *Materials and Methods*). Data points and error bars represent average and standard deviation of at least three independent experiments. Raw data and calculations are available in S1 Data.

360 **Properties of *Autographiviridae: Studiervirinae* genera *Teseptimavirus* and**
361 ***Kayfunavirus***

362 Podoviruses of *Autographiviridae* subfamily *Studiervirinae* are well-known from classical
363 representatives T3 (*Teetrevirus* genus) and T7 (*Teseptimavirus* genus) and have been frequently isolated
364 against diverse enterobacterial hosts. In our previous work we had characterized T3 and T7 together with
365 several new isolates from different genera of this subfamily [10]. As also suggested by the literature, we
366 found that all these phages depended on the LPS core of *E. coli* K-12 as host receptor when infecting this
367 host though they were invariably unable to infect this host when O-antigen expression was restored [10,
368 94]. These phages exhibited considerable flexibility in their glycan recognition in a way that truncations of
369 the LPS core reduced infectivity but that usually no individual truncation fully abolished it [10, 94]. Given
370 the ubiquity of O-antigen expression among wild *E. coli* strains and its barrier function, it seems likely that
371 these phages have evolved to target these or other surface glycans as host receptor and more accidentally
372 recognize also the LPS core of *E. coli* K-12. Previous work has already well established that diverse
373 representatives of *Autographiviridae* target specific types of O-antigen as host receptor which determines
374 the host range of these phages [29, 33, 95-97].

375 In the current study, we indeed isolated several different *Teseptimavirus* phages that depend on
376 restored O16-type O-antigen expression of *E. coli* K-12 and included three of these in the BASEL collection
377 (Bas102-104; Figs. 10A-D). Furthermore, we isolated ElsieAttenhofer (Bas105), an O16-dependent phage
378 of the distantly related *Kayfunavirus* genus that also contains various representatives known to target host
379 glycans such as phage K1F targeting the K1 capsule [98] or CLB_P1 targeting the O104-type O-antigen of
380 *E. coli* strain 55989 [99] (Fig. 10B). Our four new isolates encode a single tailspike or tail fiber in their
381 genomes analogous to other *Autographiviridae* phages and likely use it to target O16-type O-antigen (see
382 in the dedicated section below). Like their relatives, they have genomes of ca. 40kb size and are sensitive
383 particularly to type II and type III RM systems if they have a considerable number of recognition sites (Fig.
384 10D and Table S2) [10]. Beyond restriction, studies on model phages T3 and T7 as well as our previous

work suggested that *Autographiviridae* phages are specifically targeted by the PifA defense protein dependent on the allelic variant of the *gp1.2* dGTPase inhibitor gene [10, 100, 101]. Of the three new *Teseptimavirus* phages, only MeretOppenheim (Bas102) encodes a similar *gp1.2* allele as sensitive phages T7 and JacobBurckhadt (Bas65), and it is indeed significantly inhibited by PifA (Figs. 10D and S6). However, also the *Kayfunavirus* ElsieAttenhofer (Bas105) is sensitive to PifA (Fig. 10D), but it carries a distinct variant of the *gp1.2* gene (Fig. S6). These results suggest that *Autographiviridae* sensitivity to PifA is more complex than two allelic variants of one locus and / or that additional factors such as the major capsid protein may play a role (as indicated by previous work [101]).

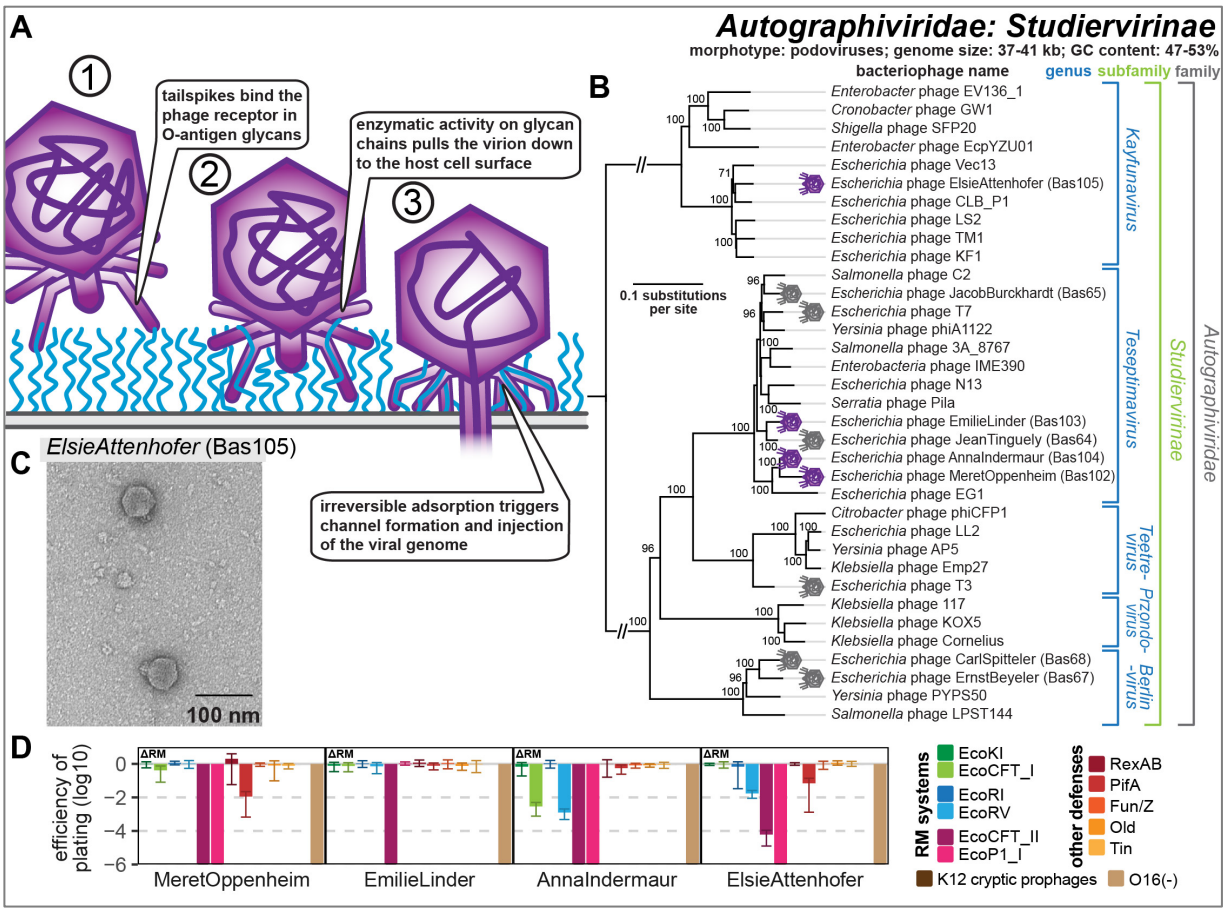

Figure 10. Overview of *Autographiviridae: Studiervirinae* phages.

(A) Schematic illustration of host recognition by podoviruses with enzymatic tailspikes targeting O-antigen (e.g., *Kayfunavirus*) based on previous work on phage T7 [71, 79]. **(B)** Maximum-Likelihood phylogeny of the *Studiervirinae* subfamily of *Autographiviridae* based on a curated whole-genome alignment with bootstrap support of branches shown if > 70/100. The phylogeny was midpoint-rooted between distantly related genus *Kayfunavirus* and the other genera. Phages of the BASEL collection are highlighted by violet (new) or grey (old) phage icons. **(C)** Representative TEM micrograph of

Kayfunavirus ElsieAttenhofer (Bas105). **(D)** The results of quantitative phenotyping experiments with *Autographiviridae* phages regarding sensitivity to altered surface glycans and bacterial immunity systems are presented as efficiency of plating (EOP). Small notes of "ΔRM" or "Δ9CP" indicate on which host strain the respective phage has been characterized (see *Materials and Methods*). Data points and error bars represent average and standard deviation of at least three independent experiments. Raw data and calculations are available in S1 Data.

393 **Tailspikes and tail fibers to overcome the O16-type O-antigen barrier**

394 Since the O-antigen barrier is ubiquitous among enterobacteria, it must be overcome or bypassed
395 by any phage infecting these hosts (Fig. 1). For classical model phages the O-antigen has been seen as a
396 facultative first receptor for initial host recognition followed by the binding to a second, terminal receptor
397 for irreversible adsorption with a distinct receptor-binding protein [29, 34]. As an example, phage T5
398 efficiently infects the *E. coli* K-12 model strain – not expressing any O-antigen – by directly targeting the
399 FhuA porin as terminal receptor with its central tail fiber [63]. While its lateral tail fibers are not required
400 to infect a host without O-antigen, increased expression of the polymannose O8-type O-antigen that they
401 target results in concomitantly faster adsorption of T5 to these hosts [102]. Conversely, increased
402 expression of O8-type O-antigen results in decreasing adsorption of a T5 mutant specifically lacking these
403 lateral tail fibers [102]. Restoration of the O16-type O-antigen of *E. coli* K-12 (which is not bound by the
404 lateral tail fibers of T5) results in complete abrogation of T5 infections (Fig. 1B and our previous work
405 [10]). Similar results have been obtained for other phages of different morphotypes that express two distinct
406 RBPs for successive recognition of O-antigen and a terminal cell surface receptor ([recently reviewed in
407 reference 29]), and the concept also applies to analogous recognition of other initial receptors like capsules
408 [103]. However, previous work had already indicated that some phages – primarily podoviruses like
409 classical models T7 and N4 – can also merely depend on a single receptor such as O-antigen or other glycans
410 for host recognition and irreversible adsorption [17, 29, 31, 70]. Similar to these, the O16-dependent phages
411 characterized in this study typically feature a single RBP to target this glycan, seemingly for both initial
412 host recognition and subsequent irreversible adsorption (Figs. 11 and 12).

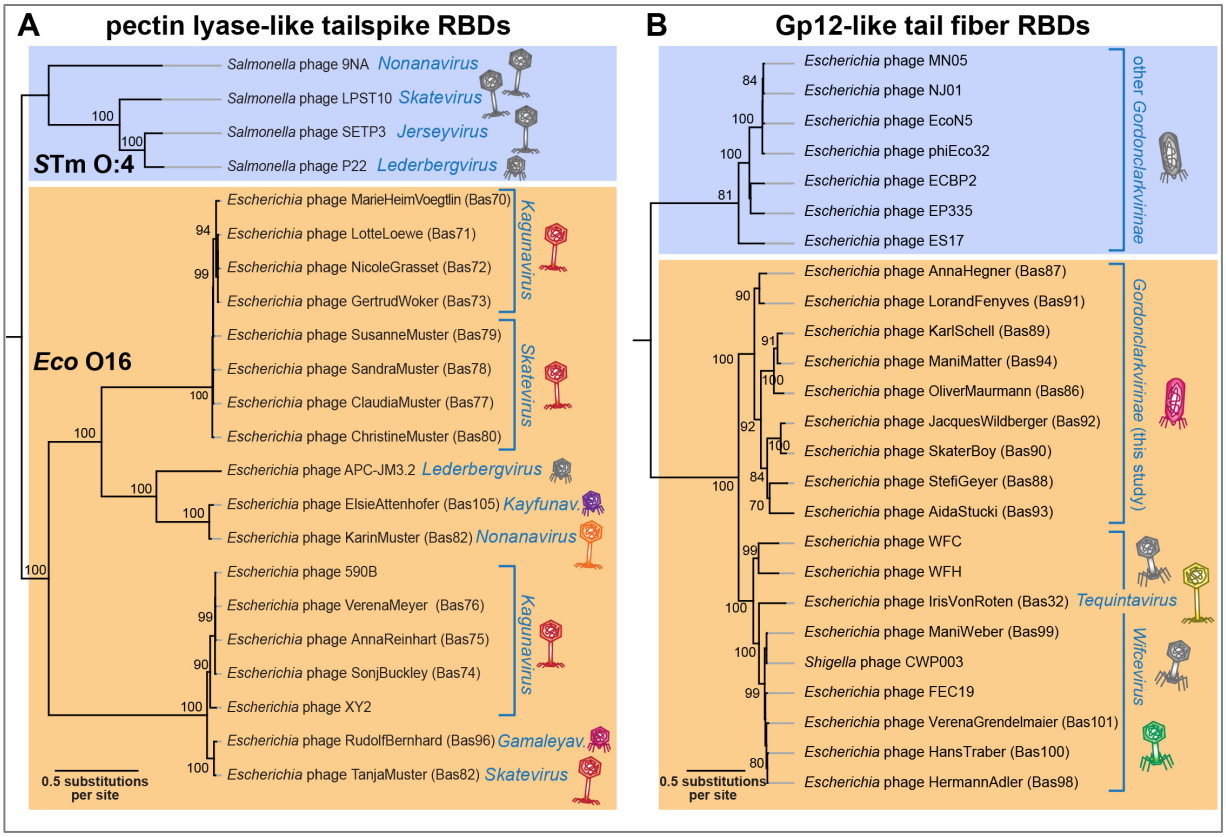

Figure 11. Phylogenetic analyses of tailspikes and tail fibers.

(A) Maximum-Likelihood phylogeny of pectin lyase-like receptor-binding domains (InterPro accession IPR011050 [104]) of tailspikes encoded by our new BASEL phages and relevant controls. The phylogeny was midpoint-rooted between previously characterized tailspikes targeting the O:4 O-antigen of *Salmonella* Typhimurium (blue) and those of our new isolates targeting *E. coli* O16-type O-antigen (orange; including a few additional previously published phages with very similar tailspikes). Bootstrap support of branches is shown if > 70/100. Phages of the BASEL collection are highlighted by colorful phage icons. **(B)** Maximum-Likelihood phylogeny of Gp12-like receptor-binding domains (InterPro accession SSF88874 [104]) of tail fibers encoded by our new BASEL phages and relevant controls. The phylogeny was midpoint-rooted between a clade of distant *Gordonclarkvirinae* tail fibers at the top (blue) and those of *Wifcevirus*, *Tequintavirus*, and the *Gordonclarkvirinae* presented in this study (orange). Note that a clade with *Wifcevirus* receptor-binding domains (bottom) includes diverse phages from the database as well as *Tequintavirus* IrisVonRoten (Bas32 [10]) scattered between the *Wifcevirus* isolates characterized in the current study.

Our new isolates of small siphoviruses in genera *Kagunavirus*, *Skatevirus*, and others encode tailspikes for recognition and enzymatic processing of the O16-type O-antigen that are encoded directly downstream of a J-like central tail fiber protein (Fig. S2). Notably, this is the same locus where the *bona fide* RBPs described in our previous work are encoded [10] as well as the capsule-targeting tailspikes of small siphoviruses targeting *Klebsiella* spp. (Fig. S2) [105]. We therefore conclude that these different RBPs are used analogously for terminal receptor recognition. Interestingly, the tailspikes of these distinct

419 siphoviruses as well as *Kayfunavirus* ElsieAttenhofer (Bas105) and *Gamaleyavirus* RudolfBernhard
420 (Bas96) are all homologous and feature an enzymatic pectin lyase-like receptor-binding domain (InterPro
421 accession IPR011050 [104]) connected to variable anchor domains (Figs. 11A and 12A). A phylogeny
422 including distant relatives known to target the O:4 O-antigen of *Salmonella* Typhimurium shows that the
423 tailspikes of our O16-targeting phages form a distinct, though diverse, group alongside tailspikes from a
424 few phages isolated in previous studies (Fig. 11A) [65]. This close relationship between tailspikes from
425 very different phages targeting O16-type O-antigen highlights the frequent horizontal exchange of loci
426 encoding these RBPs [33, 106].

427 Based on prominent examples of glycan-targeting tailspikes, we had initially expected that phages
428 depending on O-antigen as host receptor would mostly use enzymatic tailspikes to penetrate the glycan
429 barrier [33, 84, 97]. However, many of our O16-dependent phage isolates had tail fibers instead. While
430 these varied in length and the types of receptor-binding domains (RBDs), many contained an RBD
431 homologous to that of Gp12 short tail fibers of T-even phages targeting the *E. coli* LPS core [107] (InterPro
432 accession SSF88874 [104]). These Gp12-like RBDs are located in the distal parts of lateral tail fibers across
433 various phages, including myoviruses of the *Wifcevirus* genus, siphovirus IrisVonRoten (Bas32), and
434 podoviruses of the *Gordonclarkvirinae* subfamily (Fig. 11B). However, such a broad distribution of closely
435 related RBDs is not unexpected given the frequent horizontal transfer of tail fiber components [106].

436 Interestingly, a phylogeny shows that the Gp12-like RBDs of *Wifcevirus* isolates targeting O16-
437 type O-antigen are scattered between homologs from diverse other *Wifcevirus* phages, suggesting that they
438 either mediate very broad host recognition or that these other *Wifcevirus* isolates could also target this
439 specific glycan (Fig. 11B). Conversely Gp12-like RBDs of *Gordonclarkvirinae* targeting O16-type
440 O-antigen are only very distantly related to homologous domains of other phages from this group (Fig.
441 11B). For one of these others, EP335, it had been shown previously that its lateral tail fiber directly binds
442 O157-type O-antigen, suggesting that this may be a conserved feature of these tail fibers with Gp12-like
443 RBDs [76]. Other phages from the expanded BASEL collection encode different types of tail fibers with

444 other RBDs that all likely target this glycan, highlighting the versatility of these non-enzymatic RBPs (see

445 predicted structures in Figs. 12B, 12C, and S7).

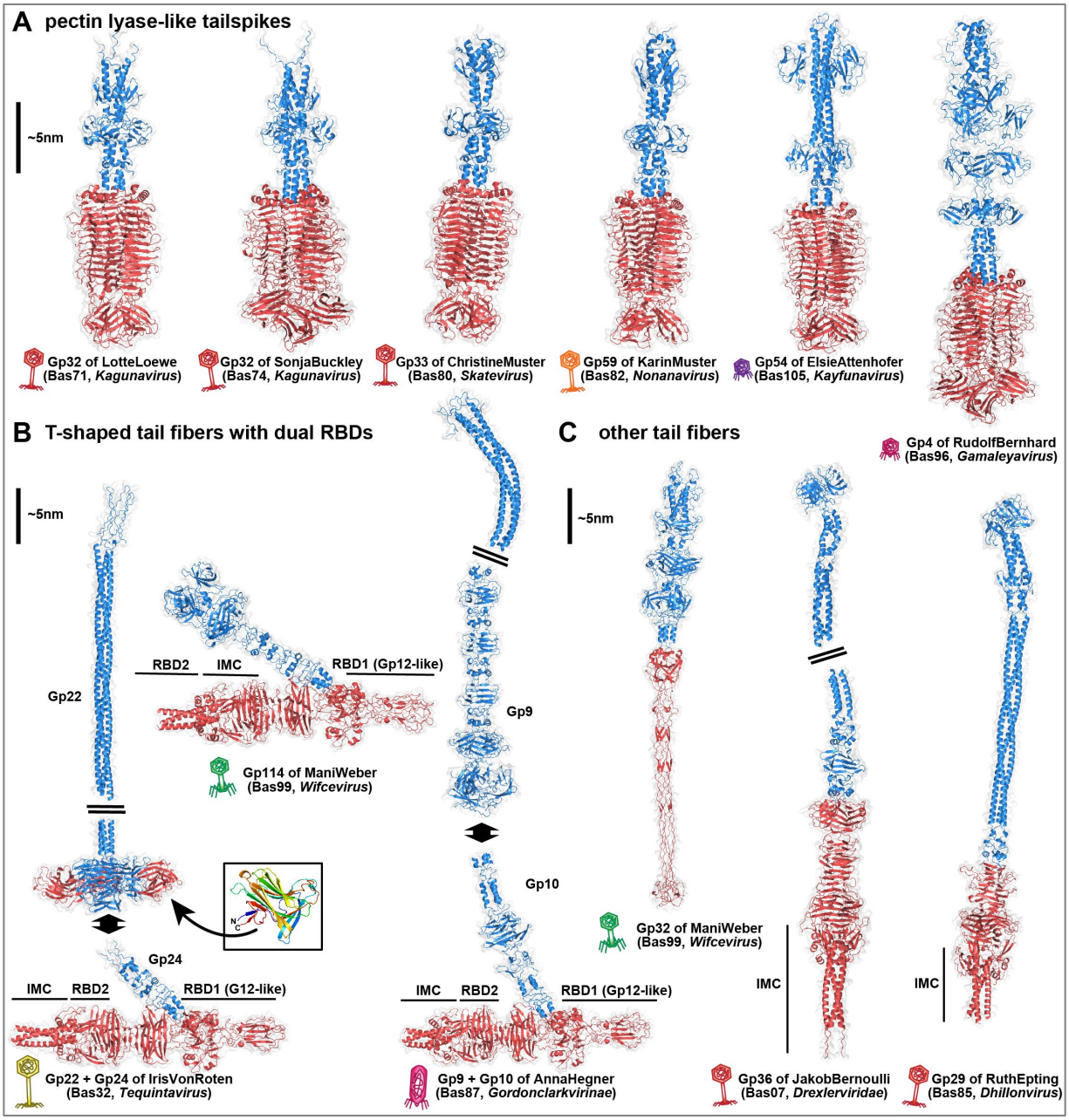

Figure 12. Predicted structures of representative tailspikes and tail fibers.

(A) AlphaFold-Multimer [108] predicted structures of homotrimeric tailspikes from selected BASEL phages (see also Fig. 11A). **(B)** Predicted structures of the representative T-shaped tail fiber complexes of IrisVonRoten (Bas32, *Tequintavirus*), AnnaHegner (Bas87, *Gordonclarkvirinae*), and ManiWeber (Bas99, *Wifcevirus*) which all feature the dual Gp12-like RBD1 and T5-like RBD2 (predicted with the C-terminal intramolecular chaperone domain (IMC) attached; see also Figs. 11B and S10). While ManiWeber features an N-terminal anchor domain for baseplate attachment, the T-shaped tail fibers of IrisVonRoten and AnnaHegner attach to proximal fibers (Gp22 and Gp9, respectively)

which connect the complete fiber structure to the distal baseplate complex. The proximal fiber protein Gp22 of IrisVonRoten contains an additional galectin-like domain (inset box; colored N- (blue) to C- (red) terminus) that protrudes from the C-terminus of the fiber and could contribute to host receptor interaction as an additional RBD. While the overall setup of the T-shaped tail fibers is highly conserved, the RBDs are highly variable and seem to be frequently transferred horizontally (Figs. 11B, S9C, and S10D). **(C)** Predicted structures of other tail fibers with single RBDs (more shown in Fig. S7). The second tail fiber of ManiWeber closely resembles the distal tip of the T4 tail fiber including conserved HxH motifs for ion coordination [109]. Tail fibers of JakobBernoulli (Bas07, *Drexlerviridae*; Gp36) and RuthEpting (Bas85, *Dhillonvirus*; Gp29) both contain elongated N-terminal coiled coils connected to receptor-binding T5-like fiber tips with C-terminal IMC domains. In (A)-(C), N-terminal anchor domains and fiber shafts are colored blue while the RBDs are colored red. A ~5 nm vertical scale bar is provided for reference. In all panels, viral morphotypes are annotated by phage icons analogous to Figs. 11A and 11B.

446 **Phages with several receptor-binding proteins or dual receptor-binding domains**

447 Notably, some of our new isolates that depend on O16-tpe O-antigen of *E. coli* K-12 encode two
448 and not only one *bona fide* RBP. Of these, *Jilinvirus* HeidiAbel encodes separate long and short tail fibers
449 that are likely used successively during host recognition analogous to the long and short tail fibers of much
450 larger T-even myoviruses [10, 73, 74] (Fig. S7). A very different situation is apparent for *Gamaleyavirus*
451 RudolfBernhard (Bas96) which encodes two tailspikes of which one carries a pectin lyase-like domain
452 closely related to others from our collection (Figs. 11A and 12A) and the other one seems unrelated. Such
453 a setup of two tailspikes is common for *Gamaleyavirus* phages and other *Schitoviridae* (see also Fig. S8)
454 [33, 84]. It seems likely that the two tailspikes are used for alternative target recognition similar to
455 *Autographiviridae* phage SP6 which carries two separate tailspikes that it can use to target different types
456 of O-antigen to infect different strains of *Salmonella* [97].

457 While the presentation of two independent RBPs is thus not uncommon for podoviruses, the
458 *Gordonclarkvirinae* are the only phages of this morphotype in the BASEL collection that encode separate
459 long and short tail fibers which are likely used successively and not alternatively [55]. The short tail fibers
460 of these phages are highly conserved and appear to be vertically inherited, indicating a conserved and
461 possibly mechanical role during infection (Fig. S9A) [55]. Similarly, the *Wifcevirus* phages also feature
462 two different tail fibers of which one – predicted to have an elongated RBD tip similar to the T4 Gp37 long
463 tail fiber [37] (Fig. 12C) – is highly conserved across this genus (Fig. S9B), suggesting a conserved or

464 mechanical role during host recognition. Conversely, both the *Gordonclarkvirinae* and *Wifcevirus* phages
465 feature a second tail fiber with a predicted distinctive T-shaped structure presenting dual RBDs, the Gp12-
466 like RBD1 (see above) and a second, T5-like RBD2 that could not be identified from primary sequence
467 alone (Figs. 12B and S10A-C). Both the Gp12-like RBD1 and the T5-like RBD2 differ widely between
468 homologs of the T-shaped tail fibers (Fig. S9C) and have a phylogenetic distribution that is scattered across
469 viral groups and morphotypes (Figs. S10D and 11B). These observations are in line with the recognition of
470 highly variable host receptors like O-antigen, suggesting that these T-shaped tail fibers may generally
471 targeted these (and possibly other) glycans.

472 This remarkable T-shaped tail fiber structure is predicted to have a very similar arrangement in
473 *Gordonclarkvirinae* (exemplified by Gp10 of AnnaHegner, Bas87), *Wifcevirus* (exemplified by Gp114 of
474 ManiWeber, Bas99) and also the lateral tail fibers of *Tequintavirus* IrisVonRoten (Gp24, Bas32; see all in
475 Fig. 12B). Using Gp24 of IrisvonRoten as a representative, the DALI server identified structural similarities
476 and shared structural elements between the Gp12-like RBD1 with X-ray crystal structures of the distal knob
477 domain (D10) of the T4 long tail fiber Gp37 [109] (Z-score 8.8, RMSD 3.2, 100 residues) and – as expected
478 from primary sequence – with the Gp12 short tail fiber distal tip [109] (Z-score 6.2, RMSD 4.1, 127
479 residues; Fig. S10A-C). Likewise, the T5-like RBD2 of Gp24 of IrisVonRoten also shares structural
480 similarity with the distal binding tip and intramolecular chaperone (IMC) domain of the phage T5 lateral
481 tail fiber [110](Z-score 6.3, RMSD 4.8, 179 residues; see Fig. S10A-C). Finally, while the T-shaped RBPs
482 of IrisVonRoten (Gp24) and AnnaHegner (Gp10) connect to a long proximal fiber (Gp23 and Gp9,
483 respectively), the T-shaped RBP of ManiWeber (Gp114) instead features a prominent attachment domain
484 at its N-terminus that likely facilitates direct baseplate attachment (Fig. 12B). This diversity highlights the
485 modular versatility of bacteriophage RBPs for host recognition and the initiation of viral infections.

486 Host range across pathogenic *E. coli* and *Salmonella* Typhimurium

487 The host range of bacteriophages is a crucial property both with regard to their ecology and for
488 applications in clinics and biotechnology [111-113]. It can be defined in different ways, but researchers

489 generally distinguish a phage's lytic host range – estimated by the ability to lyse a host strain in a spot test
490 – and its plating host range, i.e., the ability to form plaques [111, 112]. While plaque formation requires the
491 phage to bind the host cell and to overcome or bypass all layers of bacterial immunity at least partially, the
492 lytic host range is primarily informative about viral host recognition due to "lysis from without" at high
493 phage-to-host ratios even in the absence of viral replication [114]. In our previous work we had tested the
494 host range of BASEL phages and classical model phages against commonly used model strains of *E. coli*
495 and *S.* Typhimurium [10]. For the current study we had anticipated that the diverse O-antigen variants of
496 these strains would largely exclude the mostly O16-dependent phages presented here. This would make it
497 impossible to estimate their interaction with bacterial immunity. We therefore included three additional
498 *E. coli* strains encoding O16-type O-antigen that belong to sequence types (ST)-131, -144, and -8281 (see
499 section *Bacterial strains and strain construction* in *Materials and Methods*).

500 Our experiments to determine the lysis host range indeed revealed that most O16-dependent phages
501 lysed all or some of the O16-expressing strains but barely any of the strains with rough LPS or another type
502 of O-antigen (Fig. 13A). This is in line with the expected dominant role of O-antigen for the host recognition
503 of these phages, especially since most of them do not encode additional receptor-binding proteins besides
504 the O16-targeting tailspikes or tail fibers (Figs. 11 + 12) [29-31, 35]. However, there were stark differences
505 between the different groups of phages that we tested. All small siphoviruses (genera *Kagunavirus*,
506 *Skatevirus*, and relatives; Bas70-82) and many podoviruses (Bas95/96 Bas102-105) had a very narrow host
507 range beyond strains encoding O16-type O-antigen and lysed almost none of the strains without it
508 (Fig. 13A). These phages have either an O16-targeting enzymatic tailspike or simple tail fibers (Figs. 11,
509 12, and S7), suggesting that their ability to target additional host receptors is limited. Conversely, isolates
510 of *Gordonclarkvirinae* and *Wifcevirus* groups showed a very broad host recognition and could in some
511 cases even lyse strains with rough LPS (Fig. 13A). This indicates that the T-shaped tail fibers of these
512 phages are more versatile and might be able to bind different glycan structures with their two RBDs (Figs.
513 11, 12, S7, S9B-C, and S10). Previous work had indeed already observed a comparably broad recognition

514 of some isolates of large myoviruses (e.g., *Tevenvirinae*, *Vequintavirinae* and relatives, etc.) or large

515 siphoviruses (e.g., *Markadamsvirinae*) that commonly carry complex long tail fibers [10, 35, 57, 115, 116].

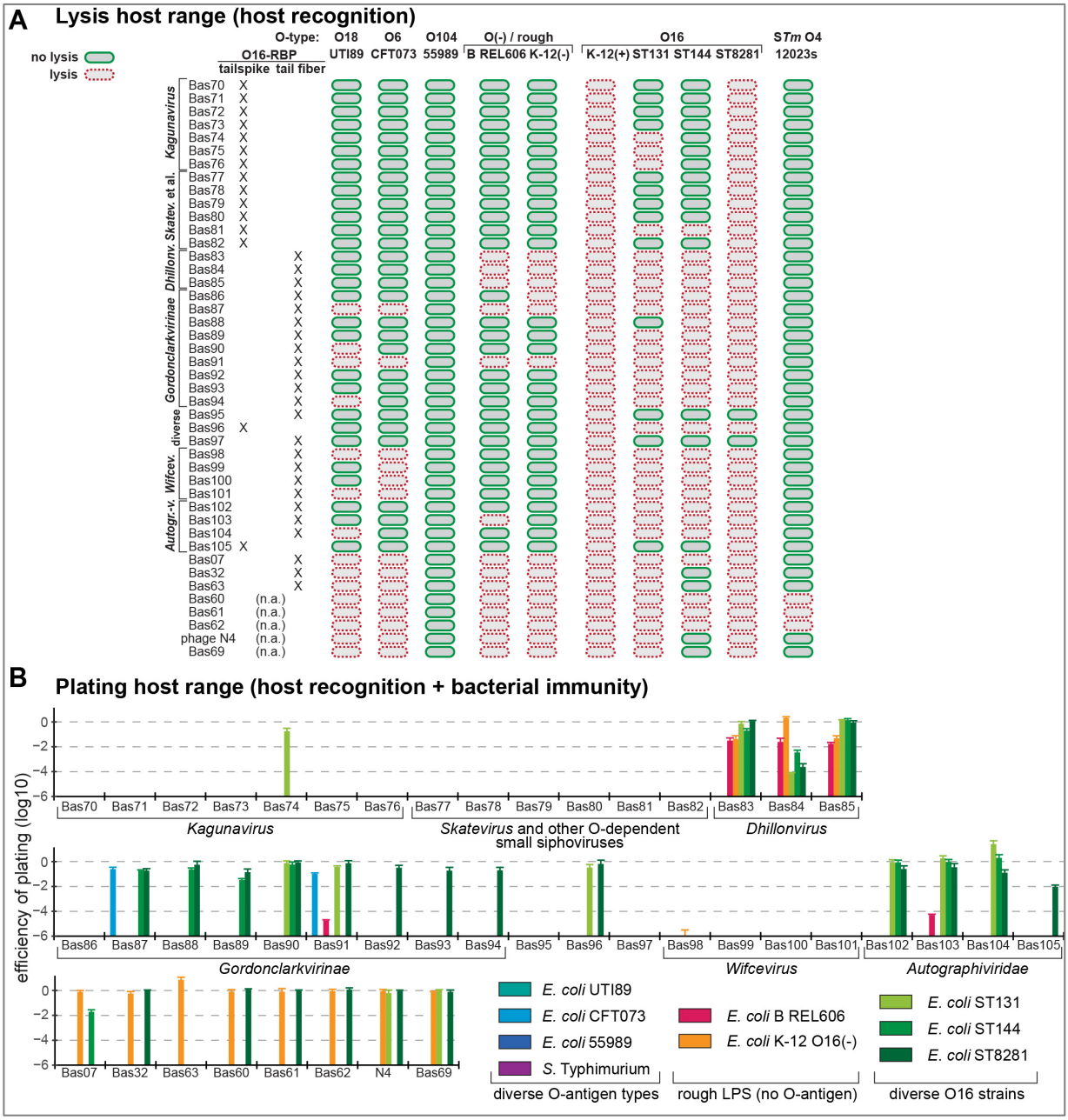

Figure 13. Host range of new phage isolates in the BASEL collection.

(A) Lysis host range of all new BASEL phages and controls (same as in Fig. S1B) as determined by qualitative spot test assays with high-titer phage stocks (>10^9 pfu/ml if possible; see *Materials and Methods*). The O-antigen type of different *E. coli* and *Salmonella* Typhimurium strains and possibly rough LPS (as O(-)) are highlighted at the top while phages with O16-targeting tail spikes or tail fibers are distinguished on the left side. Lysis of a host strain is shown by a red cell lysis icon while the inability to lyse a strain is shown as a green icon in the shape of a cell with full integrity. **(B)** Plating host range of all new BASEL phages and controls (like in (A)) as determined by quantitative efficiency-of-plating

(EOP) assays using serial dilutions of phage stocks. Data points and error bars represent average and standard deviation of at least three independent experiments. Raw data and calculations are available in S1 Data. In (A) and (B), K-12 strains have been selected differently for phages inhibited by its cryptic prophages (Δ9CP) and for those who are not (ΔRM).

516 Our data do not show unambiguously which of the two RBDs of the T-shaped tail fibers – or both
517 – may be critical for O-antigen recognition and bacterial infection in our experiments. However, the
518 phylogeny of the T5-like RBD2 does not correlate with any host recognition data (compare Figs. S10D and
519 13A). Conversely, the phylogeny of the Gp12-like RBD1 shows different clusters for *Gordonclarkvirinae*
520 with broadest host recognition (Bas97 and Bas91) and others for those with narrower host range
521 (Bas86/89/94 and Bas88/89/82/83; compare Figs. 11B and 13A). This may suggest a bigger role for the
522 Gp12-like RBD in host recognition of *Gordonclarkvirinae* across our set of host strains.

523 The siphoviruses with O16-targeting lateral tail fibers and additional central fibers to bind a porin
524 as terminal receptor – new *Dhillonvirus* isolates Bas83-85 as well as Bas07 (JakobBernoulli) and Bas32
525 (IrisVonRoten) – lysed all rough strains but differed in their ability to infect others (Fig. 13A). This confirms
526 the barrier function of mismatched O-antigen types for these phages and the expected facultative nature of
527 O-antigen binding when the terminal receptor on the cell surface is accessible [10, 28]. As shown already
528 previously [10, 12, 17], phages that can bypass O-antigen by targeting the NGR glycan (Bas60-62 and N4
529 as well as Bas69) have a very broad host recognition with the *Justusliebigvirus* phages Bas60-62 featuring
530 the largest lysis host range which even includes *Salmonella* Typhimurium (Fig. 13A). This is likely due to
531 the array of different tailspikes and tail fibers expressed by these phages which enables them to overcome
532 diverse glycan barriers [117]. Conversely, we also observed that many apparently O16-dependent phages
533 failed to lyse one or more of the strains with this O-antigen type that we tested, especially when the phages
534 use enzymatic tailspikes for host recognition (Fig. 13A). Since these phages do not encode any other
535 receptor-binding proteins, we find it unlikely that bacterial variation in other potential receptors such as the
536 LPS core may be responsible for this behavior. Instead, it seems likely to us that strain-specific chemical
537 modifications of the O-antigen chains – which are abundant and highly variable between strains ([recently

538 reviewed in reference 36]) – could prevent the binding of some highly specific tailspikes to some variants
539 of O16-type O-antigen.

540 The plating host range of all phages was usually much narrower than their lysis host range (Figs.
541 13A and 13B), which shows the impact of bacterial immunity in the diverse strains that we used. This effect
542 was particularly strong for all phages with considerable sensitivity to RM systems such as small
543 siphoviruses Bas70-82 (Fig. 13B; compare Figs. 5D and 6G). Conversely, phages with pronounced
544 resistance to RM systems of the *Gordonclarkvirinae* (Bas86-93) and *Gamaleyavirus* (Bas96) groups could
545 form plaques on many of the strains that they can lyse, indicating that this abundant and broadly targeting
546 form of defense systems has a major impact on phage host range (Fig. 13B; compare Figs. 7D and 8G) [40,
547 45, 46]. This is in line with previous work showing a broad plating host range for individual isolates of
548 *Gordonclarkvirinae* [76, 112, 118] and a narrower one for individual *Wifcevirus* phages or small
549 siphoviruses like *Kagunavirus* isolates [35, 57]. Intriguingly, *Autographiviridae* phages (Bas102-105) and
550 in particular the new *Dhillonvirus* isolates (Bas83-85) formed plaques on nearly all strains that they could
551 lyse despite their only moderate resistance to RM systems (Figs. 13A and 13B; compare Figs. 6G and 10D).
552 It would be interesting to study the underlying molecular mechanisms that apparently enable these phages
553 to overcome the native RM systems of these strains while the *Wifcevirus* phages – displaying considerable
554 resistance to restriction in the K-12 host (Fig. 9E) – fail to form plaques on any of the many strains which
555 they can lyse (Figs. 13A and 13B).

556 # Discussion

557 ## Phages depending on O-antigen glycans are diverse and abundant in nature

558 While it is curious that we find O16-targeting phages to be much more abundant in environmental
559 samples compared to sewage treatment plant inflow (Table S1), previous work has also observed such
560 differences in other contexts. As an example, phages targeting the conjugative pili of different
561 enterobacterial plasmids were much more common in wastewater compared to river water [119]. While the

562 underlying ecological phenomena remain elusive, it seems certain that wastewater does not merely contain
563 a large abundance of *E. coli* phages compared to most environmental samples but also has its own biases.
564 One interesting observation for many O16-dependent phages characterized in this work is that they
565 seem to use these glycans as terminal host receptors while their genomes lack any recognizable strategy to
566 inactivate this receptor during infections. Conversely, virulent phages targeting porins characteristically
567 encode proteins such as Cor of T1 or Llp of T5 that disable their porin receptors to prevent adsorption of
568 viral offspring to the debris of the lysed virocell [120, 121]. Similar mechanisms are also common among
569 temperate phages including those targeting O-antigen glycans which they can chemically modify, e.g., by
570 glycosylation or acetylation ([recently reviewed in reference 36]), for "superinfection exclusion" of related
571 viruses [14, 122]. These examples show that such exclusion mechanisms would in principle also be possible
572 for virulent phages, but it seems likely that the abundance of O-antigen molecules on the cell surface (e.g.,
573 compared to porins) makes a complete modification during lytic infections futile. Instead, recent work
574 suggested an alternative strategy of phages that transiently block their offspring's host recognition by
575 "caps" made of chaperones on receptor-binding proteins instead of disabling the host receptors [123]. We
576 expect that this strategy and similar concepts may be more widespread among glycan-targeting phages, and
577 we look forward to future research uncovering their molecular mechanisms and evolutionary context.
578 Traditionally, siphoviruses infecting *E. coli* were considered to exclusively target porins as terminal
579 host receptors like well-studied model phages T1 or T5 [59, 60]. However, more recent studies had already
580 described siphoviruses infecting *E. coli* or other enterobacteria that target flagella, conjugative pili, or
581 surface glycans as host receptor [33, 96, 124, 125]. Using *E. coli* K-12 with restored O16-type O-antigen
582 expression as host, we indeed isolated diverse small siphoviruses from genera *Kagunavirus*, *Skatevirus*,
583 and others which use this surface glycan as essential host receptor. It seems likely that the abundance and
584 diversity of these groups had previously been overlooked due to the traditional focus on *E. coli* laboratory
585 strains with rough LPS as host receptor (see Fig. 1A). Our results strongly suggest that O-antigen is the
586 only and terminal host receptor of these isolates because they only carry a single receptor-binding protein

587 – in all cases enzymatic tailspikes (Figs. 11A and 12A) – which is encoded directly next to the J-like central
588 tail fiber hub (Fig. S2A). This is the same locus where other small siphoviruses infecting *E. coli* encode
589 *bona fide* receptor-binding proteins as well as superinfection exclusion factors targeting different porins
590 (Fig. S2B [10, 120]), and host recognition by these central tail fibers is known to trigger irreversible
591 adsorption and genome injection [63, 64]. We look forward to future studies characterizing the mechanistic
592 link of O-antigen recognition and genome injection in more detail. One specific aspect deserving further
593 investigation is the way how these processes are linked on the molecular level compared to phages with
594 two distinct tail fibers carrying receptor-binding domains. Electron microscopy of small siphoviruses
595 depending on O-antigen clearly shows three distal tail appendages that are likely the tailspikes presented
596 on the J-like fibers (see Fig. 5B). Conversely, siphoviruses targeting porins generally have only one central
597 tail fiber targeting this terminal receptor besides three lateral tail fibers targeting O-antigen or other initial
598 receptors [126]. This indicates that the single RBPs of siphoviruses targeting only O-antigen may be
599 presented on the virion like lateral tail fibers while being functionally equivalent to central tail fibers for
600 irreversible adsorption and triggering DNA genome ejection.

601 Our study highlighted once more that – besides a few models like P22, G7C, and T4 [37, 72, 84,
602 127] – we lack a molecular understanding how many phages use their diverse tail fibers and tailspikes to
603 recognize host receptors and initiate infections. While we had initially expected to isolate many phages
604 with tailspikes targeting O16-type O-antigen that would move the virion to the cell surface by enzymatic
605 activity, many instead carried tail fibers lacking enzymatic properties (Figs. 12B-C and S7). Beyond a mere
606 binding to their LPS receptor (which has been well studied for several examples [37, 70, 110]), we speculate
607 that successive transient interactions of tail fibers with O-antigen receptors may enable the fibers to "glide"
608 through this barrier towards the cell surface (see Figs. 7A and 9A). Of particular interest are the novel
609 T-shaped tail fibers with separate Gp12-like and T5-like RBDs (Figs. 12B and S10) that – to the best of our
610 knowledge – are the first example of a tail fiber protein with two distinct RBDs in the same polypeptide.

611 Conversely, branched structures combining distinct RBPs have been well described [128] and the long tail
612 fiber tip Gp37 of phage T4 features different patches in the same RBD to target distinct receptors [37].

613 **Phage host range, glycan receptors, and bacterial immunity**

614 Understanding the molecular mechanisms underlying the host range of different bacteriophages is
615 important not only for ecological insights but also to enable effective applications in clinics [35, 52-54,
616 113]. While diverse aspects of phage-host interactions like bacterial metabolism and antiviral immunity all
617 influence phage host range, the access to and recognition of viral host receptors generally play major roles
618 [129]. As expected from previous work [10, 28, 30, 35], we observed a dominant role of the O-antigen
619 barrier for phage host range in a way that O-antigen types mismatched to the phages' receptor-binding
620 proteins abolished host recognition while phages with no other host receptor also fully depended on its
621 presence. Interestingly, our data show that phages with tail fibers tend to have a broader host recognition
622 than phages with tailspikes among the tested viruses (Fig. 13A). Understanding these differences on the
623 molecular level by studying distinct functionalities of these different types of RBPs would not only expand
624 our knowledge of phage-host interactions but could also help applications in clinics and biotechnology,
625 e.g., by phage host range engineering [130]. The complete BASEL collection with diverse phages that target
626 the same receptor – O16-type O-antigen – could be a useful tool to investigate these interactions.

627 The dual role of O-antigen as a barrier and as a host receptor is reminiscent, e.g., of the well-studied
628 capsules of *Klebsiella* spp. which form a robust barrier to phage infection but also serve as a dominant
629 factor for phage host range by specific recognition of capsule types by certain variants of RBPs [105, 131,
630 132]. The specificity and dominance of these interactions even enable their use for quite reliable phage host
631 range predictions across *Klebsiella* strains [133]. Conversely, for other hosts like *P. aeruginosa* the
632 availability of long retractable type IV pili reduces the importance of glycans as host receptors, and for
633 many Gram-positives like *Staphylococcus aureus* at least the host recognition is usually broader due to a
634 lower inter-strain diversity of bacterial surface structures [14, 134-136].

635 For *E. coli*, the picture is certainly more nuanced because, e.g., most of the O16-targeting phages
636 that can lyse our different tested strains with this O-antigen type fail to form plaques on them (compare
637 Figs. 13A and 13B). While this shows a clear influence of bacterial immunity, a recent study that
638 experimentally tested the host range of many *E. coli* phages across many strains did not observe a simple
639 correlation between phage host range and the number of predicted antiviral defense systems [35], unlike
640 what had been observed for *Pseudomonas aeruginosa* and *Vibrio* spp. [16, 137, 138]. Our results primarily
641 suggest a link between the ability to form plaques on diverse strains and viral resistance to RM systems as
642 the most common and most broadly targeting form of bacterial immunity (see above) [45, 46, 139].
643 However, the relative importance of different antiviral defense systems for observed phage host range
644 would certainly be a promising field for future study beyond mere predictions, e.g., by contrasting the phage
645 susceptibility of wildtype hosts with mutants specifically lacking one or more defense systems. Our results
646 indicate that – after removal of restriction systems in our previous work [10] – the *E. coli* K-12 genomic
647 background does not encode any antiviral defenses that play a major role for phage host range. Even when
648 all predictable defense systems are absent in the Δ9CP strain lacking all cryptic prophages (Fig. 4D; see
649 *Bacterial strains* in *Materials and Methods*), the only new group of phages that could be isolated were
650 myoviruses of the *Wifcevirus* genus and scattered isolates of few additional taxa.

651 **Expanding the BASEL collection to cover all major groups of *E. coli* phages**

652 The value of the BASEL collection as a tool for molecular biology research lies in its assorted
653 diversity across and within phage groups and on their ability to infect the model organism *E. coli* K-12 [6].
654 In this study we therefore aimed at enhancing the assorted diversity to cover all known major groups of *E.*
655 *coli* phages without a major compromise on *E. coli* K-12 as host strain (Fig. 14). However, it seemed likely
656 that the limitations of previous studies had been caused by the use of this strain background through its
657 domestication (by loss of O-antigen [27]) and its specific arsenal of bacterial immunity (see *Bacterial*
658 *strains* in *Materials and Methods*). After addressing both aspects genetically, we indeed readily isolated
659 representatives of nearly any group of *E. coli* phages that had been reported to target O-antigen as essential

660 host receptor including, e.g., diverse groups of small siphoviruses like the *Kagunavirus* genus and
661 podoviruses of *Gordonclarkvirinae* or genus *Kayfunavirus* [29, 33]. Additional isolates of *Dhillonvirus* and
662 *Gordonclarkvirinae* as well as any *Wifcevirus* could only be obtained using a host that lacks the nine cryptic
663 prophages, indicative of their inhibition by resident bacterial immunity of *E. coli* K-12. Since phages from
664 most of these diverse groups had never been isolated with any *E. coli* lab strain, there were only scarce – if
665 any – previous studies on their molecular biology. This limitation restricted our analysis of the genomic
666 and phenotypic data for some of them largely to data from the current study, while in our previous work on
667 more well-studied groups of phages we could draw heavily from the generations of previous research in the
668 field [10]. To improve the genome annotation of our new phage isolates, we therefore created a new tool –
669 GAPS (Gene Annotation Pipeline based on sequence and structure Similarity; see *Materials and Methods*)
670 to infer functional information from remote homologies and structure predictions.

671 We anticipate that the completed BASEL collection will support various applications from
672 fundamental research on viral ecology and evolution over the work on new antiviral defense systems to
673 studies on phage therapy. With an expanded biological diversity in still manageable numbers, these phages
674 can all be grown on a regular *E. coli* K-12 host by choosing the Δ9CP variant transformed with our plasmid
675 pAS001 that partially restores O16-type O-antigen expression (see *Materials and Methods*). Given the
676 increasing interest in phage therapy but also its notable incidence of treatment failure [88, 140, 141], it is
677 clear that not only fundamental research but also clinical applications could profit from a better
678 understanding of links between phage genomes and taxonomy on one side and relevant biology /
679 phenotypes + clinical properties on the other side [35, 52-54]. This is becoming increasingly evident as
680 more and more engineered phages for therapeutic applications are developed [142]. For these applications,
681 phages are mostly used as a vehicle to deliver proteins from non-viral origin such as CRISPR-Cas nucleases
682 or antibacterial toxins [61, 142-145]. This limitation highlights our lack of knowledge about the diverse
683 molecular biology of phage-host interactions beyond a few traditional models. Unraveling the molecular
684 mechanisms underlying new aspects of phage-host interactions – e.g., with tools like the BASEL collection

or modern biochemistry and structural biology – could thus open up the untapped potential of engineered phages for applications in clinics or biotechnology.

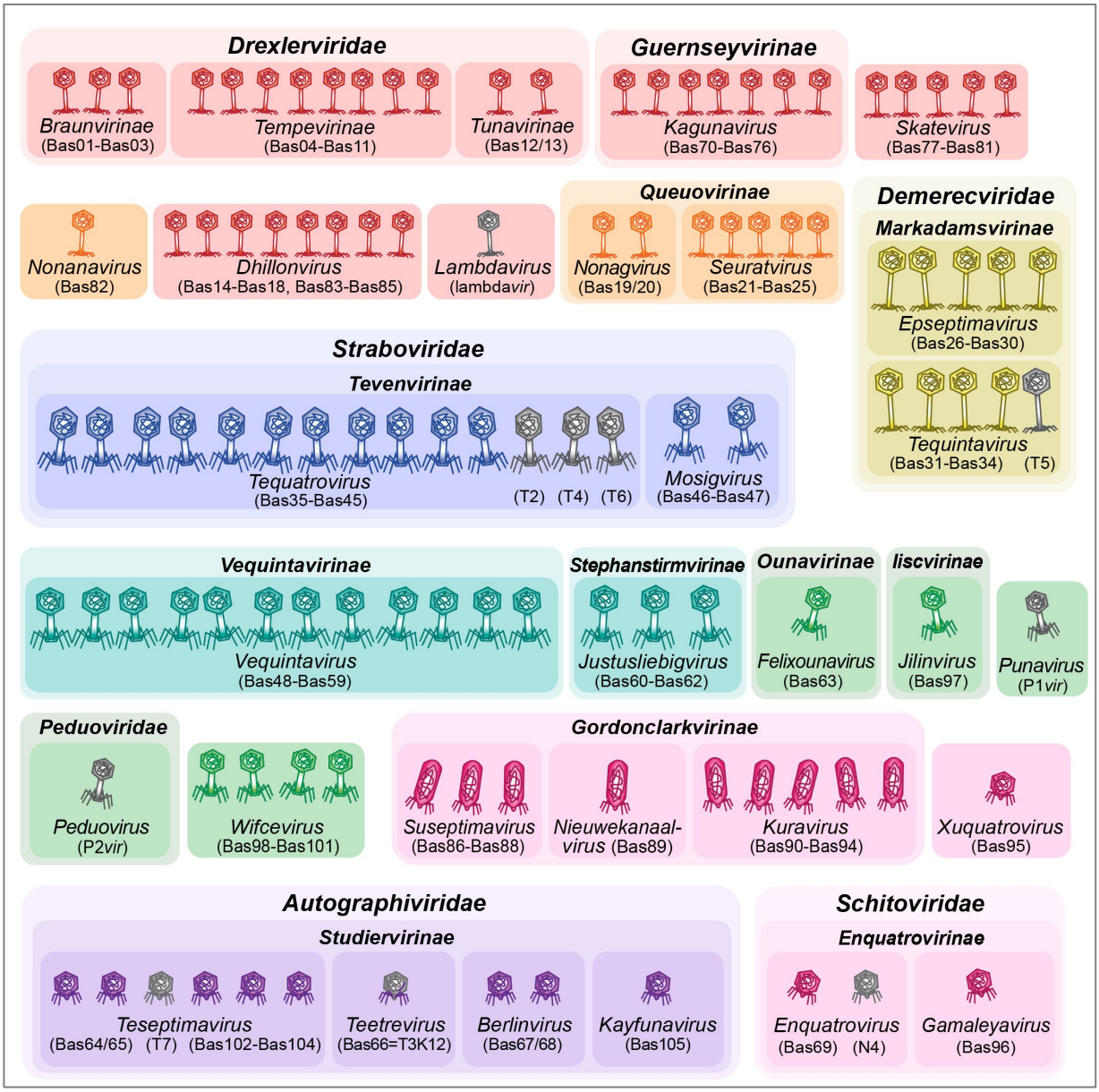

Figure 14. Overview of the complete BASEL collection.

The illustration shows all isolates of the complete BASEL collection with their Bas## identifiers. Isolates are sorted by morphotype and their current ICTV classification [58]. The color code distinguishes phages based on morphotype and genome size. For siphoviruses, small phages (ca. 30-50 kb) are shown in red, medium-sized phages (ca. 50-100 kb) are shown in orange, and large phages (>100 kb) are shown in yellow. For myoviruses, small phages (ca. 30-100 kb) are shown in green, medium-sized phages (ca. 100-150kb) are shown in cyan, and large phages (>100kb) are shown in blue. For podoviruses, small phages (ca. 30-50 kb) are shown in violet and medium-sized phages (ca. 50-100kb) are shown in pink.

688 # Materials and Methods

689 ## Preparation of culture media and solutions

690 Lysogeny Broth (LB) was prepared by dissolving 10 g/l tryptone, 5 g/l yeast extract, and 10 g/l
691 sodium chloride in Milli-Q H_2O and then sterilized by autoclaving. LB agar plates were prepared by
692 supplementing LB medium with agar at 1.5% w/v before autoclaving. Phosphate-buffered saline (PBS) was
693 prepared as a solution containing 8 g/l NaCl, 0.2 g/l KCl, 1.44 g/l $NA_2HPO_4 \cdot 2H_2O$, and 0.24 g/l KH_2PO_4
694 with the pH adjusted to 7.4 using 10 M NaOH and sterilized by autoclaving. SM buffer was prepared as
695 0.1 M NaCl, 10 mM $MgSO_4$, and 0.05 M Tris (pH 7.5) and sterilized by autoclaving.

696 ## Bacterial handling and culturing

697 *Escherichia coli* and *Salmonella enterica* subsp. *enterica* serovar Typhimurium strains were
698 routinely cultured in LB medium at 37°C in glass tubes, plastic tubes, or Erlenmeyer flasks with agitation
699 at 170 rpm. Selection for genetic modifications or plasmid maintenance was performed with ampicillin at
700 50 µg/ml, kanamycin at 25 µg/ml, and zeocin at 50 µg/ml.

701 ## Bacteriophage handling and culturing

702 Bacteriophages were generally cultured using the double-agar overlay method [146] with
703 improvements of classical techniques described by Kauffman and Polz [147]. Top agar was prepared as LB
704 agar with only 0.5% w/v agar supplemented with 20 mM $MgSO_4$ and 5 mM $CaCl_2$. Top agar plates were
705 incubated at 37°C and plaques were counted as soon as they were identified by visual inspection. However,
706 the plates were always incubated for at least 24 hours to record also slow-growing plaques.

707 High-titer stocks of bacteriophages were generated using plate-grown viruses. Briefly, phages were
708 spread with a loop throughout the top agar before solidification to achieve confluent lysis after incubation
709 for 16-24 hours at 37°C. Subsequently, top agars were scraped off from the bottom agar into each 15 ml of
710 SM buffer and centrifuged at 8’000 g for 10 minutes. Supernatants were used as high-titer stocks and stored
711 in the dark at 4°C.

712 ## Bacterial strains and strain construction

713 All bacterial strains used in this work are listed in Table S3, all oligonucleotide primers in Table
714 S4, and all plasmids in Table S5.

715 ### Variants of *Escherichia coli* K-12 MG1655 and BW25113

716 The primary host of our experimentation with *E. coli* K-12 was the ΔRM mutant of the MG1655
717 laboratory strain which we had reported in our previous work [10]. Briefly, we had engineered this strain
718 to be a more permissive host for bacteriophages by knocking out all known restriction systems of *E. coli*
719 K-12, i.e., the EcoKI type I RM system (encoded by *hsdRMS*) and the McrA, Mrr, and McrBC type IV
720 restriction systems. For phage isolation and phenotyping, the strain carried a variant of the F-plasmid in
721 which the *pifA* immunity gene had been deleted [10]. Phenotyping with plasmid-encoded antiviral defense
722 systems was done with a strain carrying pBR322_ΔP*tet* as an empty vector control [10, 148] (see Table
723 S3). Whenever indicated, we used the *E. coli* K-12 ΔRM variant with a repaired chromosomal *wbbL* gene
724 that has restored O16-type O-antigen expression from our previous work [10] (see Table S3). To rapidly
725 restore O-antigen expression in diverse strains (e.g., porin mutants of the Keio single-gene knockout
726 collection [149]) we created plasmid pAS001 that constitutively expresses *wbbL* (see below in section
727 *Plasmid construction*). Fortuitously, the plasmid-encoded *wbbL* does not fully restore the O-antigen barrier
728 (because most phages inhibited by it still show infectivity; compare Figs. 1 and S11A) but enough of it to
729 enable robust infections by all O16-dependent phages (compare Figs. 2 and S11B).

730 To identify possible limitations of phage infectivity beyond host recognition, we focused on
731 possible antiviral defenses in the K-12 genomic background beyond the restriction systems knocked out in
732 *E. coli* K-12 MG1655 ΔRM. One of these is the enigmatic enterobacterial type I-E CRISPR-Cas system
733 known to be not functional in phage defense without dedicated genetic engineering [150, 151]. In addition,
734 *E. coli* K-12 strains encode Lit (reported to cleave bacterial EF-Tu when sensing the major capsid protein
735 of some *Tevenvirinae* [152]), RnlAB (toxin-antitoxin system that aborts T4 infections in absence of the
736 viral *dmd* "master key" antitoxin [153]), DicB (inhibitor of the bacterial ManYZ inner membrane conduit

737 of lambda phage DNA translocation [154]), and a Hachiman type I system (targeting DNA replication of
738 diverse phages; also known as AbpBA [44, 46, 155]). With the exception of the seemingly inactive type
739 I-E CRISPR-Cas system, all these *bona fide* antiviral defenses are encoded in the cryptic prophages of
740 *E. coli* K-12. We therefore used the *E. coli* K-12 BW25113 Δ9CP strain devoid of all cryptic prophages as
741 an additional host for phage isolation and characterization [49]. This strain is derived from the BW25113
742 laboratory wildtype of *E. coli* K-12 that has a few minor differences compared to the MG1655 laboratory
743 wildtype [156, 157] (see also Fig. 4D). Most important for our work, *E. coli* K-12 BW25113 carries active
744 variants of the three type IV restriction systems knocked out in our MG1655 ΔRM strain as well as the
745 *hsdRMS* locus encoding the EcoKI type I RM system. Unfortunately, due to the high sensitivity of *E. coli*
746 K-12 BW25113 Δ9CP to stress and possibly also as a consequence of its already extensive genomic
747 engineering, our attempted knockouts of these systems consistently failed. However, the EcoKI locus of
748 BW25113 is restriction-deficient and we are not aware of any wildtype phages that would be sensitive to
749 the three type IV restriction systems of *E. coli* K-12, suggesting that the presence of these loci might have
750 only a negligible effect. Analogous to our work with *E. coli* K-12 MG1655 ΔRM [10], we also generated a
751 variant of *E. coli* K-12 BW25113 Δ9CP with chromosomally restored *wbbL(+)* to isolate and study phages
752 that would depend on this glycan (see Table S3). The different variants of *E. coli* K-12 BW25113 Δ9CP
753 were used for phage isolation and characterization just like the ΔRM variants with plasmid-encoded
754 antiviral defenses and a *pifA*-deficient F-plasmid (see Table S3).

755 **Other enterobacterial strains used for bacteriophage phenotyping**

756 To determine the host range of our new phage isolates and relevant controls, we initially used the
757 same strains as in our previous work (see there for details [10]). Briefly, besides the *E. coli* K-12 variants
758 with and without restored O-antigen (see above; phylogroup A, ST10, O16(+/-):H48, K-12 LPS core) these
759 were the rough *E. coli* B REL606 laboratory strain (phylogroup A, O7(-):K5:H(-), truncated R1 LPS core),
760 uropathogenic *E. coli* model strains UTI89 (phylogroup B2, ST95, O18:K1:H7, R1 LPS core) and CFT073
761 (phylogroup B2, ST73, O6:K2:H1, R1 LPS core), and enteroaggregative *E. coli* model strain 55989

762 (phylogroup B1, ST678, O104:H4, R3 LPS core). Similarly, we again used the common *Salmonella*
763 *enterica* subsp. *enterica* serovar Typhimurium laboratory strains 12023s (also known as ATCC 14028) and
764 SL1344 that share the *Salmonella* Typhimurium O4-type O-antigen. Because the results with these strains
765 were indistinguishable, only those with *S.* Typhimurium 12023s are shown in Fig. 12. Beyond these strains
766 already included for host range analyses in our previous work, we included three additional *E. coli* strains
767 with O16-type O-antigen (i.e., the same as *E. coli* K-12) belonging to ST131 (Egli lab collection isolate
768 720834-18; phylogroup B2, O16:H5), ST144 (Egli lab collection isolate 714478-19; phylogroup B2,
769 O16:H6), and ST8281 (Egli lab collection isolate 711043-19; phylogroup B2, O16:H5) [158].

770 **Plasmids and plasmid construction**

771 For the phenotyping of phage resistance or sensitivity to diverse bacterial immunity systems, we
772 used plasmids encoding different antiviral defenses constructed in our previous work (see Figs. 4B and 4C
773 as well as Table S5). Plasmid pAS001 encoding *wbbL* was cloned by inserting the *wbbL* gene downstream
774 of a constitutively expressed chloramphenicol resistance gene on a plasmid with SC101 origin of replication
775 (see details of plasmid construction in Table S6).

776 **Bacteriophage isolation**

777 **Basic procedure**

778 Phages isolates presented in this study have been isolated from diverse samples between March of
779 2020 and July of 2022. Initial experiments aimed at isolating phages that would depend on O16-type
780 O-antigen used *E. coli* K-12 MG1655 ΔRM *wbbL(+)* as host and subsequent plating on its ancestor without
781 O-antigen to identify O16-dependent isolates. Later experiments aimed at isolating phages inhibited by
782 presence of the K-12 cryptic prophages used *E. coli* K-12 BW25113 Δ9CP transformed with *wbbL*-
783 expressing pAS001 as host to obtain phages irrespective of whether they depend on O-antigen or not
784 (compare Figs. 1, 2, and S11). These isolates were later plated on *E. coli* K-12 BW25113 transformed with
785 pAS001 to screen for impaired growth in the presence of cryptic prophages and on *E. coli* K-12 BW25113

786 Δ9CP without pAS001 to screen for dependence on O-antigen expression. The isolation and screening
787 procedure is summarized in Figs. 2A and 2B.

788 We generally isolated phages by direct plating without enrichment step to avoid biases in favor of
789 fast-growing isolates. The procedure was performed similar to the approach in our previous work [10].
790 Aqueous samples were directly used in batches of 50 ml while solid samples were first agitated overnight
791 in PBS for suspension and release of viral particles. Subsequently, we centrifuged all samples at 8'000 g
792 for 10 minutes to separate viral particles – which remain in the supernatant – from larger unorganic particles
793 or bacterial cells. Viral particles were then precipitated by supplementation with $ZnCl_2$ at a final
794 concentration of 40 mM and an incubation without agitation for one hour at 37°C. Subsequently,
795 precipitates were pelleted by centrifugation at 8'000 g for 10 minutes and pellets were resuspended carefully
796 in each 0.5-1 ml of SM buffer depending on how much volume was required for a given pellet. For plating
797 of phage isolates, the suspensions were mixed with 500 µl of bacterial overnight culture and, after some
798 minutes at room temperature, with 10 ml of top agar. In case of sewage plant inflow, serial dilutions of the
799 resuspended precipitate were used due to the usually very high amount of phages. Top agars with samples
800 and bacterial inoculum were then poured onto a square LB agar plate (ca. 12 cm x 12 cm). After
801 solidification, we incubated the plates at 37°C for up to 24 hours.

802 **Isolation of clonal bacteriophage isolates**

803 After incubation, phages grew as plaques – i.e., spots of clearance – scattered across the top agar
804 that was otherwise opaque from dense bacterial growth. To screen for phages that depended on restored
805 O16-type O-antigen expression and / or showed impaired growth in presence of K-12 cryptic prophages,
806 ca. 150 plaques per plate were separately picked with sterile toothpicks and copied onto freshly inoculated
807 soft agars of hosts without O-antigen expression and / or cryptic prophages (see *Bacterial strains* above).
808 When O-antigen dependency and / or inhibition by cryptic prophages were observed, the respective isolates
809 were propagated at least three times via single plaques on top agars of their isolation host.

810 **Composition of the completed BASEL collection**

811 After phage isolation and initial screening, we sequenced the genomes of all ca. 100 isolates that
812 depended on O16-type O-antigen or were inhibited by the K-12 cryptic prophages (see below). Based on
813 phylogenetic analyses, a set of ca. 40 phages was then chosen based primarily on largest genomic distances
814 and characterized phenotypically alongside 8 phages from our previous work that grew well on *E. coli* K-12
815 with restored O-antigen expression (see below). We then chose 36 new phage isolates for inclusion in the
816 completed BASEL collection by excluding a few more closely related isolates that behaved very similarly
817 (see list in Table S2).

818 **Efficiency of Plating assays**

819 We quantified the infectivity of a phage on a host strain as the efficiency of plating (EOP) [159],
820 i.e., as the ratio of its plaque formation on that host over the plaque formation on susceptible reference
821 strains. As references we used *E. coli* K-12 MG1655 ΔRM *wbbL(+)* or *E. coli* K-12 BW251139 Δ9CP
822 *wbbL(+)*, depending on the isolates' sensitivity to presence of cryptic prophages, since all tested phages
823 grew very well with restored O16-type O-antigen expression. All variants of *E. coli* K-12 used for
824 phenotyping carried an F-plasmid without *pifA* defense gene (unless that was to be tested) and
825 pBR322_ΔP*tet* as empty vector control or plasmids expressing different antiviral defenses (see *Bacterial*
826 *strains* above and Table S3 for a list). Note that the phenotyping of phages sensitive to the presence of
827 cryptic prophages enabled us to use the isogenic host with prophages as a test condition for efficiency of
828 plating but prevented us from testing phage sensitivity to the EcoKI type I RM system because the *E. coli*
829 K-12 BW251139 Δ9CP strain has active EcoKI methylation (see *Bacterial strains* above and the genotype
830 in Table S3). It is therefore highlighted at all graphs whether ΔRM (EcoKI tested, cryptic prophage
831 sensitivity not tested) or Δ9CP (EcoKI not tested, cryptic prophage sensitivity tested) have been used as
832 hosts. To test for the effect of surface glycans on phage infectivity, we used host variants expressing no O-
833 antigen but – unlike in our previous work [10] – no mutants with deeper truncations in the LPS core because
834 almost all phages completely depended on O-antigen expression. The results with an *E. coli* K-12 mutant

835 lacking NGR expression due to the inactivation of *nfrA* are merely shown in Fig. S1A since evidently no
836 new phage isolate used this glycan for host recognition.

837 For these quantitative experiments, we prepared top agars on regular LB agar plates by overlaying
838 them with a soft agar composed of LB agar containing only 0.5% agar and additionally 20 mM $MgSO_4$ as
839 well as 5 mM $CaCl_2$ supplemented with a suitable bacterial inoculum. We used 3 ml of this soft agar with
840 100 µl of bacterial overnight culture as inoculum for regular round Petri dishes (ca. 9.4 cm diameter) and
841 10 ml of top agar supplemented with 200 µl of bacterial overnight culture for larger square Petri dishes (ca.
842 12 cm x 12 cm). EOP experiments were performed with serial dilutions of phage stocks grown on the
843 respective reference hosts prepared in sterile phosphate-buffered saline (PBS). For each experiment, 2.5 µl
844 of all serial dilutions were spotted on the top agar plates and dried into the top agar before incubation at
845 37°C for at least 24 hours. We then recorded plaque formation repeatedly throughout this time to accurately
846 quantify the infectivity of fast- and slow-growing phages. Finally, we determined the EOP of each phage
847 on each host as the ratio of plaques obtained on the experimental host over the number of plaques obtained
848 on the respective reference strain [159]. Plaque counts and the calculation of EOP of all replicates of all
849 experiments reported in this study (Figs. 5D, 6G, 7D, 8G, 9E, 10D, 13B, and S1A/B) as well as their
850 summary statistics are compiled in S1 Data.

851 In cases when visual inspection could not unambiguously record plaque formation, we determined
852 the EOP to be below the detection limit of 10^{-6} even if significant lysis from without was apparent (i.e.,
853 lysis zones caused by bacterial cell death without significant phage replication simply from the death of
854 infected cells [114]). In cases where a phage / host pair was on the edge between strong lysis from without
855 and very poor plaque formation, we cautiously recorded the result as an EOP below detection limit.

856 Qualitative top agar assays

857 We also determined the lysis host range of all tested phages on diverse *E. coli* strains (including
858 K-12 ΔRM or Δ9CP with and without restored O-antigen) as well as *Salmonella* Typhimurium, i.e., the
859 range of host strains on which a certain phage caused lysis zones irrespective of whether these were

860 accompanied by plaque formation or not (see the illustration in Fig.13A). These experiments were
861 performed as qualitative top agar assays as described in our previous work [10]. Briefly, top agar plates of
862 each host strain were prepared as described for efficiency-of-plating assays. After solidification, we spotted
863 each 2.5 µl of undiluted high-titer stocks of all tested phage isolates (typically >10^9 pfu/ml) onto the top
864 agar plates. When the spots had dried in, we incubated the plates at 37°C for at least 24 hours before visual
865 inspection. The appearance of a lysis zone in more than half of all replicates for a phage-host pair meant
866 that the host was counted as part of the lysis host range for this phage. In all such cases we subsequently
867 quantified phage infectivity in efficiency-of-plating assays (see above).

868 **Bacteriophage genome sequencing and assembly**

869 Genomic DNA of phage isolates was prepared from culture lysates using the Norgen Biotek Phage
870 DNA Isolation Kit and sequenced at SeqCenter (https://www.seqcenter.com/) or SeqCoast Genomics
871 (https://seqcoast.com/) using Illumina technology. The short reads (151bp) were trimmed and assembled
872 using the Geneious Assembler implemented in Geneious Prime 2024.0.2 with a coverage of typically 50-
873 100x (see Table S2 for each phage). Circular contigs (indicating complete assembly of a viral chromosome
874 due to the fusion of characteristic repeats at the genome ends [160]) were typically obtained easily using
875 the "Low Sensitivity / Fast" setting with ca. 100'000 reads as input for the assembly. If necessary,
876 ambiguities or incomplete assemblies were resolved by PCR amplification the high-fidelity polymerase
877 Phusion (NEB) followed by Sanger Sequencing. Sequences were linearized at the 5' end either to the first
878 nucleotide of the small or large terminase subunit gene or to the first position of the operon containing the
879 small or large terminase subunit gene.

880 **Initial bacteriophage genome annotation**

881 The genomes of new phage isolates were annotated successively in several steps. To start, we used
882 Pharokka to generate an automated, preliminary annotation of the genes in all phage genomes which
883 included tRNA prediction using tRNAscan-SE [161, 162]. Subsequently, the annotations were refined
884 manually based on identified orthologs in whole-genome alignments to different related phages generated

885 using MAFFT v7.490 [163] implemented in Geneious Prime 2024.0.2. In parallel, we used the InterPro
886 101.0 protein domain signature database to maximize the functional information accessible from the
887 primary sequence of phage proteins [104].

888 Curation of genome annotations using remote homologies and structure prediction

889 For the curation of phage genome annotations, we developed a computational pipeline called GAPS
890 (Gene Annotation Pipeline based on sequence and structure Similarity). Briefly, this pipeline employs a
891 combination of sequence and structure analyses, database searches, interpretation, annotation and
892 visualization routines to infer functional information for a given set of genes, of any organism, in an
893 automated way. For the current study, phage gene sequences were fed to GAPS as features in a .gb file and
894 translated to protein. For each protein sequence: (i) the protein and domain families were determined by
895 searching the Pfam, NCBI_CD, CATH_S40 and PHROGS databases with HHblits [164-169]; (ii) identical
896 sequences were found by searching the PDB, SwissProt and RefSeq databases [170-172]; (iii) similar
897 sequences were found by searching the UniRef30 and PDB70 databases with HHblits [168-171]; (iv) the
898 protein structures were predicted with AlphaFold2 [173]; (v) similar structures were found by searching the
899 PDB, AlphaFold-Proteome and AlphaFold-UniProt50 databases with Foldseek [170, 173, 174]. The results
900 were parsed and integrated programmatically for presentation in an interactive report file that summarizes
901 the available information for all genes of the input genome in one combined overview page. Detailed results
902 of all individual genes are presented in sub-pages. An exemplary report for *Jilinvirus* HeidiAbel (Bas97) is
903 included in this publication as Data S2 and the added value of GAPS for the functional annotation of its
904 genes is highlighted in Fig. S12. GAPS is written in Python 3.8 and is open-source. The code used to run
905 GAPS for generating the data presented in this manuscript can is available on GitHub
906 (https://github.com/hiller-lab/gaps) in the form of a Jupyter notebook.

907 Bacteriophage naming and taxonomy

908 Phage isolates were classified according to applicable rules of the International Committee on the
909 Taxonomy of Viruses (ICTV) [58, 175] largely as described in our previous work BASEL [10] (see Table

910 S2). Briefly, phages were first roughly assigned to viral family and, if possible, genus based on whole-
911 genome blastn searches against the non-redundant nucleotide collection database
912 [https://blast.ncbi.nlm.nih.gov/Blast.cgi; see also reference 176]. Subsequently, we unraveled the
913 evolutionary relationships between our new isolates and reference sequences from NCBI GenBank across
914 the diversity of relevant viral groups by calculating phylogenies based on either whole-genome alignments
915 or alignments of conserved marker genes (see details in the dedicated section below). We then compared
916 the clusters of viral sequences observed in these phylogenies to phage taxonomy as established by the ICTV
917 and the relevant literature [58, 177]. For classification on the species level, whole-genome alignments of
918 new phage isolates with close relatives were generated as described below and the nucleotide sequence
919 identity was determined as the fraction of aligned genome sequence multiplied by the nucleotide identity
920 of aligned segments. Phage isolates were classified as the same species as previously described relatives if
921 their genomes showed >95% nucleotide sequence identity [178].

922 We named most phages in honor of scientists or historically significant persons linked to the city
923 of Basel, Switzerland, where most of the phages had been isolated. To overcome the inherent gender
924 imbalance due to historical biases, we included diverse female personalities from across the whole of
925 Switzerland. Phages of *Skatevirus* and *Nonanavirus* genera were given names composed of common female
926 first names in Switzerland in 1971 (when Swiss women obtained voting rights in federal elections) and
927 "Muster" as surname (German word for paradigm or example).

928 Sequence alignments and phylogenetic analyses

929 Sequence alignments of bacteriophage genomes, specific loci, or certain genes / proteins were
930 generated using MAFFT v7.490 implemented in Geneious Prime 2024.0.2 [163]. Occasionally, we
931 supplemented poor or missing annotations in these sequences using the ORF finder tool of Geneious Prime
932 2024.0.2 guided by orthologous loci. Alignments were typically constructed using default settings of
933 MAFFT with the fast FFT-NS-2 algorithm and 200PAM/k=2 or BLOSUM62 scoring matrices for

934 nucleotide and amino acid sequences, respectively. Subsequently, we curated the alignments manually and
935 masked non-homologous parts for exclusion during phylogenetic analyses.

936 Maximum-Likelihood phylogenies were calculated using PhyML 3.3.20180621 implemented in
937 Geneious Prime 2024.0.2 from sequence alignments of orthologous genes / proteins or orthologous
938 sequence stretches of different bacteriophage genomes [179]. We used the HYK85 and LG substitution
939 models for nucleotide and amino acid sequences, respectively, and always calculated 100 bootstraps.
940 Phylogenetic relationships between phage genomes were inferred from whole-genome alignments
941 (whenever possible) or from concatenated sequence alignments of conserved core genes on nucleotide or
942 amino acid level as indicated for each phylogeny.

943 Structure predictions and analyses of receptor-binding proteins

944 Structure predictions were performed using AlphaFold-Multimer on the Cosmic^2 platform or on
945 the AlphaFold3 webserver [108, 180, 181]. All predictions presented high internal confidence scores which
946 are presented in Table S7. Illustrations were generated using the PyMOL Molecular Graphics System
947 (Version 2.4.1, Schrodinger LLC). The Dali server was used to identify structural homologs in the Protein
948 Data Bank (PDB) [182].

949 Morphological analyses by transmission electron microscopy

950 We analyzed the virion morphology of representative isolates from the different taxonomic groups
951 covered in this manuscript by negative-stain transmission electron microscopy [183]. Briefly, we applied
952 5 µl drops of high-titer phage lysates to 400 mesh carbon-coated grids that had been rendered hydrophilic
953 using a glow-discharger at low vacuum conditions. Subsequently, virions were stained on 5 µl drops of 2%
954 (w/v) uranyl acetate and examined using an FEI Tecnai G2 Spirit transmission electron microscope (FEI
955 Company) at 80-kV accelerating voltage, a Hitachi HT7700 transmission electron microscope (Hitachi) at
956 100 kV, or an FEI Talos F200C transmission electron microscope (FEI Company) at 200 kV. Images were
957 recorded with a side-mounted Olympus Veleta CCD camera 4k (Tecnai G2 Spirit), an AMT XR81B Peltier

958 cooled CCD camera (8 M pixel; Hitachi HT7700), or a Thermo Fisher Scientific Ceta 16M CCD camera
959 (Talos F200C) using EMSIS RADIUS software at a nominal magnification of typically 150'000x.

960 **Quantification and statistical analysis**

961 Data sets were analyzed quantitatively by calculating mean and standard deviation of at least three
962 independent biological replicates per experiment. Detailed information about replicates and statistical
963 analyses is provided in the figure legends.

964 # Acknowledgments

965 The authors are grateful to Dr. Julie Sollier for valuable input and critical reading of the manuscript.
966 We thank high school students participating in the Biozentrum Summer Science Academy 2022 for
967 assistance with the isolation of multiple bacteriophages described in this study (Table S2). The authors are
968 indebted to Dr. Mohamed Chami and Carola Alampi of the BioEM lab of the Biozentrum, University of
969 Basel (Switzerland), and the ScopeM facility at ETH Zürich (Switzerland) for their support with
970 transmission electron microscopy. We further thank ARA Basel, ARA Canius (Lenzerheide), and ARA
971 Triengen for samples of sewage plant inflow. The authors are grateful to David Schwegler for pioneering
972 work on the annotation of phage genomes using remote homologies and structure prediction with GAPS.
973 Dr. Toomas Mets (University of Tartu, Estonia) is acknowledged for the initial discovery that partial
974 restoration of O16-type O-antigen expression with pAS001 can still inhibit the growth of some phages. The
975 authors are grateful to Dr. Jiemin Du, Dr. Samuel Kilcher, and Prof. Dr. Martin Loessner (ETH Zürich,
976 Switzerland) for helpful discussions about the role of bacterial O-antigen for phage infections. Dr. Artem
977 Isaev is acknowledged for a helpful comment on anti-phage defense systems in cryptic prophages. This
978 work was supported by the Swiss National Science Foundation (SNSF) Ambizione Fellowship
979 PZ00P3_180085 (to A.H.), SNSF Starting Grant TMSGI3_211369 (to A.H.), and SNSF National Centre
980 of Competence in Research (NCCR) AntiResist (grant number 180541).

981 # References

982 1. Dion MB, Oechslin F, Moineau S. Phage diversity, genomics and phylogeny. Nat Rev Microbiol.
983 2020;18(3):125-38. Epub 2020/02/06. doi: 10.1038/s41579-019-0311-5. PubMed PMID: 32015529.

984 2. Cobian Güemes AG, Youle M, Cantu VA, Felts B, Nulton J, Rohwer F. Viruses as Winners in the
985 Game of Life. Annu Rev Virol. 2016;3(1):197-214. Epub 2016/10/16. doi: 10.1146/annurev-virology-
986 100114-054952. PubMed PMID: 27741409.

987 3. Ofir G, Sorek R. Contemporary Phage Biology: From Classic Models to New Insights. Cell.
988 2018;172(6):1260-70. doi: 10.1016/j.cell.2017.10.045. PubMed PMID: 29522746.

989 4. Gordillo Altamirano FL, Barr JJ. Phage Therapy in the Postantibiotic Era. Clin Microbiol Rev.
990 2019;32(2). Epub 2019/01/18. doi: 10.1128/CMR.00066-18. PubMed PMID: 30651225; PubMed Central
991 PMCID: PMCPMC6431132.

992 5. Kolter R. Small Things Considered [Internet]. Schaechter M, Kolter R, editors.
993 https://schaechter.asmblog.org/schaechter/2022/03/the-phage-treaty.html2022. [cited 2022]. Available
994 from: https://schaechter.asmblog.org/schaechter/2022/03/the-phage-treaty.html.

995 6. Shaidullina A, Harms A. Toothpicks, logic, and next-generation sequencing: systematic
996 investigation of bacteriophage-host interactions. Curr Opin Microbiol. 2022;70:102225. Epub 20221031.
997 doi: 10.1016/j.mib.2022.102225. PubMed PMID: 36327691.

998 7. Demerec M, Fano U. Bacteriophage-Resistant Mutants in *Escherichia Coli*. Genetics.
999 1945;30(2):119-36. Epub 1945/03/01. PubMed PMID: 17247150; PubMed Central PMCID:
1000 PMCPMC1209279.

1001 8. Abedon ST. The murky origin of Snow White and her T-even dwarfs. Genetics. 2000;155(2):481-6.
1002 Epub 2000/06/03. PubMed PMID: 10835374; PubMed Central PMCID: PMCPMC1461100.

1003 9. Ruiz N, Silhavy TJ. How *Escherichia coli* Became the Flagship Bacterium of Molecular Biology. J
1004 Bacteriol. 2022;204(9):e0023022. Epub 20220802. doi: 10.1128/jb.00230-22. PubMed PMID: 35916528;
1005 PubMed Central PMCID: PMCPMC9487582.

1006 10. Maffei E, Shaidullina A, Burkolter M, Heyer Y, Estermann F, Druelle V, et al. Systematic exploration
1007 of *Escherichia coli* phage-host interactions with the BASEL phage collection. PLoS Biol.
1008 2021;19(11):e3001424. Epub 2021/11/17. doi: 10.1371/journal.pbio.3001424. PubMed PMID: 34784345;
1009 PubMed Central PMCID: PMCPMC8594841.

1010 11. Kelly A, Went SC, Mariano G, Shaw LP, Picton DM, Duffner SJ, et al. Diverse Durham collection
1011 phages demonstrate complex BREX defense responses. Appl Environ Microbiol. 2023;89(9):e0062323.
1012 Epub 20230905. doi: 10.1128/aem.00623-23. PubMed PMID: 37668405; PubMed Central PMCID:
1013 PMCPMC10537673.

1014 12. Nicolas M, Trotereau A, Culot A, Moodley A, Atterbury R, Wagemans J, et al. Isolation and
1015 Characterization of a Novel Phage Collection against Avian-Pathogenic *Escherichia coli*. Microbiol Spectr.
1016 2023;11(3):e0429622. Epub 20230504. doi: 10.1128/spectrum.04296-22. PubMed PMID: 37140373;
1017 PubMed Central PMCID: PMCPMC10269720.

1018 13. University of Southampton MIL. KlebPhaCol: an open collection of phages targeting Klebsiella spp.
1019 for your research. Evergreen International Phage Meeting2023.

1020 14. Bondy-Denomy J, Qian J, Westra ER, Buckling A, Guttman DS, Davidson AR, et al. Prophages
1021 mediate defense against phage infection through diverse mechanisms. ISME J. 2016;10(12):2854-66. Epub
1022 2016/06/04. doi: 10.1038/ismej.2016.79. PubMed PMID: 27258950; PubMed Central PMCID:
1023 PMCPMC5148200.

1024 15. Brauer A, Rosendahl S, Kangsep A, Lewanczyk AC, Rikberg R, Horak R, et al. Isolation and
1025 characterization of a phage collection against *Pseudomonas putida*. Environ Microbiol.
1026 2024;26(6):e16671. doi: 10.1111/1462-2920.16671. PubMed PMID: 38863081.

1027 16. Costa AR, van den Berg DF, Esser JQ, Muralidharan A, van den Bossche H, Bonilla BE, et al.
1028 Accumulation of defense systems in phage-resistant strains of *Pseudomonas aeruginosa*. Sci Adv.
1029 2024;10(8):eadj0341. Epub 20240223. doi: 10.1126/sciadv.adj0341. PubMed PMID: 38394193; PubMed
1030 Central PMCID: PMCPMC10889362.

1031 17. Sellner B, Prakapaite R, van Berkum M, Heinemann M, Harms A, Jenal U. A New Sugar for an Old
1032 Phage: a c-di-GMP-Dependent Polysaccharide Pathway Sensitizes *Escherichia coli* for Bacteriophage
1033 Infection. mBio. 2021;12(6):e0324621. Epub 2021/12/15. doi: 10.1128/mbio.03246-21. PubMed PMID:
1034 34903045; PubMed Central PMCID: PMCPMC8669472.

1035 18. Nyerges A, Vinke S, Flynn R, Owen SV, Rand EA, Budnik B, et al. A swapped genetic code prevents
1036 viral infections and gene transfer. Nature. 2023;615(7953):720-7. Epub 20230315. doi: 10.1038/s41586-
1037 023-05824-z. PubMed PMID: 36922599; PubMed Central PMCID: PMCPMC10151025.

1038 19. Hantke K, Friz S. The TonB-dependent uptake of pyrroloquinoline-quinone (PQQ) and secretion of
1039 gluconate by *Escherichia coli* K-12. Mol Microbiol. 2022;118(4):417-25. Epub 20220914. doi:
1040 10.1111/mmi.14975. PubMed PMID: 36054785.

1041 20. Mulla Y, Müller J, Trimcev D, Bollenbach T. Extreme diversity of phage amplification rates and
1042 phage-antibiotic interactions revealed by PHORCE. bioRxiv. 2024:2024.06.07.597930. doi:
1043 10.1101/2024.06.07.597930.

1044 21. Zhang T, Tamman H, Coppieters 't Wallant K, Kurata T, LeRoux M, Srikant S, et al. Direct activation
1045 of a bacterial innate immune system by a viral capsid protein. Nature. 2022;612(7938):132-40. Epub
1046 20221116. doi: 10.1038/s41586-022-05444-z. PubMed PMID: 36385533; PubMed Central PMCID:
1047 PMCPMC9712102.

1048 22. Zhong A, Jiang X, Hickman AB, Klier K, Teodoro GIC, Dyda F, et al. Toxic antiphage defense proteins
1049 inhibited by intragenic antitoxin proteins. Proc Natl Acad Sci U S A. 2023;120(31):e2307382120. Epub
1050 20230724. doi: 10.1073/pnas.2307382120. PubMed PMID: 37487082; PubMed Central PMCID:
1051 PMCPMC10400941.

1052 23. Skutel M, Andriianov A, Zavialova M, Kirsanova M, Shodunke O, Zorin E, et al. T5-like phage BF23
1053 evades host-mediated DNA restriction and methylation. microLife. 2023;4. doi:
1054 10.1093/femsml/uqad044.

1055 24. Hu H, Hughes TCD, Popp PF, Roa-Eguiara A, Martin FJO, Rutbeek NR, et al. Structure and
1056 mechanism of Zorya anti-phage defense system. bioRxiv. 2023:2023.12.18.572097. doi:
1057 10.1101/2023.12.18.572097.

1058 25. Vizzarro G, Lemopoulos A, Adams DW, Blokesch M. *Vibrio cholerae* pathogenicity island 2 encodes
1059 two distinct types of restriction systems. J Bacteriol. 2024:e0014524. Epub 20240812. doi:
1060 10.1128/jb.00145-24. PubMed PMID: 39133004.

1061 26. Blount ZD. The unexhausted potential of *E. coli*. Elife. 2015;4. doi: 10.7554/eLife.05826. PubMed
1062 PMID: 25807083; PubMed Central PMCID: PMCPMC4373459.

1063 27. Liu D, Reeves PR. *Escherichia* coli K12 regains its O antigen. Microbiology. 1994;140 (Pt 1):49-57.
1064 doi: 10.1099/13500872-140-1-49. PubMed PMID: 7512872.

1065 28. van der Ley P, de Graaff P, Tommassen J. Shielding of *Escherichia coli* outer membrane proteins
1066 as receptors for bacteriophages and colicins by O-antigenic chains of lipopolysaccharide. J Bacteriol.
1067 1986;168(1):449-51. doi: 10.1128/jb.168.1.449-451.1986. PubMed PMID: 2428812; PubMed Central
1068 PMCID: PMCPMC213476.

1069 29. Letarov AV. Bacterial Virus Forcing of Bacterial O-Antigen Shields: Lessons from Coliphages. Int J
1070 Mol Sci. 2023;24(24). Epub 20231212. doi: 10.3390/ijms242417390. PubMed PMID: 38139217; PubMed
1071 Central PMCID: PMCPMC10743462.

1072 30. Berryhill BA, Burke KB, Fontaine J, Brink CE, Harvill MG, Goldberg DA, et al. Enteric Populations of
1073 *Escherichia coli* are Likely to be Resistant to Phages Due to O Antigen Expression. bioRxiv.
1074 2024:2023.11.08.566299. doi: 10.1101/2023.11.08.566299.

1075 31. Broeker NK, Barbirz S. Not a barrier but a key: How bacteriophages exploit host's O-antigen as an
1076 essential receptor to initiate infection. Mol Microbiol. 2017;105(3):353-7. Epub 2017/06/16. doi:
1077 10.1111/mmi.13729. PubMed PMID: 28618013.

1078 32. Henderson JC, Zimmerman SM, Crofts AA, Boll JM, Kuhns LG, Herrera CM, et al. The Power of
1079 Asymmetry: Architecture and Assembly of the Gram-Negative Outer Membrane Lipid Bilayer. Annu Rev
1080 Microbiol. 2016;70:255-78. Epub 2016/07/01. doi: 10.1146/annurev-micro-102215-095308. PubMed
1081 PMID: 27359214.

1082 33. Pas C, Latka A, Fieseler L, Briers Y. Phage tailspike modularity and horizontal gene transfer reveals
1083 specificity towards *E. coli* O-antigen serogroups. Virol J. 2023;20(1):174. Epub 20230807. doi:
1084 10.1186/s12985-023-02138-4. PubMed PMID: 37550759; PubMed Central PMCID: PMCPMC10408124.

1085 34. Iglesias SM, Li F, Briani F, Cingolani G. Viral Genome Delivery Across Bacterial Cell Surfaces. Annu
1086 Rev Microbiol. 2024. Epub 20240709. doi: 10.1146/annurev-micro-041222-124727. PubMed PMID:
1087 38986128.

1088 35. Gaborieau B, Vaysset H, Tesson F, Charachon I, Dib N, Bernier J, et al. Predicting phage-bacteria
1089 interactions at the strain level from genomes. bioRxiv. 2023:2023.11.22.567924. doi:
1090 10.1101/2023.11.22.567924.

1091 36. Whitfield C, Williams DM, Kelly SD. Lipopolysaccharide O-antigens-bacterial glycans made to
1092 measure. J Biol Chem. 2020;295(31):10593-609. Epub 20200518. doi: 10.1074/jbc.REV120.009402.
1093 PubMed PMID: 32424042; PubMed Central PMCID: PMCPMC7397119.

1094 37. Islam MZ, Fokine A, Mahalingam M, Zhang Z, Garcia-Doval C, van Raaij MJ, et al. Molecular
1095 anatomy of the receptor binding module of a bacteriophage long tail fiber. PLoS Pathog.
1096 2019;15(12):e1008193. Epub 20191219. doi: 10.1371/journal.ppat.1008193. PubMed PMID: 31856258;
1097 PubMed Central PMCID: PMCPMC6957217.

1098 38. Zivanovic Y, Confalonieri F, Ponchon L, Lurz R, Chami M, Flayhan A, et al. Insights into
1099 bacteriophage T5 structure from analysis of its morphogenesis genes and protein components. J Virol.
1100 2014;88(2):1162-74. Epub 20131106. doi: 10.1128/JVI.02262-13. PubMed PMID: 24198424; PubMed
1101 Central PMCID: PMCPMC3911642.

1102 39. Steven AC, Trus BL, Maizel JV, Unser M, Parry DA, Wall JS, et al. Molecular substructure of a viral
1103 receptor-recognition protein. The gp17 tail-fiber of bacteriophage T7. J Mol Biol. 1988;200(2):351-65. doi:
1104 10.1016/0022-2836(88)90246-x. PubMed PMID: 3259634.

1105 40. Georjon H, Bernheim A. The highly diverse antiphage defence systems of bacteria. Nat Rev
1106 Microbiol. 2023;21(10):686-700. Epub 20230717. doi: 10.1038/s41579-023-00934-x. PubMed PMID:
1107 37460672.

1108 41. Lopatina A, Tal N, Sorek R. Abortive Infection: Bacterial Suicide as an Antiviral Immune Strategy.
1109 Annu Rev Virol. 2020;7(1):371-84. Epub 2020/06/20. doi: 10.1146/annurev-virology-011620-040628.
1110 PubMed PMID: 32559405.

1111 42. Yirmiya E, Leavitt A, Lu A, Ragucci AE, Avraham C, Osterman I, et al. Phages overcome bacterial
1112 immunity via diverse anti-defence proteins. Nature. 2023. Epub 20231122. doi: 10.1038/s41586-023-
1113 06869-w. PubMed PMID: 37992756.

1114 43. Samson JE, Magadan AH, Sabri M, Moineau S. Revenge of the phages: defeating bacterial
1115 defences. Nat Rev Microbiol. 2013;11(10):675-87. Epub 2013/08/28. doi: 10.1038/nrmicro3096. PubMed
1116 PMID: 23979432.

1117 44. Doron S, Melamed S, Ofir G, Leavitt A, Lopatina A, Keren M, et al. Systematic discovery of
1118 antiphage defense systems in the microbial pangenome. Science. 2018;359(6379). Epub 2018/01/27. doi:
1119 10.1126/science.aar4120. PubMed PMID: 29371424; PubMed Central PMCID: PMCPMC6387622.

1120 45. Tesson F, Herve A, Mordret E, Touchon M, d'Humieres C, Cury J, et al. Systematic and quantitative
1121 view of the antiviral arsenal of prokaryotes. Nat Commun. 2022;13(1):2561. Epub 2022/05/11. doi:
1122 10.1038/s41467-022-30269-9. PubMed PMID: 35538097; PubMed Central PMCID: PMCPMC9090908.

1123 46. Payne LJ, Todeschini TC, Wu Y, Perry BJ, Ronson CW, Fineran PC, et al. Identification and
1124 classification of antiviral defence systems in bacteria and archaea with PADLOC reveals new system types.
1125 Nucleic Acids Res. 2021;49(19):10868-78. Epub 2021/10/05. doi: 10.1093/nar/gkab883. PubMed PMID:
1126 34606606; PubMed Central PMCID: PMCPMC8565338.

1127 47. Vassallo CN, Doering CR, Littlehale ML, Teodoro GIC, Laub MT. A functional selection reveals
1128 previously undetected anti-phage defence systems in the *E. coli* pangenome. Nat Microbiol.
1129 2022;7(10):1568-79. Epub 20220919. doi: 10.1038/s41564-022-01219-4. PubMed PMID: 36123438;
1130 PubMed Central PMCID: PMCPMC9519451.

1131 48. Beamud B, Benz F, Bikard D. Going viral: The role of mobile genetic elements in bacterial
1132 immunity. Cell Host Microbe. 2024;32(6):804-19. doi: 10.1016/j.chom.2024.05.017. PubMed PMID:
1133 38870898.

1134 49. Wang X, Kim Y, Ma Q, Hong SH, Pokusaeva K, Sturino JM, et al. Cryptic prophages help bacteria
1135 cope with adverse environments. Nat Commun. 2010;1:147. doi: 10.1038/ncomms1146. PubMed PMID:
1136 21266997; PubMed Central PMCID: PMCPMC3105296.

1137 50. Olsen NS, Forero-Junco L, Kot W, Hansen LH. Exploring the Remarkable Diversity of Culturable
1138 *Escherichia coli* Phages in the Danish Wastewater Environment. Viruses. 2020;12(9). Epub 2020/09/10.
1139 doi: 10.3390/v12090986. PubMed PMID: 32899836; PubMed Central PMCID: PMCPMC7552041.

1140 51. Michniewski S, Redgwell T, Grigonyte A, Rihtman B, Aguilo-Ferretjans M, Christie-Oleza J, et al.
1141 Riding the wave of genomics to investigate aquatic coliphage diversity and activity. Environ Microbiol.
1142 2019;21(6):2112-28. Epub 2019/03/19. doi: 10.1111/1462-2920.14590. PubMed PMID: 30884081;
1143 PubMed Central PMCID: PMCPMC6563131.

1144 52. Mutalik VK, Arkin AP. A Phage Foundry Framework to Systematically Develop Viral
1145 Countermeasures to Combat Antibiotic-Resistant Bacterial Pathogens. iScience. 2022;25(4):104121. Epub
1146 2022/04/12. doi: 10.1016/j.isci.2022.104121. PubMed PMID: 35402883; PubMed Central PMCID:
1147 PMCPMC8983348.

1148 53. Venturini C, Petrovic Fabijan A, Fajardo Lubian A, Barbirz S, Iredell J. Biological foundations of
1149 successful bacteriophage therapy. EMBO Mol Med. 2022;n/a(n/a):e12435. Epub 2022/05/28. doi:
1150 10.15252/emmm.202012435. PubMed PMID: 35620963.

1151 54. Lood C, Boeckaerts D, Stock M, De Baets B, Lavigne R, van Noort V, et al. Digital phagograms:
1152 predicting phage infectivity through a multilayer machine learning approach. Curr Opin Virol.
1153 2022;52:174-81. Epub 20211221. doi: 10.1016/j.coviro.2021.12.004. PubMed PMID: 34952265.

1154 55. Siborova M, Fuzik T, Prochazkova M, Novacek J, Benesik M, Nilsson AS, et al. Tail proteins of phage
1155 SU10 reorganize into the nozzle for genome delivery. Nat Commun. 2022;13(1):5622. Epub 20220924.
1156 doi: 10.1038/s41467-022-33305-w. PubMed PMID: 36153309; PubMed Central PMCID:
1157 PMCPMC9509320.

1158 56. Korf IHE, Meier-Kolthoff JP, Adriaenssens EM, Kropinski AM, Nimtz M, Rohde M, et al. Still
1159 Something to Discover: Novel Insights into *Escherichia coli* Phage Diversity and Taxonomy. Viruses.
1160 2019;11(5). doi: 10.3390/v11050454. PubMed PMID: 31109012; PubMed Central PMCID:
1161 PMCPMC6563267.

1162 57. Vitt AR, Sørensen AN, Bojer MS, Bortolaia V, Sørensen MCH, Brøndsted L. Diverse bacteriophages
1163 for biocontrol of ESBL- and AmpC-β-lactamase-producing *E. coli*. iScience. 2024;27(2):108826. doi:
1164 https://doi.org/10.1016/j.isci.2024.108826.

1165 58. Zerbini FM, Siddell SG, Lefkowitz EJ, Mushegian AR, Adriaenssens EM, Alfenas-Zerbini P, et al.
1166 Changes to virus taxonomy and the ICTV Statutes ratified by the International Committee on Taxonomy
1167 of Viruses (2023). Arch Virol. 2023;168(7):175. Epub 20230610. doi: 10.1007/s00705-023-05797-4.
1168 PubMed PMID: 37296227; PubMed Central PMCID: PMCPMC10861154.

1169 59. Bertozzi Silva J, Storms Z, Sauvageau D. Host receptors for bacteriophage adsorption. FEMS
1170 Microbiol Lett. 2016;363(4). Epub 2016/01/13. doi: 10.1093/femsle/fnw002. PubMed PMID: 26755501.

1171 60. Hantke K. Compilation of *Escherichia coli* K-12 outer membrane phage receptors - their function
1172 and some historical remarks. FEMS Microbiol Lett. 2020;367(2). Epub 2020/02/06. doi:
1173 10.1093/femsle/fnaa013. PubMed PMID: 32009155.

1174 61. Du J, Meile S, Baggenstos J, Jaggi T, Piffaretti P, Hunold L, et al. Enhancing bacteriophage
1175 therapeutics through in situ production and release of heterologous antimicrobial effectors. Nat Commun.
1176 2023;14(1):4337. Epub 20230720. doi: 10.1038/s41467-023-39612-0. PubMed PMID: 37474516; PubMed
1177 Central PMCID: PMCPMC10359290.

1178 62. Mohammed M, Casjens SR, Millard AD, Harrison C, Gannon L, Chattaway MA. Genomic analysis
1179 of Anderson typing phages of *Salmonella* Typhimrium [sic]: towards understanding the basis of bacteria-
1180 phage interaction. Sci Rep. 2023;13(1):10484. Epub 20230628. doi: 10.1038/s41598-023-37307-6.
1181 PubMed PMID: 37380724; PubMed Central PMCID: PMCPMC10307801.

1182 63. Linares R, Arnaud CA, Effantin G, Darnault C, Epalle NH, Boeri Erba E, et al. Structural basis of
1183 bacteriophage T5 infection trigger and *E. coli* cell wall perforation. Sci Adv. 2023;9(12):eade9674. Epub
1184 20230324. doi: 10.1126/sciadv.ade9674. PubMed PMID: 36961893; PubMed Central PMCID:
1185 PMCPMC10038345.

1186 64. Ge X, Wang J. Structural mechanism of bacteriophage lambda tail's interaction with the bacterial
1187 receptor. Nat Commun. 2024;15(1):4185. Epub 20240517. doi: 10.1038/s41467-024-48686-3. PubMed
1188 PMID: 38760367; PubMed Central PMCID: PMCPMC11101478.

1189 65. Zeng C, Gilcrease EB, Hendrix RW, Xie Y, Jalfon MJ, Gill JJ, et al. DNA Packaging and Genomics of
1190 the *Salmonella* 9NA-Like Phages. J Virol. 2019;93(22). Epub 20191029. doi: 10.1128/JVI.00848-19.
1191 PubMed PMID: 31462565; PubMed Central PMCID: PMCPMC6819911.

1192 66. Hutinet G, Kot W, Cui L, Hillebrand R, Balamkundu S, Gnanakalai S, et al. 7-Deazaguanine
1193 modifications protect phage DNA from host restriction systems. Nat Commun. 2019;10(1):5442. Epub
1194 2019/12/01. doi: 10.1038/s41467-019-13384-y. PubMed PMID: 31784519; PubMed Central PMCID:
1195 PMCPMC6884629.

1196 67. Khan Mirzaei M, Eriksson H, Kasuga K, Haggard-Ljungquist E, Nilsson AS. Genomic, proteomic,
1197 morphological, and phylogenetic analyses of vB_EcoP_SU10, a podoviridae phage with C3 morphology.
1198 PLoS One. 2014;9(12):e116294. Epub 20141231. doi: 10.1371/journal.pone.0116294. PubMed PMID:
1199 25551446; PubMed Central PMCID: PMCPMC4281155.

1200 68. Batinovic S, Fujii Y, Nittami T. Expansion of *Kuravirus*-like Phage Sequences within the Past
1201 Decade, including *Escherichia* Phage YF01 from Japan, Prompt the Creation of Three New Genera. Viruses.
1202 2023;15(2). Epub 20230211. doi: 10.3390/v15020506. PubMed PMID: 36851720; PubMed Central PMCID:
1203 PMCPMC9965538.

1204 69. Zulk JJ, Clark JR, Ottinger S, Ballard MB, Mejia ME, Mercado-Evans V, et al. Phage Resistance
1205 Accompanies Reduced Fitness of Uropathogenic *Escherichia coli* in the Urinary Environment. mSphere.
1206 2022;7(4):e0034522. Epub 20220803. doi: 10.1128/msphere.00345-22. PubMed PMID: 35920561;
1207 PubMed Central PMCID: PMCPMC9429881.

1208 70. Gonzalez-Garcia VA, Pulido-Cid M, Garcia-Doval C, Bocanegra R, van Raaij MJ, Martin-Benito J, et
1209 al. Conformational changes leading to T7 DNA delivery upon interaction with the bacterial receptor. J Biol
1210 Chem. 2015;290(16):10038-44. Epub 2015/02/24. doi: 10.1074/jbc.M114.614222. PubMed PMID:
1211 25697363; PubMed Central PMCID: PMCPMC4400320.

1212 71. Hu B, Margolin W, Molineux IJ, Liu J. The bacteriophage T7 virion undergoes extensive structural
1213 remodeling during infection. Science. 2013;339(6119):576-9. Epub 2013/01/12. doi:
1214 10.1126/science.1231887. PubMed PMID: 23306440; PubMed Central PMCID: PMCPMC3873743.

1215 72. Trojet SN, Caumont-Sarcos A, Perrody E, Comeau AM, Krisch HM. The gp38 adhesins of the T4
1216 superfamily: a complex modular determinant of the phage's host specificity. Genome Biol Evol.
1217 2011;3:674-86. Epub 2011/07/13. doi: 10.1093/gbe/evr059. PubMed PMID: 21746838; PubMed Central
1218 PMCID: PMCPMC3157838.

1219 73. Washizaki A, Yonesaki T, Otsuka Y. Characterization of the interactions between *Escherichia coli*
1220 receptors, LPS and OmpC, and bacteriophage T4 long tail fibers. Microbiologyopen. 2016;5(6):1003-15.
1221 Epub 2016/06/09. doi: 10.1002/mbo3.384. PubMed PMID: 27273222; PubMed Central PMCID:
1222 PMCPMC5221442.

1223 74. Efimov AD, Golomidova AK, Kulikov EE, Belalov IS, Ivanov PA, Letarov AV. RB49-like
1224 Bacteriophages Recognize O Antigens as One of the Alternative Primary Receptors. Int J Mol Sci.
1225 2022;23(19). Epub 20220926. doi: 10.3390/ijms231911329. PubMed PMID: 36232640; PubMed Central
1226 PMCID: PMCPMC9569957.

1227 75. Weigele P, Raleigh EA. Biosynthesis and Function of Modified Bases in Bacteria and Their Viruses.
1228 Chem Rev. 2016;116(20):12655-87. Epub 2016/06/21. doi: 10.1021/acs.chemrev.6b00114. PubMed
1229 PMID: 27319741.

1230 76. Witte S, Zinsli LV, Gonzalez-Serrano R, Matter CI, Loessner MJ, van Mierlo JT, et al. Structural and
1231 functional characterization of the receptor binding proteins of *Escherichia coli* O157 phages EP75 and
1232 EP335. Comput Struct Biotechnol J. 2021;19:3416-26. Epub 20210604. doi: 10.1016/j.csbj.2021.06.001.
1233 PubMed PMID: 34194667; PubMed Central PMCID: PMCPMC8217332.

1234 77. Sidi Mabrouk A, Ongenae V, Claessen D, Brenzinger S, Briegel A. A Flexible and Efficient
1235 Microfluidics Platform for the Characterization and Isolation of Novel Bacteriophages. Appl Environ
1236 Microbiol. 2023;89(1):e0159622. Epub 20230105. doi: 10.1128/aem.01596-22. PubMed PMID: 36602353;
1237 PubMed Central PMCID: PMCPMC9888219.

1238 78. Adler BA, Al-Shimary MJ, Patel JR, Armbruster E, Colognori D, Charles EJ, et al. Genome-wide
1239 Characterization of Diverse Bacteriophages Enabled by RNA-Binding CRISPRi. bioRxiv.
1240 2023:2023.09.18.558157. doi: 10.1101/2023.09.18.558157.

1241 79. Swanson NA, Lokareddy RK, Li F, Hou CD, Leptihn S, Pavlenok M, et al. Cryo-EM structure of the
1242 periplasmic tunnel of T7 DNA-ejectosome at 2.7 A resolution. Mol Cell. 2021;81(15):3145-59 e7. Epub
1243 20210701. doi: 10.1016/j.molcel.2021.06.001. PubMed PMID: 34214465; PubMed Central PMCID:
1244 PMCPMC8349896.

1245 80. Santos TM, Bicalho RC. Complete genome sequence of vB_EcoM_ECO1230-10: a coliphage with
1246 therapeutic potential for bovine metritis. Vet Microbiol. 2011;148(2-4):267-75. Epub 20100908. doi:
1247 10.1016/j.vetmic.2010.08.034. PubMed PMID: 20875932.

1248 81. Lv M, Wang S, Yan G, Sun C, Feng X, Gu J, et al. Genome sequencing and analysis of an *Escherichia*
1249 *coli* phage vB_EcoM-ep3 with a novel lysin, Lysep3. Virus Genes. 2015;50(3):487-97. Epub 20150405. doi:
1250 10.1007/s11262-015-1195-8. PubMed PMID: 25842152.

1251 82. Kawato Y, Yasuike M, Nakamura Y, Shigenobu Y, Fujiwara A, Sano M, et al. Complete genome
1252 sequence analysis of two *Pseudomonas plecoglossicida* phages, potential therapeutic agents. Appl Environ
1253 Microbiol. 2015;81(3):874-81. Epub 20141121. doi: 10.1128/AEM.03038-14. PubMed PMID: 25416766;
1254 PubMed Central PMCID: PMCPMC4292507.

1255 83. Wishart DS, Han S, Saha S, Oler E, Peters H, Grant JR, et al. PHASTEST: faster than PHASTER, better
1256 than PHAST. Nucleic Acids Res. 2023;51(W1):W443-W50. doi: 10.1093/nar/gkad382. PubMed PMID:
1257 37194694; PubMed Central PMCID: PMCPMC10320120.

1258 84. Prokhorov NS, Riccio C, Zdorovenko EL, Shneider MM, Browning C, Knirel YA, et al. Function of
1259 bacteriophage G7C esterase tailspike in host cell adsorption. Mol Microbiol. 2017;105(3):385-98. Epub
1260 2017/05/18. doi: 10.1111/mmi.13710. PubMed PMID: 28513100.

1261 85. Tikhe CV, Gissendanner CR, Husseneder C. Whole-Genome Sequence of the Novel *Enterobacter*
1262 Bacteriophage Arya with an Integrase Pseudogene, Isolated from the Gut of the Formosan Subterranean
1263 Termite. Genome Announc. 2018;6(1). Epub 20180104. doi: 10.1128/genomeA.00838-17. PubMed PMID:
1264 29301894; PubMed Central PMCID: PMCPMC5754474.

1265 86. Boeckman J, Korn A, Yao G, Ravindran A, Gonzalez C, Gill J. Sheep in wolves' clothing: Temperate
1266 T7-like bacteriophages and the origins of the *Autographiviridae*. Virology. 2022;568:86-100. Epub
1267 20220131. doi: 10.1016/j.virol.2022.01.013. PubMed PMID: 35149347.

1268 87. Onallah H, Hazan R, Nir-Paz R, group Ps, Brownstein MJ, Fackler JR, et al. Refractory *Pseudomonas*
1269 *aeruginosa* infections treated with phage PASA16: A compassionate use case series. Med. 2023;4(9):600-
1270 11 e4. Epub 20230809. doi: 10.1016/j.medj.2023.07.002. PubMed PMID: 37562400.

1271 88. Pirnay JP, Djebara S, Steurs G, Griselain J, Cochez C, De Soir S, et al. Personalized bacteriophage
1272 therapy outcomes for 100 consecutive cases: a multicentre, multinational, retrospective observational
1273 study. Nat Microbiol. 2024;9(6):1434-53. Epub 20240604. doi: 10.1038/s41564-024-01705-x. PubMed
1274 PMID: 38834776; PubMed Central PMCID: PMCPMC11153159.

1275 89. Li F, Hou CD, Lokareddy RK, Yang R, Forti F, Briani F, et al. High-resolution cryo-EM structure of
1276 the *Pseudomonas* bacteriophage E217. Nat Commun. 2023;14(1):4052. Epub 20230708. doi:
1277 10.1038/s41467-023-39756-z. PubMed PMID: 37422479; PubMed Central PMCID: PMCPMC10329688.

1278 90. Necel A, Bloch S, Nejman-Falenczyk B, Grabski M, Topka G, Dydecka A, et al. Characterization of a
1279 bacteriophage, vB_Eco4M-7, that effectively infects many *Escherichia coli* O157 strains. Sci Rep.
1280 2020;10(1):3743. Epub 20200228. doi: 10.1038/s41598-020-60568-4. PubMed PMID: 32111934; PubMed
1281 Central PMCID: PMCPMC7048862.

1282 91. Heineman RH, Bull JJ. Testing optimality with experimental evolution: lysis time in a
1283 bacteriophage. Evolution. 2007;61(7):1695-709. doi: 10.1111/j.1558-5646.2007.00132.x. PubMed PMID:
1284 17598749; PubMed Central PMCID: PMCPMC1974807.

1285 92. Maffei E, Woischnig A-K, Burkolter MR, Heyer Y, Humolli D, Thürkauf N, et al. Phage Paride can
1286 kill dormant, antibiotic-tolerant cells of Pseudomonas aeruginosa by direct lytic replication. Nature
1287 Communications. 2024;15(1):175. doi: 10.1038/s41467-023-44157-3.

1288 93. Kropinski AM, Chan L, Jarrell K, Milazzo FH. The nature of *Pseudomonas aeruginosa* strain PAO
1289 bacteriophage receptors. Can J Microbiol. 1977;23(6):653-8. doi: 10.1139/m77-098. PubMed PMID:
1290 406024.

1291 94. Mutalik VK, Adler BA, Rishi HS, Piya D, Zhong C, Koskella B, et al. High-throughput mapping of the
1292 phage resistance landscape in *E. coli*. PLoS Biol. 2020;18(10):e3000877. Epub 2020/10/14. doi:
1293 10.1371/journal.pbio.3000877. PubMed PMID: 33048924; PubMed Central PMCID: PMCPMC7553319
1294 following competing interests: VKM, AMD, and APA consult for and hold equity in Felix Biotechnology,
1295 Inc.

1296 95. Kiljunen S, Vilen H, Pajunen M, Savilahti H, Skurnik M. Nonessential genes of phage phiYeO3-12
1297 include genes involved in adaptation to growth on *Yersinia enterocolitica* serotype O:3. J Bacteriol.

1298 2005;187(4):1405-14. Epub 2005/02/03. doi: 10.1128/JB.187.4.1405-1414.2005. PubMed PMID:
1299 15687205; PubMed Central PMCID: PMCPMC545605.

1300 96. Adler BA, Kazakov AE, Zhong C, Liu H, Kutter E, Lui LM, et al. The genetic basis of phage
1301 susceptibility, cross-resistance and host-range in *Salmonella*. Microbiology (Reading). 2021;167(12). Epub
1302 2021/12/16. doi: 10.1099/mic.0.001126. PubMed PMID: 34910616; PubMed Central PMCID:
1303 PMCPMC8744999.

1304 97. Tu J, Park T, Morado DR, Hughes KT, Molineux IJ, Liu J. Dual host specificity of phage SP6 is
1305 facilitated by tailspike rotation. Virology. 2017;507:206-15. Epub 20170426. doi:
1306 10.1016/j.virol.2017.04.017. PubMed PMID: 28456019; PubMed Central PMCID: PMCPMC5503682.

1307 98. Scholl D, Merril C. The genome of bacteriophage K1F, a T7-like phage that has acquired the ability
1308 to replicate on K1 strains of *Escherichia coli*. J Bacteriol. 2005;187(24):8499-503. Epub 2005/12/03. doi:
1309 10.1128/JB.187.24.8499-8503.2005. PubMed PMID: 16321955; PubMed Central PMCID:
1310 PMCPMC1317022.

1311 99. Lourenco M, Chaffringeon L, Lamy-Besnier Q, Titecat M, Pedron T, Sismeiro O, et al. The gut
1312 environment regulates bacterial gene expression which modulates susceptibility to bacteriophage
1313 infection. Cell Host Microbe. 2022;30(4):556-69 e5. Epub 2022/04/15. doi: 10.1016/j.chom.2022.03.014.
1314 PubMed PMID: 35421351.

1315 100. Molineux IJ, Spence JL. Virus-plasmid interactions: mutants of bacteriophage T3 that abortively
1316 infect plasmid F-containing (F+) strains of *Escherichia coli*. Proc Natl Acad Sci U S A. 1984;81(5):1465-9.
1317 Epub 1984/03/01. doi: 10.1073/pnas.81.5.1465. PubMed PMID: 6324192; PubMed Central PMCID:
1318 PMCPMC344857.

1319 101. Schmitt CK, Molineux IJ. Expression of gene 1.2 and gene 10 of bacteriophage T7 is lethal to F
1320 plasmid-containing *Escherichia coli*. J Bacteriol. 1991;173(4):1536-43. Epub 1991/02/01. doi:
1321 10.1128/jb.173.4.1536-1543.1991. PubMed PMID: 1995595; PubMed Central PMCID: PMCPMC207293.

1322 102. Heller K, Braun V. Polymannose O-antigens of *Escherichia coli*, the binding sites for the reversible
1323 adsorption of bacteriophage T5+ via the L-shaped tail fibers. J Virol. 1982;41(1):222-7. Epub 1982/01/01.
1324 doi: 10.1128/JVI.41.1.222-227.1982. PubMed PMID: 7045389; PubMed Central PMCID: PMCPMC256742.

1325 103. Gong Q, Wang X, Huang H, Sun Y, Qian X, Xue F, et al. Novel Host Recognition Mechanism of the
1326 K1 Capsule-Specific Phage of *Escherichia coli*: Capsular Polysaccharide as the First Receptor and
1327 Lipopolysaccharide as the Secondary Receptor. J Virol. 2021;95(18):e0092021. Epub 20210825. doi:
1328 10.1128/JVI.00920-21. PubMed PMID: 34191582; PubMed Central PMCID: PMCPMC8387036.

1329 104. Paysan-Lafosse T, Blum M, Chuguransky S, Grego T, Pinto BL, Salazar GA, et al. InterPro in 2022.
1330 Nucleic Acids Res. 2023;51(D1):D418-D27. doi: 10.1093/nar/gkac993. PubMed PMID: 36350672; PubMed
1331 Central PMCID: PMCPMC9825450.

1332 105. Beamud B, Garcia-Gonzalez N, Gomez-Ortega M, Gonzalez-Candelas F, Domingo-Calap P, Sanjuan
1333 R. Genetic determinants of host tropism in *Klebsiella* phages. Cell Rep. 2023;42(2):112048. Epub
1334 20230206. doi: 10.1016/j.celrep.2023.112048. PubMed PMID: 36753420; PubMed Central PMCID:
1335 PMCPMC9989827.

1336 106. Smug BJ, Szczepaniak K, Rocha EPC, Dunin-Horkawicz S, Mostowy RJ. Ongoing shuffling of protein
1337 fragments diversifies core viral functions linked to interactions with bacterial hosts. Nat Commun.

1338 2023;14(1):7460. Epub 20231128. doi: 10.1038/s41467-023-43236-9. PubMed PMID: 38016962; PubMed
1339 Central PMCID: PMCPMC10684548.

1340 107. Hu B, Margolin W, Molineux IJ, Liu J. Structural remodeling of bacteriophage T4 and host
1341 membranes during infection initiation. Proc Natl Acad Sci U S A. 2015;112(35):E4919-28. Epub
1342 2015/08/19. doi: 10.1073/pnas.1501064112. PubMed PMID: 26283379; PubMed Central PMCID:
1343 PMCPMC4568249.

1344 108. Evans R, O'Neill M, Pritzel A, Antropova N, Senior A, Green T, et al. Protein complex prediction
1345 with AlphaFold-Multimer. bioRxiv. 2022:2021.10.04.463034. doi: 10.1101/2021.10.04.463034.

1346 109. Bartual SG, Otero JM, Garcia-Doval C, Llamas-Saiz AL, Kahn R, Fox GC, et al. Structure of the
1347 bacteriophage T4 long tail fiber receptor-binding tip. Proc Natl Acad Sci U S A. 2010;107(47):20287-92.
1348 Epub 20101101. doi: 10.1073/pnas.1011218107. PubMed PMID: 21041684; PubMed Central PMCID:
1349 PMCPMC2996694.

1350 110. Garcia-Doval C, Caston JR, Luque D, Granell M, Otero JM, Llamas-Saiz AL, et al. Structure of the
1351 Receptor-Binding Carboxy-Terminal Domain of the Bacteriophage T5 L-Shaped Tail Fibre with and without
1352 Its Intra-Molecular Chaperone. Viruses. 2015;7(12):6424-40. Epub 20151208. doi: 10.3390/v7122946.
1353 PubMed PMID: 26670244; PubMed Central PMCID: PMCPMC4690869.

1354 111. Hyman P. Phages for Phage Therapy: Isolation, Characterization, and Host Range Breadth.
1355 Pharmaceuticals (Basel). 2019;12(1). Epub 2019/03/14. doi: 10.3390/ph12010035. PubMed PMID:
1356 30862020; PubMed Central PMCID: PMCPMC6469166.

1357 112. Khan Mirzaei M, Nilsson AS. Isolation of phages for phage therapy: a comparison of spot tests and
1358 efficiency of plating analyses for determination of host range and efficacy. PLoS One.
1359 2015;10(3):e0118557. doi: 10.1371/journal.pone.0118557. PubMed PMID: 25761060; PubMed Central
1360 PMCID: PMCPMC4356574.

1361 113. Holtappels D, Alfenas-Zerbini P, Koskella B. Drivers and consequences of bacteriophage host
1362 range. FEMS Microbiol Rev. 2023;47(4). doi: 10.1093/femsre/fuad038. PubMed PMID: 37422441.

1363 114. Abedon ST. Lysis from without. Bacteriophage. 2011;1(1):46-9. doi: 10.4161/bact.1.1.13980.
1364 PubMed PMID: 21687534; PubMed Central PMCID: PMCPMC3109453.

1365 115. Meile S, Du J, Staubli S, Grossmann S, Koliwer-Brandl H, Piffaretti P, et al. Engineered reporter
1366 phages for detection of *Escherichia coli*, *Enterococcus*, and *Klebsiella* in urine. Nat Commun.
1367 2023;14(1):4336. Epub 20230720. doi: 10.1038/s41467-023-39863-x. PubMed PMID: 37474554; PubMed
1368 Central PMCID: PMCPMC10359277.

1369 116. Loose M, Saez Moreno D, Mutti M, Hitzenhammer E, Visram Z, Dippel D, et al. Natural Bred ε2-
1370 Phages Have an Improved Host Range and Virulence against Uropathogenic *Escherichia coli* over Their
1371 Ancestor Phages. Antibiotics (Basel). 2021;10(11). Epub 20211101. doi: 10.3390/antibiotics10111337.
1372 PubMed PMID: 34827275; PubMed Central PMCID: PMCPMC8614997.

1373 117. Schwarzer D, Buettner FF, Browning C, Nazarov S, Rabsch W, Bethe A, et al. A multivalent
1374 adsorption apparatus explains the broad host range of phage phi92: a comprehensive genomic and
1375 structural analysis. J Virol. 2012;86(19):10384-98. Epub 2012/07/13. doi: 10.1128/JVI.00801-12. PubMed
1376 PMID: 22787233; PubMed Central PMCID: PMCPMC3457257.

1377 118. Manohar P, Tamhankar AJ, Lundborg CS, Ramesh N. Isolation, characterization and in vivo efficacy
1378 of *Escherichia* phage myPSH1131. PLoS One. 2018;13(10):e0206278. Epub 20181024. doi:
1379 10.1371/journal.pone.0206278. PubMed PMID: 30356310; PubMed Central PMCID: PMCPMC6200275.

1380 119. He Z, Parra B, Nesme J, Smets BF, Dechesne A. Quantification and fate of plasmid-specific
1381 bacteriophages in wastewater: Beyond the F-coliphages. Water Res. 2022;227:119320. Epub 20221104.
1382 doi: 10.1016/j.watres.2022.119320. PubMed PMID: 36395568.

1383 120. Wietzorrek A, Schwarz H, Herrmann C, Braun V. The genome of the novel phage Rtp, with a
1384 rosette-like tail tip, is homologous to the genome of phage T1. J Bacteriol. 2006;188(4):1419-36. Epub
1385 2006/02/03. doi: 10.1128/JB.188.4.1419-1436.2006. PubMed PMID: 16452425; PubMed Central PMCID:
1386 PMCPMC1367250.

1387 121. Decker K, Krauel V, Meesmann A, Heller KJ. Lytic conversion of *Escherichia coli* by bacteriophage
1388 T5: blocking of the FhuA receptor protein by a lipoprotein expressed early during infection. Mol Microbiol.
1389 1994;12(2):321-32. doi: 10.1111/j.1365-2958.1994.tb01020.x. PubMed PMID: 8057856.

1390 122. Silveira CB, Luque A, Rohwer F. The landscape of lysogeny across microbial community density,
1391 diversity and energetics. Environ Microbiol. 2021;23(8):4098-111. Epub 2021/06/15. doi: 10.1111/1462-
1392 2920.15640. PubMed PMID: 34121301.

1393 123. Gonzalez-Serrano R, Rosselli R, Roda-Garcia JJ, Martin-Cuadrado AB, Rodriguez-Valera F, Dunne
1394 M. Distantly related *Alteromonas* bacteriophages share tail fibers exhibiting properties of transient
1395 chaperone caps. Nat Commun. 2023;14(1):6517. Epub 20231016. doi: 10.1038/s41467-023-42114-8.
1396 PubMed PMID: 37845226; PubMed Central PMCID: PMCPMC10579305.

1397 124. Quinones-Olvera N, Owen SV, McCully LM, Marin MG, Rand EA, Fan AC, et al. Diverse and
1398 abundant phages exploit conjugative plasmids. Nat Commun. 2024;15(1):3197. Epub 20240412. doi:
1399 10.1038/s41467-024-47416-z. PubMed PMID: 38609370; PubMed Central PMCID: PMCPMC11015023.

1400 125. Gambino M, Sorensen MCH. Flagellotropic phages: common yet diverse host interaction
1401 strategies. Curr Opin Microbiol. 2024;78:102451. Epub 20240306. doi: 10.1016/j.mib.2024.102451.
1402 PubMed PMID: 38452595.

1403 126. Nobrega FL, Vlot M, de Jonge PA, Dreesens LL, Beaumont HJE, Lavigne R, et al. Targeting
1404 mechanisms of tailed bacteriophages. Nat Rev Microbiol. 2018;16(12):760-73. Epub 2018/08/15. doi:
1405 10.1038/s41579-018-0070-8. PubMed PMID: 30104690.

1406 127. Iglesias SM, Lokareddy RK, Yang R, Li F, Yeggoni DP, David Hou CF, et al. Molecular Architecture of
1407 *Salmonella Typhimurium* [sic]Virus P22 Genome Ejection Machinery. J Mol Biol. 2023;435(24):168365.
1408 Epub 20231110. doi: 10.1016/j.jmb.2023.168365. PubMed PMID: 37952769; PubMed Central PMCID:
1409 PMCPMC10842050.

1410 128. Ouyang R, Ongenae V, Muok A, Claessen D, Briegel A. Phage fibers and spikes: a nanoscale Swiss
1411 army knife for host infection. Curr Opin Microbiol. 2024;77:102429. Epub 20240126. doi:
1412 10.1016/j.mib.2024.102429. PubMed PMID: 38277900.

1413 129. Gordillo Altamirano FL, Barr JJ. Unlocking the next generation of phage therapy: the key is in the
1414 receptors. Curr Opin Biotechnol. 2020;68:115-23. Epub 2020/11/18. doi: 10.1016/j.copbio.2020.10.002.
1415 PubMed PMID: 33202354.

130. Dunne M, Prokhorov NS, Loessner MJ, Leiman PG. Reprogramming bacteriophage host range: design principles and strategies for engineering receptor binding proteins. Curr Opin Biotechnol. 2021;68:272-81. Epub 20210318. doi: 10.1016/j.copbio.2021.02.006. PubMed PMID: 33744824; PubMed Central PMCID: PMCPMC10163921.

131. Haudiquet M, Le Bris J, Nucci A, Bonnin RA, Domingo-Calap P, Rocha EPC, et al. Capsules and their traits shape phage susceptibility and plasmid conjugation efficiency. Nat Commun. 2024;15(1):2032. Epub 20240306. doi: 10.1038/s41467-024-46147-5. PubMed PMID: 38448399; PubMed Central PMCID: PMCPMC10918111.

132. Ferriol-Gonzalez C, Concha-Eloko R, Bernabeu-Gimeno M, Fernandez-Cuenca F, Canada-Garcia JE, Garcia-Cobos S, et al. Targeted phage hunting to specific *Klebsiella pneumoniae* clinical isolates is an efficient antibiotic resistance and infection control strategy. Microbiol Spectr. 2024:e0025424. Epub 20240828. doi: 10.1128/spectrum.00254-24. PubMed PMID: 39194291.

133. Boeckaerts D, Stock M, Ferriol-Gonzalez C, Oteo-Iglesias J, Sanjuan R, Domingo-Calap P, et al. Prediction of *Klebsiella* phage-host specificity at the strain level. Nat Commun. 2024;15(1):4355. Epub 20240522. doi: 10.1038/s41467-024-48675-6. PubMed PMID: 38778023; PubMed Central PMCID: PMCPMC11111740.

134. Wright RCT, Friman VP, Smith MCM, Brockhurst MA. Cross-resistance is modular in bacteria-phage interactions. PLoS Biol. 2018;16(10):e2006057. Epub 2018/10/04. doi: 10.1371/journal.pbio.2006057. PubMed PMID: 30281587; PubMed Central PMCID: PMCPMC6188897.

135. Göller PC, Elsener T, Lorge D, Radulovic N, Bernardi V, Naumann A, et al. Multi-species host range of staphylococcal phages isolated from wastewater. Nat Commun. 2021;12(1):6965. Epub 2021/12/01. doi: 10.1038/s41467-021-27037-6. PubMed PMID: 34845206; PubMed Central PMCID: PMCPMC8629997.

136. Walsh SK, Imrie RM, Matuszewska M, Paterson GK, Weinert LA, Hadfield JD, et al. The host phylogeny determines viral infectivity and replication across *Staphylococcus* host species. PLoS Pathog. 2023;19(6):e1011433. Epub 20230608. doi: 10.1371/journal.ppat.1011433. PubMed PMID: 37289828; PubMed Central PMCID: PMCPMC10284401.

137. Piel D, Bruto M, Labreuche Y, Blanquart F, Goudenege D, Barcia-Cruz R, et al. Phage-host coevolution in natural populations. Nat Microbiol. 2022;7(7):1075-86. Epub 2022/06/28. doi: 10.1038/s41564-022-01157-1. PubMed PMID: 35760840.

138. Hussain FA, Dubert J, Elsherbini J, Murphy M, VanInsberghe D, Arevalo P, et al. Rapid evolutionary turnover of mobile genetic elements drives bacterial resistance to phages. Science. 2021;374(6566):488-92. Epub 20211021. doi: 10.1126/science.abb1083. PubMed PMID: 34672730.

139. Roberts RJ, Vincze T, Posfai J, Macelis D. REBASE--a database for DNA restriction and modification: enzymes, genes and genomes. Nucleic Acids Res. 2015;43(Database issue):D298-9. Epub 2014/11/08. doi: 10.1093/nar/gku1046. PubMed PMID: 25378308; PubMed Central PMCID: PMCPMC4383893.

140. Kortright KE, Chan BK, Koff JL, Turner PE. Phage Therapy: A Renewed Approach to Combat Antibiotic-Resistant Bacteria. Cell Host Microbe. 2019;25(2):219-32. Epub 2019/02/15. doi: 10.1016/j.chom.2019.01.014. PubMed PMID: 30763536.

141. Aslam S, Lampley E, Wooten D, Karris M, Benson C, Strathdee S, et al. Lessons Learned From the First 10 Consecutive Cases of Intravenous Bacteriophage Therapy to Treat Multidrug-Resistant Bacterial

1457 Infections at a Single Center in the United States. Open Forum Infect Dis. 2020;7(9):ofaa389. Epub
1458 2020/10/03. doi: 10.1093/ofid/ofaa389. PubMed PMID: 33005701; PubMed Central PMCID:
1459 PMCPMC7519779.

1460 142. Meile S, Du J, Dunne M, Kilcher S, Loessner MJ. Engineering therapeutic phages for enhanced
1461 antibacterial efficacy. Curr Opin Virol. 2022;52:182-91. Epub 20211221. doi:
1462 10.1016/j.coviro.2021.12.003. PubMed PMID: 34952266.

1463 143. Gencay YE, Jasinskyte D, Robert C, Semsey S, Martinez V, Petersen AO, et al. Engineered phage
1464 with antibacterial CRISPR-Cas selectively reduce *E. coli* burden in mice. Nat Biotechnol. 2024;42(2):265-
1465 74. Epub 20230504. doi: 10.1038/s41587-023-01759-y. PubMed PMID: 37142704; PubMed Central
1466 PMCID: PMCPMC10869271.

1467 144. Brödel AK, Charpenay LH, Galtier M, Fuche FJ, Terrasse R, Poquet C, et al. In situ targeted base
1468 editing of bacteria in the mouse gut. Nature. 2024. Epub 20240710. doi: 10.1038/s41586-024-07681-w.
1469 PubMed PMID: 38987595.

1470 145. Kim P, Sanchez AM, Penke TJR, Tuson HH, Kime JC, McKee RW, et al. Safety, pharmacokinetics,
1471 and pharmacodynamics of LBP-EC01, a CRISPR-Cas3-enhanced bacteriophage cocktail, in uncomplicated
1472 urinary tract infections due to *Escherichia coli* (ELIMINATE): the randomised, open-label, first part of a
1473 two-part phase 2 trial. Lancet Infect Dis. 2024. Epub 20240809. doi: 10.1016/S1473-3099(24)00424-9.
1474 PubMed PMID: 39134085.

1475 146. Kropinski AM, Mazzocco A, Waddell TE, Lingohr E, Johnson RP. Enumeration of bacteriophages by
1476 double agar overlay plaque assay. Methods Mol Biol. 2009;501:69-76. doi: 10.1007/978-1-60327-164-6_7.
1477 PubMed PMID: 19066811.

1478 147. Kauffman KM, Polz MF. Streamlining standard bacteriophage methods for higher throughput.
1479 MethodsX. 2018;5:159-72. Epub 2019/01/10. doi: 10.1016/j.mex.2018.01.007. PubMed PMID: 30622914;
1480 PubMed Central PMCID: PMCPMC6318102.

1481 148. Pleska M, Qian L, Okura R, Bergmiller T, Wakamoto Y, Kussell E, et al. Bacterial Autoimmunity Due
1482 to a Restriction-Modification System. Curr Biol. 2016;26(3):404-9. Epub 2016/01/26. doi:
1483 10.1016/j.cub.2015.12.041. PubMed PMID: 26804559.

1484 149. Baba T, Ara T, Hasegawa M, Takai Y, Okumura Y, Baba M, et al. Construction of *Escherichia coli* K-
1485 12 in-frame, single-gene knockout mutants: the Keio collection. Mol Syst Biol. 2006;2:2006 0008. doi:
1486 10.1038/msb4100050. PubMed PMID: 16738554; PubMed Central PMCID: PMC1681482.

1487 150. Xue C, Sashital DG. Mechanisms of Type I-E and I-F CRISPR-Cas Systems in *Enterobacteriaceae*.
1488 EcoSal Plus. 2019;8(2). doi: 10.1128/ecosalplus.ESP-0008-2018. PubMed PMID: 30724156; PubMed
1489 Central PMCID: PMCPMC6368399.

1490 151. Strotskaya A, Savitskaya E, Metlitskaya A, Morozova N, Datsenko KA, Semenova E, et al. The action
1491 of *Escherichia coli* CRISPR-Cas system on lytic bacteriophages with different lifestyles and development
1492 strategies. Nucleic Acids Res. 2017;45(4):1946-57. Epub 2017/01/29. doi: 10.1093/nar/gkx042. PubMed
1493 PMID: 28130424; PubMed Central PMCID: PMCPMC5389539.

1494 152. Yu YT, Snyder L. Translation elongation factor Tu cleaved by a phage-exclusion system. Proc Natl
1495 Acad Sci U S A. 1994;91(2):802-6. Epub 1994/01/18. doi: 10.1073/pnas.91.2.802. PubMed PMID: 8290603;
1496 PubMed Central PMCID: PMCPMC43037.

1497 153. Koga M, Otsuka Y, Lemire S, Yonesaki T. *Escherichia coli rnlA* and *rnlB* compose a novel toxin-
1498 antitoxin system. Genetics. 2011;187(1):123-30. Epub 2010/10/29. doi: 10.1534/genetics.110.121798.
1499 PubMed PMID: 20980243; PubMed Central PMCID: PMCPmc3018318.

1500 154. Ragunathan PT, Vanderpool CK. Cryptic-Prophage-Encoded Small Protein DicB Protects
1501 *Escherichia coli* from Phage Infection by Inhibiting Inner Membrane Receptor Proteins. J Bacteriol.
1502 2019;201(23). Epub 2019/09/19. doi: 10.1128/JB.00475-19. PubMed PMID: 31527115; PubMed Central
1503 PMCID: PMCPMC6832061.

1504 155. Sasaki T, Takita S, Fujishiro T, Shintani Y, Nojiri S, Yasui R, et al. Phage single-stranded DNA-binding
1505 protein or host DNA damage triggers the activation of the AbpAB phage defense system. mSphere.
1506 2023:e0037223. Epub 20231026. doi: 10.1128/msphere.00372-23. PubMed PMID: 37882551.

1507 156. Grenier F, Matteau D, Baby V, Rodrigue S. Complete Genome Sequence of *Escherichia coli*
1508 BW25113. Genome Announc. 2014;2(5). Epub 20141016. doi: 10.1128/genomeA.01038-14. PubMed
1509 PMID: 25323716; PubMed Central PMCID: PMCPMC4200154.

1510 157. Bachmann BJ. Pedigrees of some mutant strains of *Escherichia coli* K-12. Bacteriol Rev.
1511 1972;36(4):525-57. doi: 10.1128/br.36.4.525-557.1972. PubMed PMID: 4568763; PubMed Central
1512 PMCID: PMCPMC408331.

1513 158. Cuenod A, Agnetti J, Seth-Smith HMB, Roloff T, Walchli D, Shcherbakov D, et al. Bacterial genome-
1514 wide association study substantiates *papGII* of *Escherichia coli* as a major risk factor for urosepsis. Genome
1515 Med. 2023;15(1):89. Epub 20231030. doi: 10.1186/s13073-023-01243-x. PubMed PMID: 37904175;
1516 PubMed Central PMCID: PMCPMC10614358.

1517 159. Abedon ST, Katsaounis TI. Basic Phage Mathematics. Methods Mol Biol. 2018;1681:3-30. Epub
1518 2017/11/15. doi: 10.1007/978-1-4939-7343-9_1. PubMed PMID: 29134583.

1519 160. Garneau JR, Depardieu F, Fortier LC, Bikard D, Monot M. PhageTerm: a tool for fast and accurate
1520 determination of phage termini and packaging mechanism using next-generation sequencing data. Sci
1521 Rep. 2017;7(1):8292. Epub 2017/08/16. doi: 10.1038/s41598-017-07910-5. PubMed PMID: 28811656;
1522 PubMed Central PMCID: PMCPMC5557969.

1523 161. Bouras G, Nepal R, Houtak G, Psaltis AJ, Wormald PJ, Vreugde S. Pharokka: a fast scalable
1524 bacteriophage annotation tool. Bioinformatics. 2023;39(1). doi: 10.1093/bioinformatics/btac776.
1525 PubMed PMID: 36453861; PubMed Central PMCID: PMCPMC9805569.

1526 162. Chan PP, Lowe TM. tRNAscan-SE: Searching for tRNA Genes in Genomic Sequences. Methods Mol
1527 Biol. 2019;1962:1-14. Epub 2019/04/26. doi: 10.1007/978-1-4939-9173-0_1. PubMed PMID: 31020551;
1528 PubMed Central PMCID: PMCPMC6768409.

1529 163. Katoh K, Standley DM. MAFFT multiple sequence alignment software version 7: improvements in
1530 performance and usability. Mol Biol Evol. 2013;30(4):772-80. Epub 2013/01/19. doi:
1531 10.1093/molbev/mst010. PubMed PMID: 23329690; PubMed Central PMCID: PMCPMC3603318.

1532 164. Mistry J, Chuguransky S, Williams L, Qureshi M, Salazar GA, Sonnhammer ELL, et al. Pfam: The
1533 protein families database in 2021. Nucleic Acids Res. 2021;49(D1):D412-D9. doi: 10.1093/nar/gkaa913.
1534 PubMed PMID: 33125078; PubMed Central PMCID: PMCPMC7779014.

165. Wang J, Chitsaz F, Derbyshire MK, Gonzales NR, Gwadz M, Lu S, et al. The conserved domain database in 2023. Nucleic Acids Res. 2023;51(D1):D384-D8. doi: 10.1093/nar/gkac1096. PubMed PMID: 36477806; PubMed Central PMCID: PMCPMC9825596.

166. Sillitoe I, Bordin N, Dawson N, Waman VP, Ashford P, Scholes HM, et al. CATH: increased structural coverage of functional space. Nucleic Acids Res. 2021;49(D1):D266-D73. doi: 10.1093/nar/gkaa1079. PubMed PMID: 33237325; PubMed Central PMCID: PMCPMC7778904.

167. Terzian P, Olo Ndela E, Galiez C, Lossouarn J, Perez Bucio RE, Mom R, et al. PHROG: families of prokaryotic virus proteins clustered using remote homology. NAR Genom Bioinform. 2021;3(3):lqab067. Epub 20210805. doi: 10.1093/nargab/lqab067. PubMed PMID: 34377978; PubMed Central PMCID: PMCPMC8341000.

168. Steinegger M, Meier M, Mirdita M, Vohringer H, Haunsberger SJ, Söding J. HH-suite3 for fast remote homology detection and deep protein annotation. BMC Bioinformatics. 2019;20(1):473. Epub 20190914. doi: 10.1186/s12859-019-3019-7. PubMed PMID: 31521110; PubMed Central PMCID: PMCPMC6744700.

169. Steinegger M, Söding J. Clustering huge protein sequence sets in linear time. Nat Commun. 2018;9(1):2542. Epub 20180629. doi: 10.1038/s41467-018-04964-5. PubMed PMID: 29959318; PubMed Central PMCID: PMCPMC6026198.

170. Berman HM, Westbrook J, Feng Z, Gilliland G, Bhat TN, Weissig H, et al. The Protein Data Bank. Nucleic Acids Res. 2000;28(1):235-42. doi: 10.1093/nar/28.1.235. PubMed PMID: 10592235; PubMed Central PMCID: PMCPMC102472.

171. UniProt C. UniProt: the Universal Protein Knowledgebase in 2023. Nucleic Acids Res. 2023;51(D1):D523-D31. doi: 10.1093/nar/gkac1052. PubMed PMID: 36408920; PubMed Central PMCID: PMCPMC9825514.

172. O'Leary NA, Wright MW, Brister JR, Ciufo S, Haddad D, McVeigh R, et al. Reference sequence (RefSeq) database at NCBI: current status, taxonomic expansion, and functional annotation. Nucleic Acids Res. 2016;44(D1):D733-45. Epub 20151108. doi: 10.1093/nar/gkv1189. PubMed PMID: 26553804; PubMed Central PMCID: PMCPMC4702849.

173. Jumper J, Evans R, Pritzel A, Green T, Figurnov M, Ronneberger O, et al. Highly accurate protein structure prediction with AlphaFold. Nature. 2021;596(7873):583-9. Epub 2021/07/16. doi: 10.1038/s41586-021-03819-2. PubMed PMID: 34265844; PubMed Central PMCID: PMCPMC8371605.

174. van Kempen M, Kim SS, Tumescheit C, Mirdita M, Lee J, Gilchrist CLM, et al. Fast and accurate protein structure search with Foldseek. Nat Biotechnol. 2024;42(2):243-6. Epub 20230508. doi: 10.1038/s41587-023-01773-0. PubMed PMID: 37156916; PubMed Central PMCID: PMCPMC10869269.

175. Adriaenssens E, Brister JR. How to Name and Classify Your Phage: An Informal Guide. Viruses. 2017;9(4). doi: 10.3390/v9040070. PubMed PMID: 28368359; PubMed Central PMCID: PMCPMC5408676.

176. Tolstoy I, Kropinski AM, Brister JR. Bacteriophage Taxonomy: An Evolving Discipline. Methods Mol Biol. 2018;1693:57-71. Epub 2017/11/10. doi: 10.1007/978-1-4939-7395-8_6. PubMed PMID: 29119432.

177. Grose JH, Casjens SR. Understanding the enormous diversity of bacteriophages: the tailed phages that infect the bacterial family *Enterobacteriaceae*. Virology. 2014;468-470:421-43. Epub 2014/09/23. doi: 10.1016/j.virol.2014.08.024. PubMed PMID: 25240328; PubMed Central PMCID: PMCPMC4301999.

1575 178. Turner D, Adriaenssens EM, Lehman SM, Moraru C, Kropinski AM. Bacteriophage Taxonomy: A
1576 Continually Evolving Discipline. Methods Mol Biol. 2024;2734:27-45. doi: 10.1007/978-1-0716-3523-0_3.
1577 PubMed PMID: 38066361.

1578 179. Guindon S, Dufayard JF, Lefort V, Anisimova M, Hordijk W, Gascuel O. New algorithms and
1579 methods to estimate maximum-likelihood phylogenies: assessing the performance of PhyML 3.0. Syst Biol.
1580 2010;59(3):307-21. Epub 2010/06/09. doi: 10.1093/sysbio/syq010. PubMed PMID: 20525638.

1581 180. Cianfrocco MA, Wong-Barnum M, Youn C, Wagner R, Leschziner A. COSMIC2: A Science Gateway
1582 for Cryo-Electron Microscopy Structure Determination. Practice and Experience in Advanced Research
1583 Computing 2017: Sustainability, Success and Impact; New Orleans, LA, USA: Association for Computing
1584 Machinery; 2017. p. Article 22.

1585 181. Abramson J, Adler J, Dunger J, Evans R, Green T, Pritzel A, et al. Accurate structure prediction of
1586 biomolecular interactions with AlphaFold 3. Nature. 2024;630(8016):493-500. Epub 20240508. doi:
1587 10.1038/s41586-024-07487-w. PubMed PMID: 38718835; PubMed Central PMCID: PMCPMC11168924.

1588 182. Holm L. Dali server: structural unification of protein families. Nucleic Acids Res.
1589 2022;50(W1):W210-W5. doi: 10.1093/nar/gkac387. PubMed PMID: 35610055; PubMed Central PMCID:
1590 PMCPMC9252788.

1591 183. Aziz RK, Ackermann HW, Petty NK, Kropinski AM. Essential Steps in Characterizing Bacteriophages:
1592 Biology, Taxonomy, and Genome Analysis. Methods Mol Biol. 2018;1681:197-215. Epub 2017/11/15. doi:
1593 10.1007/978-1-4939-7343-9_15. PubMed PMID: 29134597.

1594 184. Abedon ST. Detection of Bacteriophages: Phage Plaques. In: Harper DR, Abedon ST, Burrowes BH,
1595 McConville ML, editors. Bacteriophages: Biology, Technology, Therapy. Cham: Springer International
1596 Publishing; 2018. p. 1-32.

1597 185. Pick K, Ju T, Willing BP, Raivio TL. Isolation and Characterization of a Novel Temperate *Escherichia*
1598 *coli* Bacteriophage, Kapi1, Which Modifies the O-Antigen and Contributes to the Competitiveness of Its
1599 Host during Colonization of the Murine Gastrointestinal Tract. mBio. 2022;13(1):e0208521. Epub
1600 20220125. doi: 10.1128/mbio.02085-21. PubMed PMID: 35073745; PubMed Central PMCID:
1601 PMCPMC8787464.

1602 186. Bertani B, Ruiz N. Function and Biogenesis of Lipopolysaccharides. EcoSal Plus. 2018;8(1). Epub
1603 2018/08/02. doi: 10.1128/ecosalplus.ESP-0001-2018. PubMed PMID: 30066669; PubMed Central PMCID:
1604 PMCPMC6091223.

1605 187. North OI, Sakai K, Yamashita E, Nakagawa A, Iwazaki T, Buttner CR, et al. Phage tail fibre assembly
1606 proteins employ a modular structure to drive the correct folding of diverse fibres. Nat Microbiol.
1607 2019;4(10):1645-53. Epub 20190617. doi: 10.1038/s41564-019-0477-7. PubMed PMID: 31209305.

1608

1609 # Data reporting

1610 All data generated or analyzed during this study are included in this published article. The raw data
1611 of every replicate experiment underlying the plots shown in Figs. 5D, 6G, 7D, 8G, 9E, 10D, 11A/B, and
1612 S1A/B as well as all calculations underlying the summary data in these figures are compiled in S1 Data.
1613 The code that has been used to run GAPS for the results presented in this work is available at
1614 https://github.com/hiller-lab/gaps.

1615 # Accession numbers

1616 The annotated genome sequences of all 36 newly isolated phages will be available at the NCBI
1617 GenBank database under accession numbers listed in Table S2 with the final publication after peer review.

1618 # Figure Legends

1619 (Figure legends are included with the figures in the main text)

1620 # Supporting Information Captions

1621 **Table S1. Isolation of O16-dependent and K12-prophage-inhibited phages from**
1622 **sewage and environmental samples**

1623 **Table S2. List of all phages used in this study.**

1624 This table presents the taxonomic classification, isolation / source, host receptors, and genomic
1625 features of all phages characterized in this study.

1626 **Table S3. List of all bacterial strains used in this study.**

1627 This table presents all bacterial strains that have been used in this work. The abbreviations in the
1628 selection column indicate the drug and its concentration that were used. Amp = ampicillin, Cam =

1629 chloramphenicol, Kan = kanamycin, Zeo = zeocin; 25 / 50 / 100 refer to 25 µg/ml, 50 µg/ml, and 100 = 100
1630 µg/ml, respectively.

1631 **Table S4. List of all oligonucleotide primers used in this study.**

1632 **Table S5. List of all plasmids used in this study.**

1633 Abbreviations in the selection column highlight the drug and its concentration that were used to
1634 select for plasmid maintenance. Amp = ampicillin, Cam = chloramphenicol, Kan = kanamycin; 25 / 50 /
1635 100 refer to 25 µg/ml, 50 µg/ml, and 100 = 100 µg/ml, respectively.

1636 **Table S6. Construction of all plasmids generated in this study.**

1637 **Table S7. Construction of all plasmids generated in this study.**

1638 Confidence scores of AlphaFold-generated models. Confidence per residue is calculated as a
1639 predicted Local Distance Difference Test score (pLDDT; values 0-100), with an average of all residues
1640 within the models provided below. A pLDDT ≥ 90 have very high model confidence, residues with 90 >
1641 pLDDT ≥ 70 are classified as confident, while residues with 70 > pLDDT > 50 have low confidence, and
1642 residues with pLDDT <50 correspond to very low confidence. Interface pTM scores ("iptm+ptm") are a
1643 measure of predicted protein multimer accuracy by AlphaFold-Multimer using the with confidence scored
1644 0 to 1 for the complete model. All structures were predicted using the COSMIC^2 platform [180], except
1645 structures highlighted with an asterisk which had been solved using the AlphaFold3 server (see the
1646 dedicated section in *Materials and Methods*) [181].

1647 **S1 Data. Raw data and calculations of all efficiency-of-plating (EOP) assays and**
1648 **qualitative top agar experiments.** This file is not included in the preprint of this
1649 manuscript.

1650 **S2 Data. GAPS report for the HeidiAbel genome.**

1651

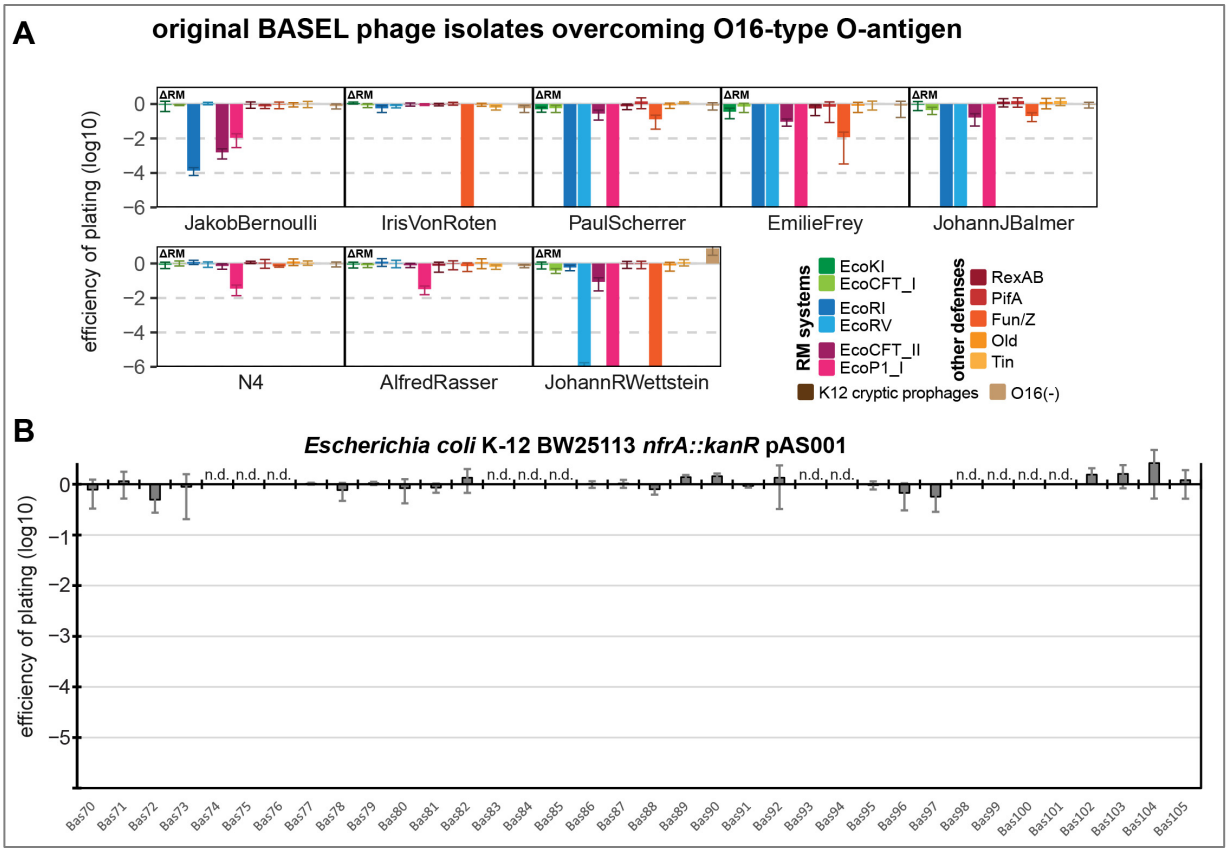

S1 Figure. Supplemental data for Fig. 4.

(A) Phages that had shown significant growth on *E. coli* K-12 with restored O-antigen in our previous work [10] were now phenotypically characterized in the presence of this glycan. The results of these quantitative phenotyping experiments regarding sensitivity to altered surface glycans and bacterial immunity systems are presented as efficiency of plating (EOP). The small note of "ΔRM" indicates that this experiment has been performed using *E. coli* K-12 ΔRM *wbbL(+)* as host (i.e., with restored O-antigen expression). Data points and error bars represent average and standard deviation of at least three independent experiments. Raw data and calculations are available in S1 Data. **(B)** The results of quantitative phenotyping experiments with all newly presented BASEL phages infecting an *nfrA* knockout (specifically lacking the NGR glycan [17]) are presented as efficiency of plating (EOP). This strain had been transformed with plasmid pAS001 to restore O16-type O-antigen expression (see *Materials and Methods*). Data points and error bars represent average and standard deviation of at least three independent experiments. Raw data and calculations are available in S1 Data. It is evident that no newly included BASEL phage depends partially or completely on the NGR glycan for infection of *E. coli* K-12. Phages sensitive to the presence of cryptic prophages in the K-12 genomic background could not be tested, but since all carry tailspikes or tail fibers targeting O16-type O-antigen as sole receptor-binding proteins (Figs. 11 and 12) it seems highly unlikely that they would be affected by the absence of NGR.

.

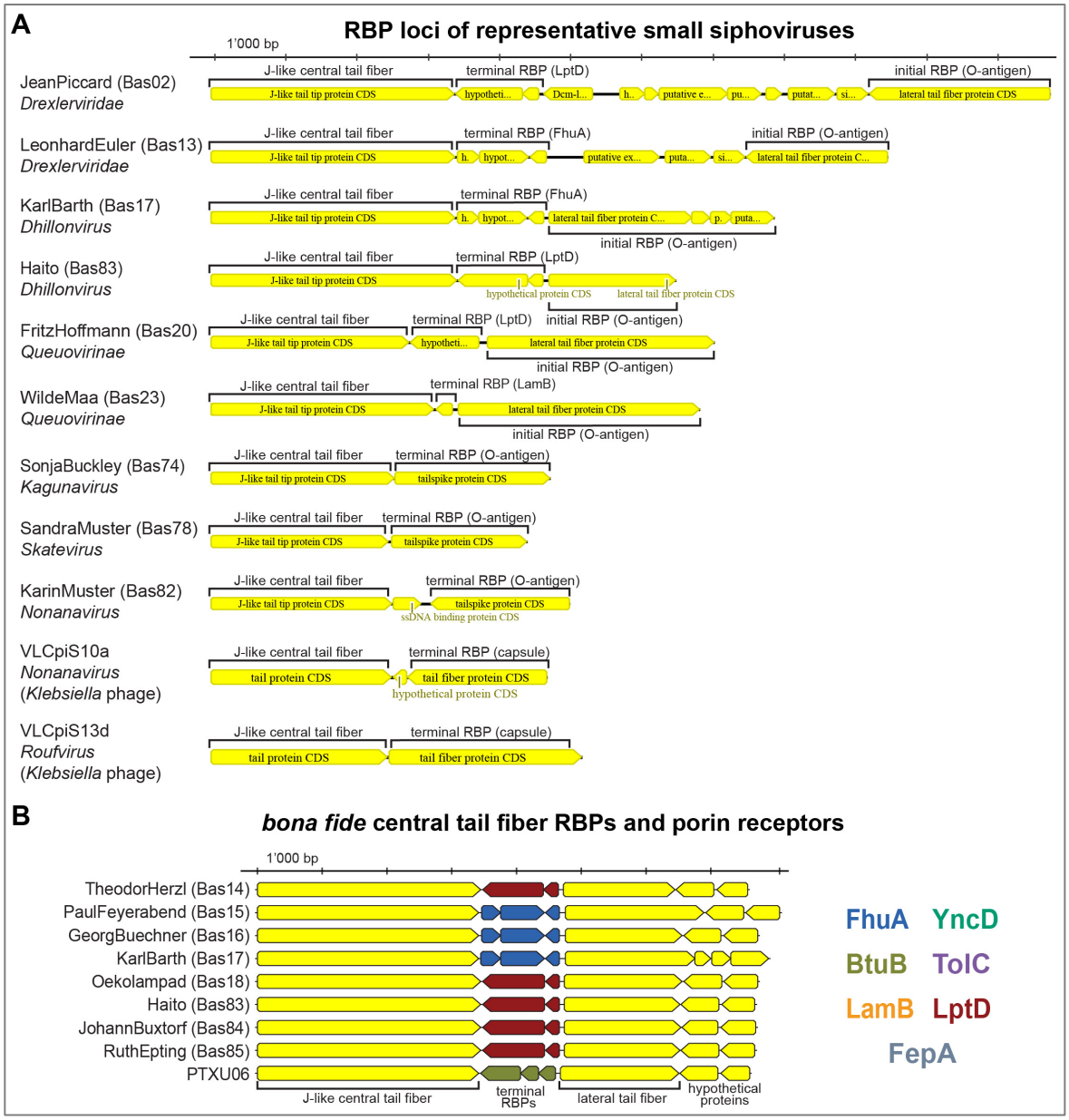

S2 Figure. Supplemental data for Fig. 6.

(A) The illustration compares the tail fiber and tailspike loci of diverse small siphoviruses from the original BASEL collection and the current study and porin-targeting receptor-binding proteins (RBPs) are annotated based on the *bona fide* central tail fiber caps identified previously [10]. It is apparent that the single RBPs of the three exemplary O16-dependent phages SonjaBuckley (*Kagunavirus*, Bas74), SandraMuster (*Skatevirus*, Bas78), and KarinMuster (*Nonanavirus*, Bas82) are encoded at the same locus as the porin-targeting RBPs for terminal receptor recognition in the other genomes. For comparison, we also included two small siphoviruses targeting *Klebsiella* capsules that had been classified in previous work as belonging to *Nonanavirus* (see Fig. 6E) and *Roufvirus* (see Fig. 6D) [48]. Despite the annotation as "tail fiber", both viruses encode tailspikes directly downstream of the orthologs of the J-like central tail fiber proteins [48]. **(B)** Comparison of *bona fide* central tail fiber RBP loci of all *Dhillonvirus* isolates in the BASEL collection and PTXU06 for comparison [10, 56]. The

association of different variants of this locus with porin specificity is color-coded as in our previous work – all new isolates from the current study are predicted to target LptD (red) as terminal receptor [10].

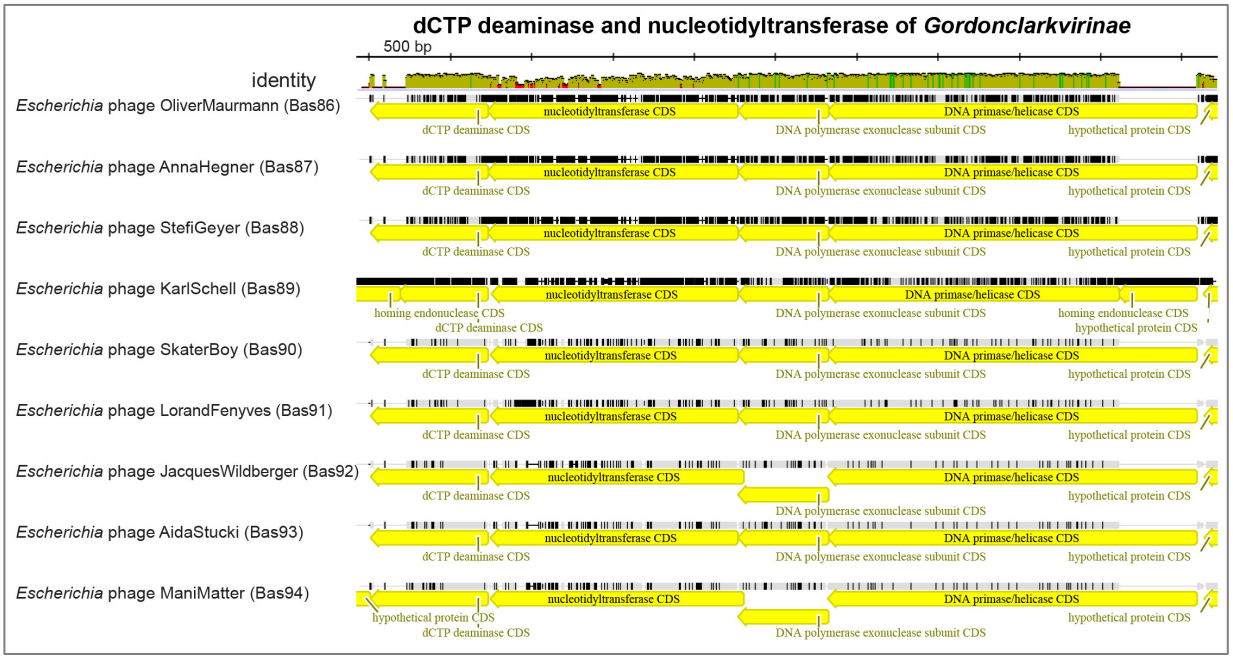

S3 Figure. Supplemental data for Fig. 7.

The conserved locus encoding dCTP deaminase, nucleotidyltransferase, and DNA replication genes of all included *Gordonclarkvirinae* isolates is shown in a sequence alignment (see *Materials and Mehtods*). Colors in the sequence identity graph above the alignment indicate the sequence identity at each individual position with green representing 100% identity, greenish brown 30%-99% identity, and red <30% identity. Besides homing endonuclease insertions, the locus is fully syntenic across these isolates (and many other *Gordonclarkvirinae*).

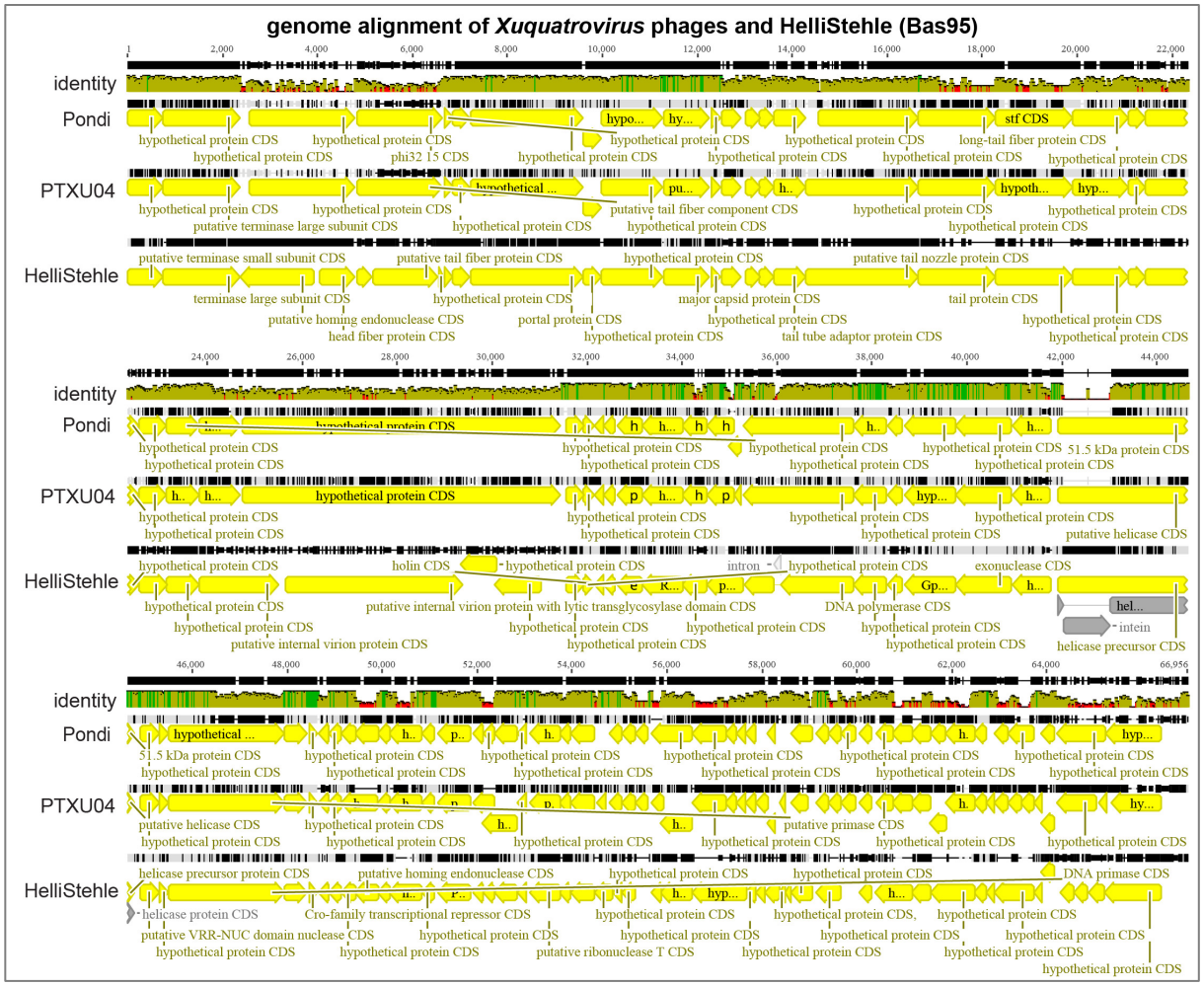

S4 Figure. Supplemental data for Fig. 8.

The genomes of our new isolate HelliStehle (Bas95) and *Xuquatrovirus* phages Pondi (GenBank accession OP136151.1) and PTXU04 (NCBI GenBank accession NC_048193.1) are shown in a sequence alignment with the putative small terminase subunit as starting point (see *Materials and Methods*). Colors in the sequence identity graph above the alignment indicate the sequence identity at each individual position with green representing 100% identity, greenish brown 30%-99% identity, and red <30% identity. The pairwise sequence identity of prototypic phage PTXU04 to fellow *Xuquatrovirus* Pondi is 83.8% and to HelliStehle (Bas95) merely 58.3%.

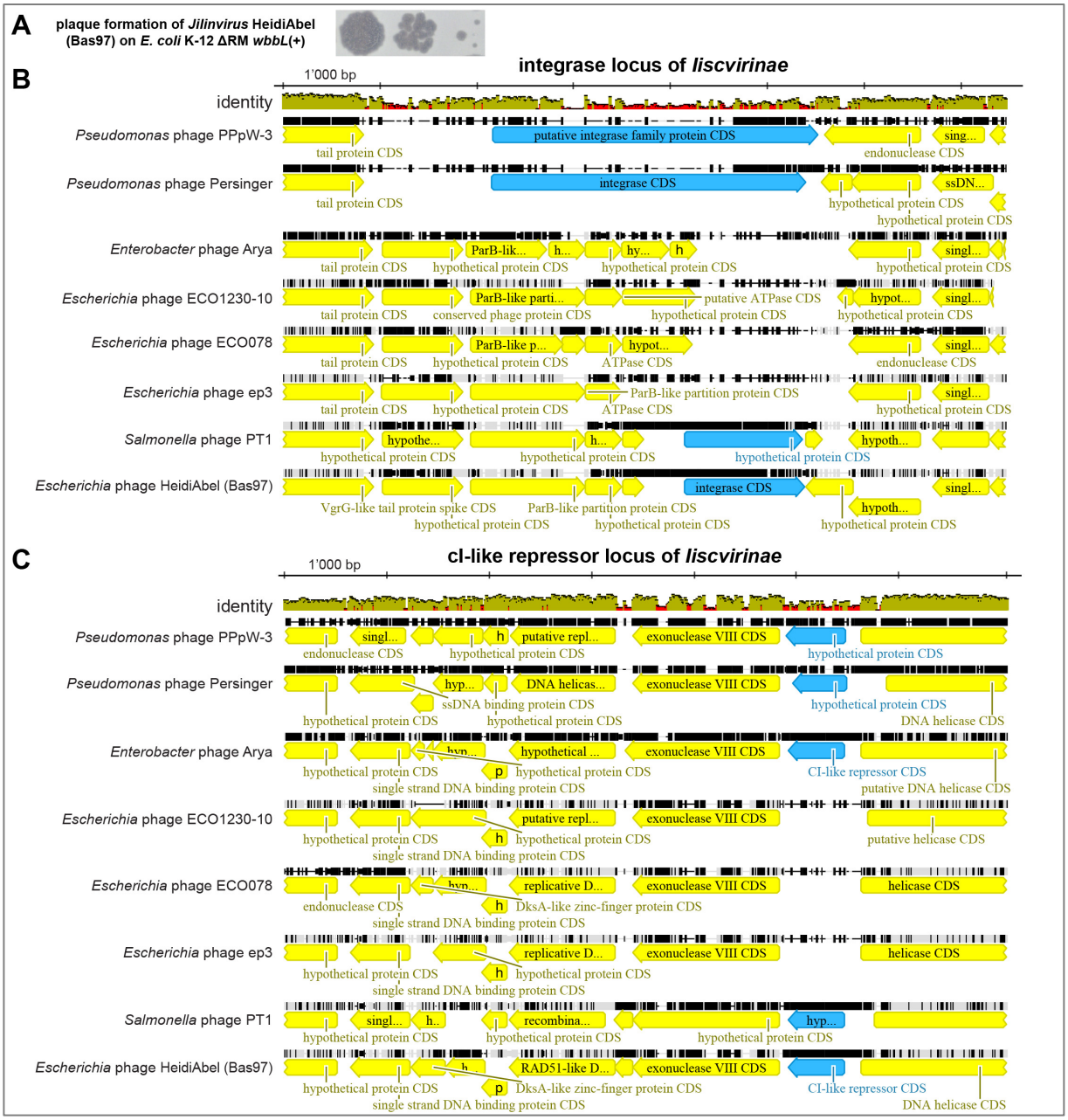

S5 Figure. Supplemental data for Fig. 9.

(A) Serial dilutions of *Jilinvirus* HeidiAbel (from left to right) were spotted on a soft agar of *E. coli* K-12 ΔRM *wbbL(+)* and grown overnight at 37°C before imaging. The lysis zones and plaques show no classical signs of lysogen formation such as turbidity or marked growth of (self-immune) lysogens in the middle [184] – compare, e.g., the growth of temperate *Lederbergvirus* phage Kap1 on a host enabling lysogeny and a host without its preferred integration site in Fig. 3 of Pick et al. [185]. Instead, upon prolonged incubation merely an abundance of dotted individual colonies is found that we typically observe for phages requiring the LPS O-antigen as host receptor which is a huge mutational target [186]. **(B, C)** The illustrations show sequence alignments of the integrase locus of *Iiscvirinae* phages (B) and – encoded slightly downstream – their cI-like repressor locus (C; see *Materials and Methods*). Both genes of interest are highlighted in blue. Colors in the sequence identity graphs above the alignments indicate the sequence identity at each individual position with green representing 100% identity, greenish brown

30%-99% identity, and red <30% identity. The alignments show that only the two *Pseudomonas* phages (top) and *Salmonella* phage PT1 as well as our isolate HeidiAbel encode seemingly intact integrase and cI-like repressor genes. These observations are further discussed in the main text.

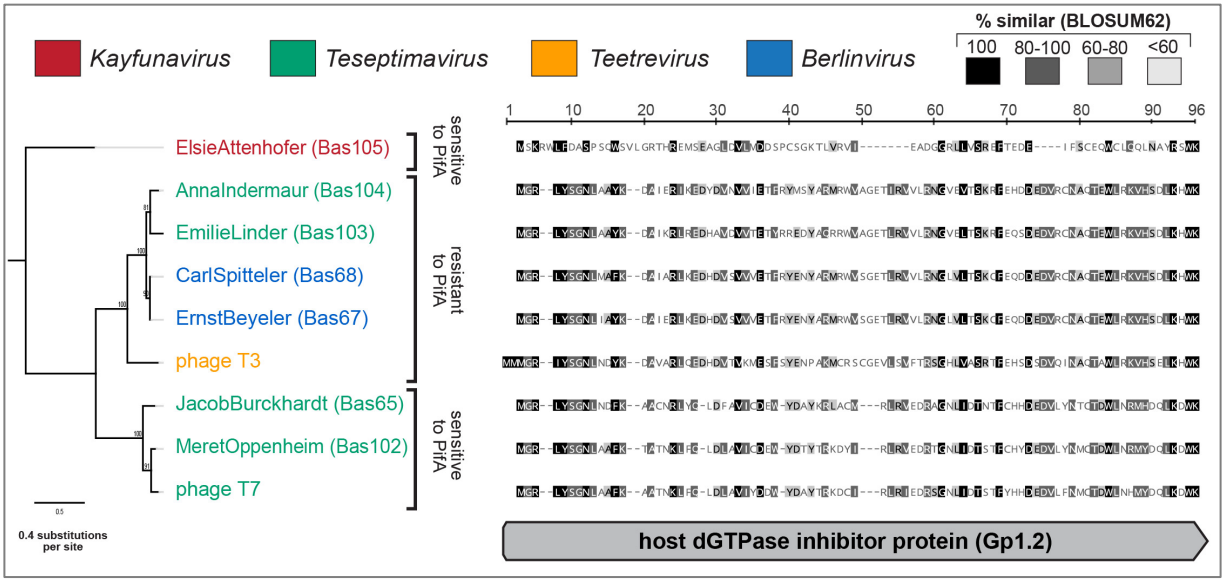

S6 Figure. Supplemental data for Fig. 10.

The illustration shows a Maximum-Likelihood phylogeny (left) and a sequence alignment (right) of Gp1.2 orthologs in all tested *Autographiviridae* phages in the complete BASEL collection. Experimental details are explained in *Materials and Methods*. Resistance to the PifA defense system (see Fig. 10D and our previous work [10]) correlates with one specific clade of Gp1.2 homologs (the middle one).

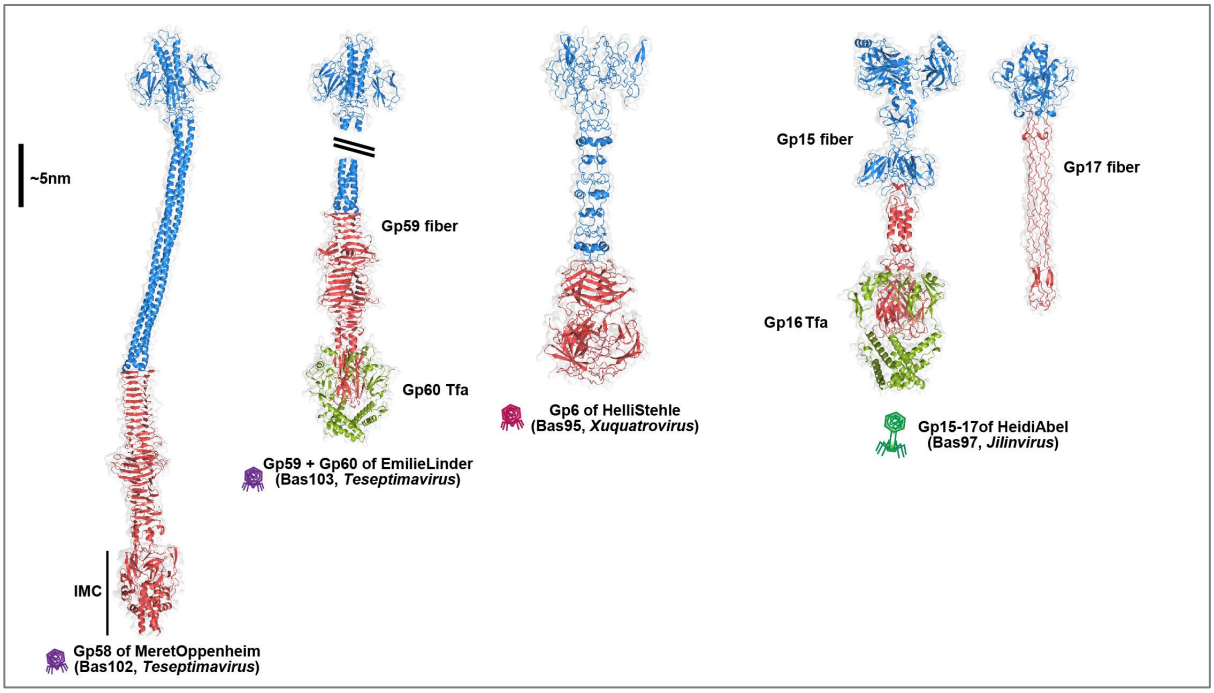

S7 Figure. Supplemental data for Figs. 11 and 12.

AlphaFold-Multimer [108] predicted structures of additional tail fibers from selected BASEL phages with a single receptor-binding domain (RBD). Tail fibers of *Teseptimavirus* phages MeretOppenheim (Bas102) and EmilieLinder (Bas103) are formed by a homotrimer of Gp58 or Gp59, respectively. Note that the tail fiber of MeretOppenheim contains a C-terminal intramolecular chaperone (IMC) domain. Conversely, EmilieLinder encodes a separate Mu-like tail fiber assembly protein (Tfa, Gp60; green) downstream of the Gp59 tail fiber that are predicted to form a hexameric complex as observed for the tail fiber of phage Mu [187]. The homotrimeric tail fibers of *Xuquatrovirus* HelliStehle (Bas95) and *Jilinvirus* HeidiAbel (Bas97) feature comparably short fiber stalks. HeidiAbel also encodes a Tfa protein (Gp16; green) that is predicted to form a complex with the tail fiber similar to the complex predicted for EmilieLinder. In addition, HeidiAbel also encodes a separate tail fiber with a distal tip that is similar, but truncated, to the T4 Gp37 long tail fiber and the Gp32 tail fiber of *Wifcevirus* ManiWeber [37] (see Fig. 12C). Based on the size and genetic arrangement, we speculate that the Gp15 fiber of HeidiAbel serves as a lateral tail fiber for initial host recognition while Gp17 forms a short tail fiber for irreversible adsorption triggering viral genome injection (analogous to the much larger T-even myoviruses [10, 73, 74]). In all predicted structures, N-terminal anchor domains and fiber shafts are colored blue with the RBDs colored red. A ~5 nm vertical scale bar is provided for reference and viral morphotypes are annotated by phage icons analogous to Figs. 11A and 11B.

1662

1663

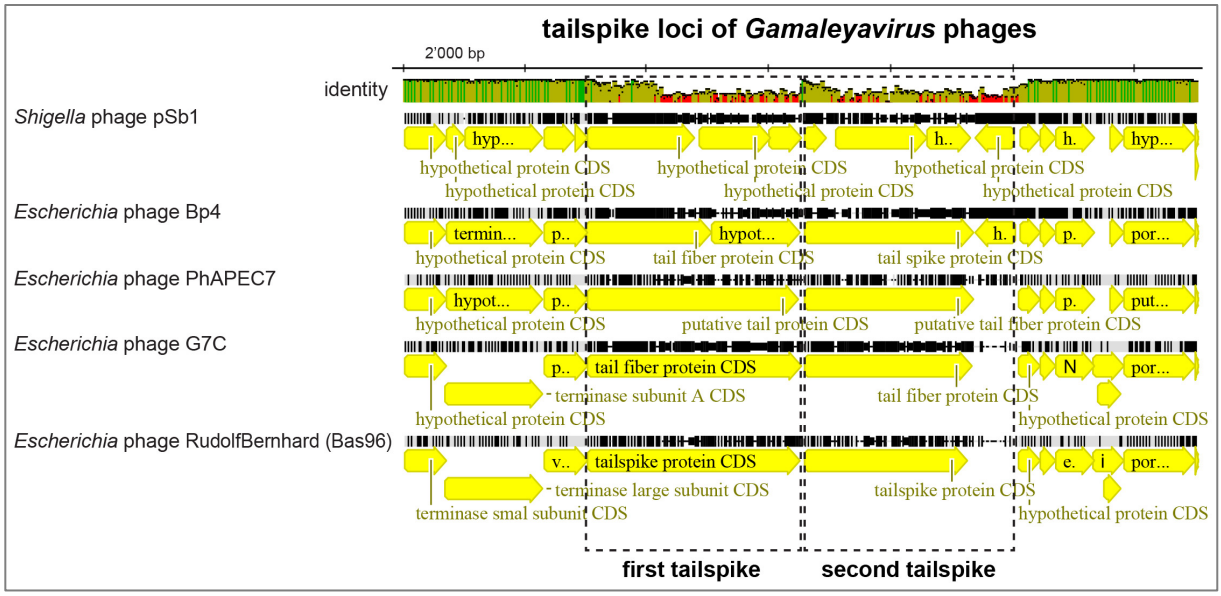

S8 Figure. Supplemental data for Figs. 11 and 12.

The illustration shows a sequence alignment of the tailspike locus of different *Gamaleyavirus* phages (compare Fig. 8E; see *Materials and Methods*). Colors in the sequence identity graph above the alignment indicate the sequence identity at each individual position with green representing 100% identity, greenish brown 30%-99% identity, and red <30% identity. The alignment shows that the most 5' parts of the two tailspike loci – encoding the N-terminal ends of the (proximal subunits of the) tailspikes – are highly conserved, likely encoding conserved structural elements that anchor them at the virion. The receptor-binding domains of all tailspikes vary greatly. These observations are further discussed in the main text.

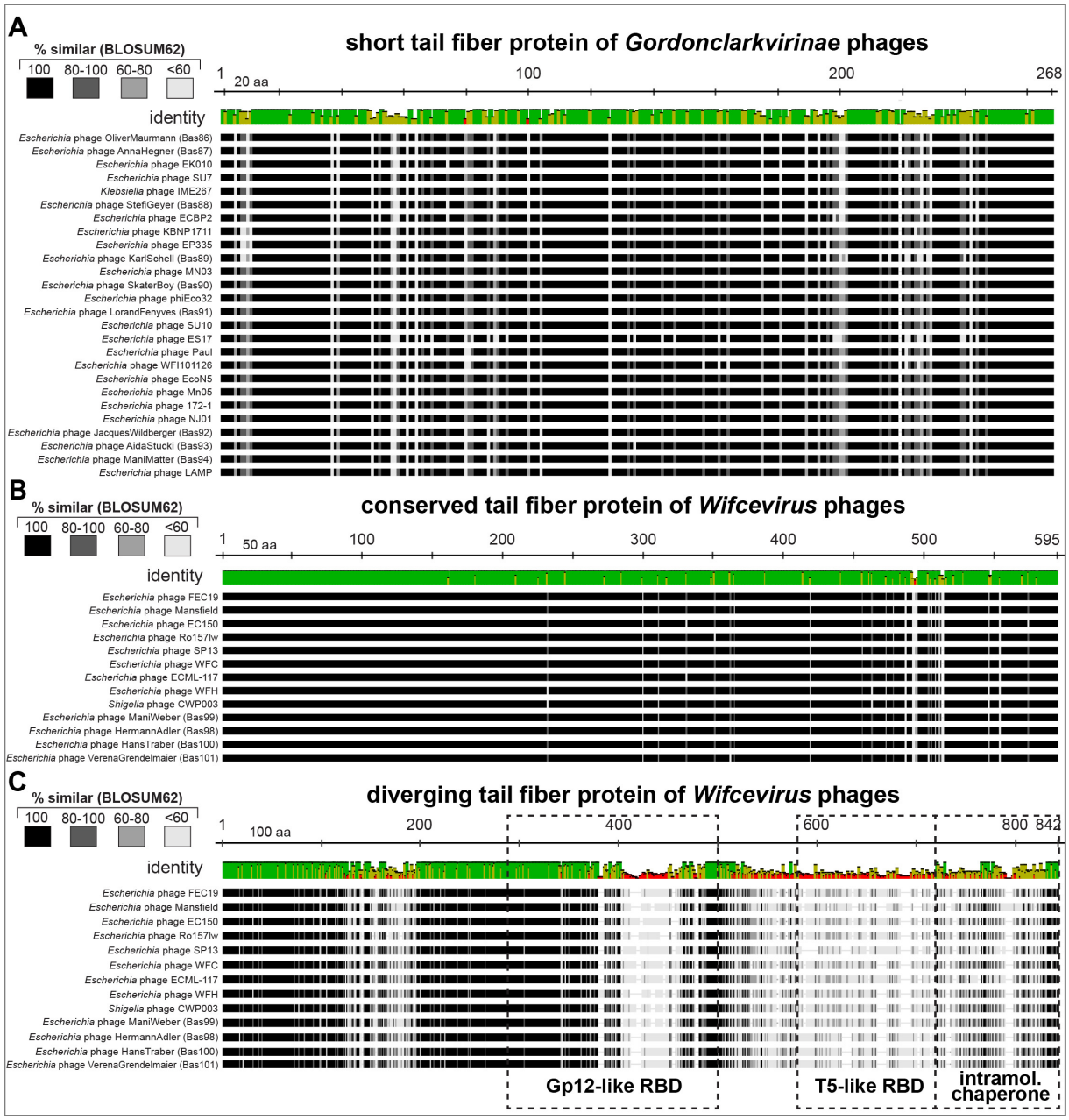

S9 Figure. Supplemental data for Figs. 11 and 12.

(**A**) The illustration shows an amino acid sequence alignment of the short tail fiber proteins of all *Gordonclarkvirinae* included in Fig. 7C in the same order (see *Materials and Methods*). It is apparent that short tail fiber proteins are highly conserved across the *Gordonclarkvirinae* subfamily with only minor differences. Across all sequences there are 163 of 267 fully identical sites (60.8%). **(B)** Amino acid sequence alignment of the conserved tail fiber of *Wifcevirus* phages encoded with their tail fiber locus (Gp32 of ManiWeber / Bas99, see Fig. 12C). It is clear from the alignment that all orthologs are very similar in amino acid sequence, suggesting a conserved and invariable function. **(C)** Amino acid sequence alignment of the T-shaped tail fibers of *Wifcevirus* phages (see Figs. 11B, 12B, and S10D). The alignment shows that the N-terminus of all orthologs is highly conserved while the two receptor-binding domains (RBDs) as well as – to lesser extent – the intramolecular chaperone of the T5-like RBD2 vary a lot between sequences. In (A) to (C), colors in the sequence identity graph above the alignment

indicate the sequence identity at each individual position with green representing 100% identity, greenish brown 30%-99% identity, and red <30% identity.

1666

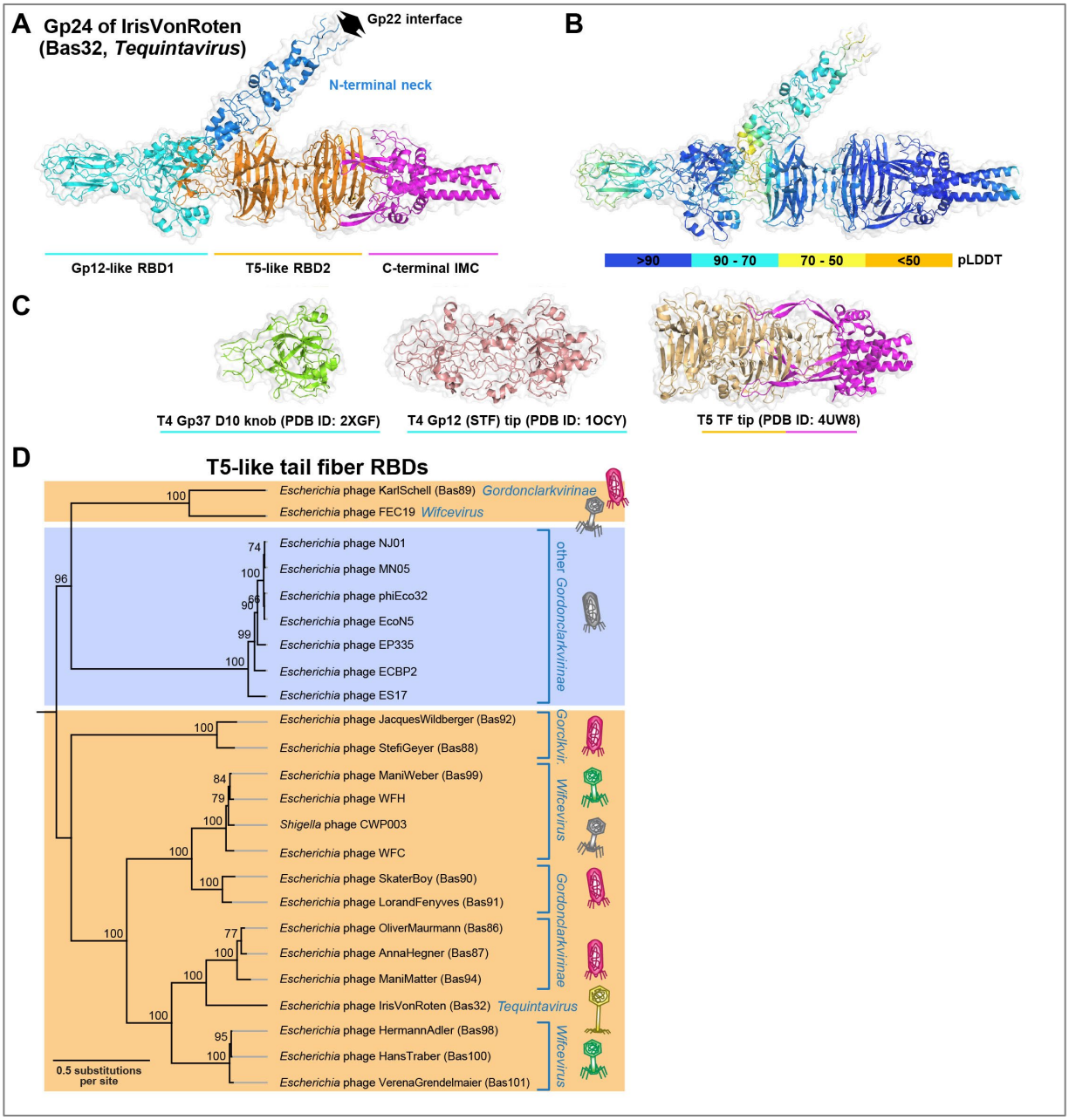

S10 Figure. Supplemental data for Figs. 11 and 12.

(A) The AlphaFold-Multimer [108] predicted structure of the T-shaped tail fiber of IrisVonRoten (Gp24) was colored to highlight the domain boundaries of this unique dual RBD tail fiber. **(B)** The same structure as in (A) was colored by predicted local distance difference test (pLDDT) confidence scores as generated by AlphaFold to demonstrate the high level of confidence (overall average = 72.6) in the predicted T-shaped tail fiber structure. **(C)** The DALI server [182] identified structural similarities between the Gp12-like RBD1 with crystal structures of the distal knob domain (D10) of the T4 long tail fiber Gp37 [109] (Z-score 8.8, RMSD 3.2, 100 residues) and unsurprisingly with the Gp12 short tail fiber

distal tip itself [109] (Z-score 6.2, RMSD 4.1, 127 residues) as well as similarity between the T5-like RBD2 with the distal binding tip and IMC domain of the phage T5 lateral tail fiber [110] (Z-score 6.3, RMSD 4.8, 179 residues). **(D)** Maximum-Likelihood phylogeny of T5-like receptor-binding domains of T-shaped tail fibers together with their intramolecular chaperone domain as identified by structure prediction (see *Materials and Methods*). The phylogeny was midpoint-rooted between a clade of distant *Gordonclarkvirinae* tail fibers at the top (blue) together with two other sequences and all other RBDs mostly belonging to phages presented in this study (orange). Note how RBDs of *Wifcevirus*, *Gordonclarkvirinae*, and *Tequintavirus* isolates are scattered over the phylogeny in small clusters, suggesting frequent horizontal gene transfer as often observed for viral receptor-binding domains [10, 33, 106]. Phage AidaStucki (Bas93, *Gordonclarkvirinae*) was not included due to a large truncation in its intramolecular chaperone domain.

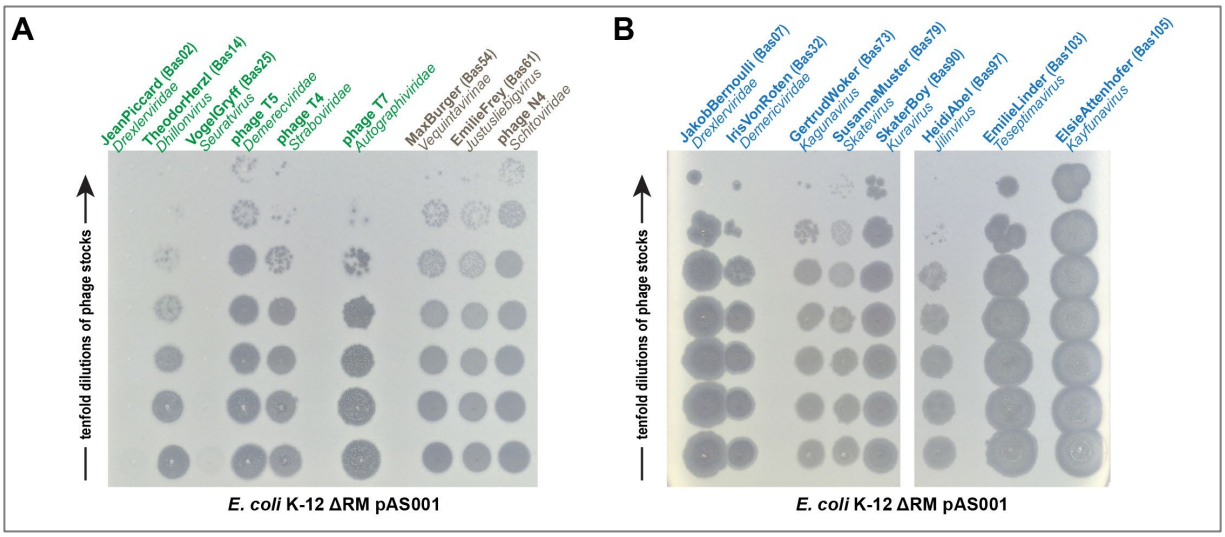

S11 Figure. Supplemental data for Materials and Methods.

The same serial dilutions as in Figs. 1B (for (A)) and 2B (for (B)) were spotted on the *E. coli* K-12 ΔRM strain with partially restored O16-type O-antigen due to ectopic expression of *wbbL* from plasmid pAS001 (see *Materials and Methods*). Most but not all phages inhibited by a full O16-type O-antigen barrier (green) show robust growth on this host (compare Fig. 1B) while those that can bypass it (brown; compare Fig. 1B) or that depend on it (blue; compare Fig. 2B) grow very well. Notably, a weak inhibition of phage growth had already been observed previously for intermediate restoration of the *E. coli* K-12 O16-type O-antigen [30].

S12 Figure. Supplemental data for Materials and Methods.

The illustration shows the genome of phage HeidiAbel (Bas97; see Fig. 8F) with annotations highlighted in different colors. Blue annotations had been predicted by Pharokka in a similar functional context but could be improved by GAPS while red annotations had only been predicted as hypothetical proteins by Pharokka [161]. The genes highlighted in grey had not been predicted by Pharokka in this setup but were inferred by manual analysis of a whole-genome alignment between HeidiAbel and related phages (see *Materials and Methods*). A tRNA is highlighted in pink. The GAPS output for HeidiAbel based on the Pharokka-annotated genome as input is included as S2 Data.